# The challenge of regulating angiogenesis in tissue engineered implants

C.J. Kirkpatrick

*Repair lab, Institute of Pathology, Johannes Gutenberg University, Mainz, Germany*

The success of tissue engineering (TE) implants will depend in large measure on the ability of the chosen system to provide an adequate oxygen supply to the cells involved, as practically all cell types in the human body (with the exception of cartilage) have an aerobic metabolism. Thus, it is important to develop relevant assays for human angiogenesis in order to better understand the underlying molecular mechanisms and to test new TE concepts for vascularization [1]. Cell cultures form an essential model system in studying vascular system-biomaterial interactions for TE applications, irrespective of whether a biomaterial scaffold or matrix will be pre-seeded with cells prior to implantation or the cell-material interactions are induced in vivo, for example by a suitable drug-delivery system to promote angiogenesis. The author will discuss in detail the underlying biological mechanisms and present data on human endothelial cell (EC) cultures, both as established cell lines and as primary isolated cells, in assays designed to unravel the mechanisms of vascularization of biomaterial matrices and scaffolds.

We have developed two-and three-dimensional assays using human EC of both macro- and microvascular origin (HUVEC, HDMEC, HPMEC). This assay system includes pro-angiogenic factors and suitable matrices (collagen I and fibrin) and promotes formation of lumen-containing vascular sprouts [2]. In order to test novel 3D scaffolds for TE we have performed detailed studies on the silk protein, fibroin, in the form of a fibre network [3]. Molecular biological methods, such as RT-PCR are employed to study the functional status of the cells. Seeding fibroin scaffolds with EC, followed by later addition of collagen I with fibrin to fill the scaffold interstices, permits extensive growth of EC on the network and vascular sprouting into the gel matrix, as studied using confocal laser scanning microscopy (CLSM). With such cultures we have shown that it is possible to establish in vitro assays to test the suitability of different biomaterial scaffolds for vascularization. RT-PCR has shown, for example, that the EC on the fibroin network are not activated [4]. Similar work is being performed on porous ceramics and metal surfaces.

Currently, co-cultures of EC and osteoblasts are being established to simulate more closely the in vivo situation during bone regeneration. These models offer possibilities to study other wound healing forms, such as for skin regeneration (EC together with keratinocytes and dermal fibroblasts). In addition, studies with endothelial progenitor cells (EPC) from human blood are also being performed, as this gives the possibility of employing autologous cells for vascularization. The latter probably represents the most attractive possibility for vascularisation of TE implants, although it must be stressed that many fundamental biological issues with respect to endothelial lineage differentiation still remain to be clarified. In particular, it is still unclear how pure the EPC population must be to achieve maximum success. Thus, it is possible that heterotypic cell interactions might be essential to regulate lineage differentiation. A further issue concerns the possible activation of immunogenic signals (even) in autologous cells induced by the artificial situation of in vitro cultivation.

In conclusion, as TE applications approach possible clinical use, the requirement for detailed knowledge on how human vascular cells interact with biomaterials will become increasingly important, as vascularisation and control of the inflammatory and healing responses are prerequisites for clinical success.

**REFERENCES:** [1].Kirkpatrick CJ, Unger RE, Krump-Konvalinkova V, Schmidt H, Kamp G, Peters K. Experimental approaches to study vascularisation in tissue engineering and biomaterial applications. J Mater Sci Mater Med 2003; 14: 677-681. [2].Peters K, Schmidt H, Unger RE, Otto M, Kamp G, Kirkpatrick CJ.Software-supported image quantification of angiogenesis in an in vitro culture system: Application to studies of biocompatibility. Biomaterials 2002; 23, 3413-3419. [3].Unger RE, Wolf M, Peters K, Motta A, Migliaresi C, Kirkpatrick CJ. Growth of human cells on a non-woven silk fibroin net: a potential for use in tissue engineering. Biomaterials 2004; 25: 1069-1075. [4].Unger RE, Peters K, Wolf M, Motta A, Migliaresi C, Kirkpatrick CJ. Endothelialization of a non-woven silk fibroin net for use in tissue engineering: growth and gene regulation of human endothelial cells. Biomaterials 2004; 25: 5137-5146.

**Acknowledgements:** The author kindly acknowledges the input of the scientific staff, Ron Unger PhD, Kirsten Peters PhD, Sabine Fuchs PhD & Iris Hermanns MSc, the expert technical help of Sabine Aust, Susanne Barth, Luise Meyer & Anne Sartoris with the tissue culture experimentation. Thanks also to the German Research Foundation (DFG) for the generous financial support (Priority Programme "Biosystem", Grant KI 601/1-3).

# Alterations in Gene Expression in a 3D Spheroidal Co-Culture Model of Endothelial Cells and Osteoblasts Regarding Angiogenesis and Differentiation

A.Wenger, A.Stahl, U. Kneser, G.B. Stark, G. Finkenzeller

[1] *Department of Plastic Surgery, University Hospital Freiburg, 79106 Freiburg, Germany*

**INTRODUCTION:** Angiogenesis is a fundamental process in bone formation and fracture healing which requires intercommunication between endothelial and osteoblastic cells. Neovascularization is also a very important issue in tissue engineering since implantation of voluminous grafts without sufficient vascularity results in hypoxic cell death in engineered tissues. Therefore, strategies that enhance angiogenesis should have positive effects on cell survival in tissue engineering. In this context, we have developed a three-dimensional spheroidal co-culture system consisting of human primary osteoblasts and human endothelial cells to improve angiogenesis in bone tissue engineering.[1,2]

**METHODS:** We investigated the intercellular communication between endothelial and osteoblastic cells in mono- and co-culture spheroids with emphasis on putative alterations in gene expression of endothelial and osteoblastic cell specific genes, playing a role in angiogenesis or differentiation[3]. By using quantitative RT PCR and ELISA techniques, we have detected pleiotropic effects on gene expression depending on the cell culture technique applied i.e. whether the cells were grown in spheroid or monolayer culture.

**RESULTS:** In endothelial cell spheroids, expression of Tie-1, Tie-2 and CD31 is upregulated in comparison to endothelial cell monolayer culture, whereas spheroidal culture of osteoblasts results in a weak upregulation of osteocalcin mRNA and a strong upregulation in the expression of the angiopoietin-2 gene.
Spheroidal co-cultivation of osteoblasts and endothelial cells induces a moderate upregulation of VEGFR-2 in endothelial cells and a very pronounced upregulation of the osteoblast differentiation marker alkaline phosphatase in osteoblasts.

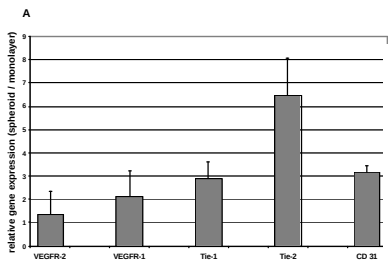


*Fig. 2: Comparison of collagen type I, osteocalcin, alkaline phosphatase, Angiopoetin-1 and –2 expression in hOB spheroids vs.*

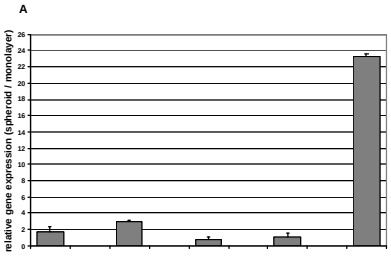


*Fig. 1: Comparison of mRNA expression in EC spheroids vs. EC monolyer culture after 48h. Gene expression were determined by quantitative real time rt PCR.*

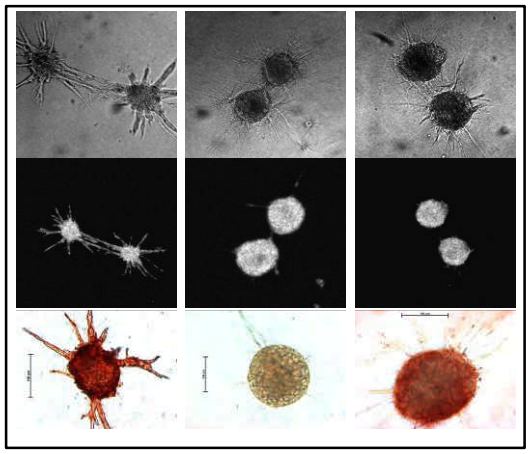

*Fig. 3 A-C: Phase contrast images (200X mag) of HUVEC spheroids (A), hOB spheroids (B) and HUVEC/hOB co-spheroids (C) with corresponding confocal laser microscopy images (50X mag) of the same spheroids labelled with DRAQ 5 as a specific marker for DNA. Sumview projections of optical sections through HUVEC spheroids reveal distinct DRAQ 5 signals within HUVEC spheroid sprouts with linear alignment of DRAQ-positive cell nuclei (A). Sprouts emerging from hOB and HUVEC/hOB co-spheroids display only few if any DRAQ 5 positive signals within spheroid sprouts (B, C).for CD31-positive tube like sprouts emerging from HUVEC spheroid in a collagen matrix (right).*

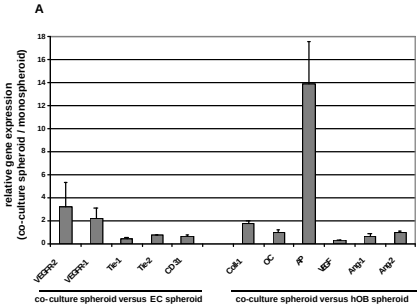


*Fig. 4: Comparison of levels of gene expression in co-culture spheroids vs. the corresponding monospheroids after 48h of culture.*

**DISCUSSION & CONCLUSIONS:** The effects displayed are not mediated by a paracrine mechanism but are most likely due to the establishment of heterotypic cell contacts within the co-culture spheroid demonstrating complex bi-directional gene regulation mechanisms between EC and OB. The data presented in this study demonstrates the spheroidal co-culture system to be a powerful tool to study paracrine and/or cell contact mediated interactions between endothelial cells and osteoblasts for applications in bone tissue engineering.

**REFERENCES:** [1]T. Korff, H.G. Augustin (1999) *J Cell Sci* 112**:** 3249–3258. [2]Wenger A, Stahl A., Weber H., Finkenzeller G., Augustin H.G., Stark G.B., Kneser U. (2004) Tissue Engineering (accepted). [3]F. Villars, L. Bordenave, R. Bareille, J. Amédée (2000) J Cell Biochem. 79 672-685

# Scaffolds for Cartilage Tissue Engineering: Effect of Pore Size

S.Grad[1], K.Gorna[2], S.Gogolewski[2], M.Alini[1]

[1]*Biochemistry & Cell Biology,* [2]*Polymer Research, AO Research Institute, Davos, Switzerland*

**INTRODUCTION:** Three-dimensional porous scaffolds prepared from experimental linear biodegradable polyurethane may serve as suitable carriers for cartilage tissue engineering [1]. The main limitations of the system were the poor retention of matrix molecules within the scaffold and the maintenance of the appropriate chondrocytic phenotype of the cells. We hypothesized that the decrease of the scaffold pore size might be a possible strategy to overcome these problems. The present study investigated the effect of the scaffold pore size on the proliferation, differentiation and extracellular matrix production of chondrocytes seeded onto polyurethane carriers.

**METHODS:** 3D porous polyurethane scaffolds with different pore sizes (Table 1) [2] were cut into discs of 8 mm in diameter and 4 mm in thickness. After sterilization with ethylene oxide, discs were seeded with bovine articular chondrocytes using a vacuum cell seeding system. 5 x $10^6$ cells were seeded per scaffold, and cell-polymer constructs were cultured in DMEM containing 10% FCS, nonessential amino acids, ascorbic acid and L-proline for up to 6 weeks. After 2 days, 2, 4, and 6 weeks, they were analyzed biochemically and histologically. The DNA contents of the constructs were measured, and the amounts of sulfated glycosaminoglycans were determined in constructs and in the culture media. Gene expression of procollagen types I and II and aggrecan core was quantified by real-time RT-PCR. For histological evaluation, constructs were embedded in methyl methacrylate, and sections were stained with toluidine blue.

| SP000 | SP001 | SP004 | ISO K |
|---|---|---|---|
| 50-200 | 80-350 | 50-200 | 50-400 |

**Table 1.** Approximate pore size [µm] of the four polyurethane scaffolds used for the study.

**RESULTS:** Histological analysis 2 days after cell seeding demonstrated a uniform distribution of the cells throughout the SP000, SP004 and ISO K scaffolds, whereas the cells mainly accumulated at the edge of the SP001 constructs. After 6 weeks in culture, accumulation of intensely stained extra-cellular matrix was most pronounced in ISO K scaffolds (Fig.1). The DNA content within constructs did not vary between the different scaffolds at day 2 and was highest in ISO K scaffolds after 6 weeks of culture. Consistent with histological observations, amounts of GAG were significantly enhanced in ISO K compared to smaller pore size scaffolds. 25-30% of the synthesized GAG was retained in SP000, whereas 15-20% was retained in the other scaffold types. The mRNA expression of collagen II decreased in all constructs; the decrease was significantly less in ISO K compared to the others after 6 weeks. An increase in collagen I mRNA and decrease in aggrecan mRNA was noticeable in all scaffolds.

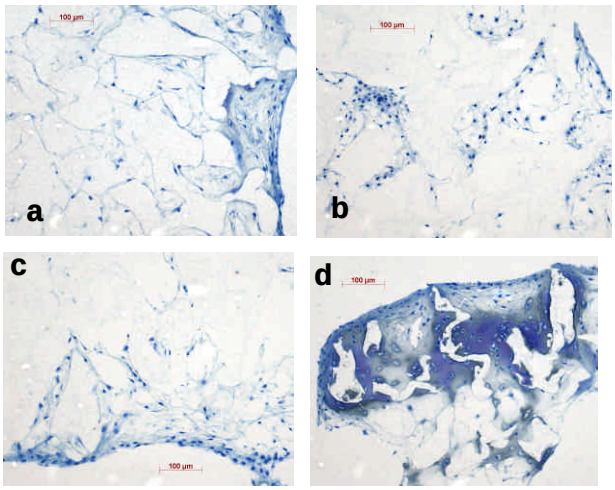


**Figure 1.** Histological sections after 6 weeks in culture. (a) SP000 (b) SP001 (c) SP004 (d) ISO K

**DISCUSSION & CONCLUSIONS:** The results of this study indicate that decreasing the pore size of polyurethane scaffolds does not improve the phenotype expression and cartilaginous matrix synthesis of incorporated chondrocytes. Although a homogeneous cell distribution could be obtained in most of the constructs, an edge effect was noticed in particular in the scaffolds with the smallest pores. In addition, a low pore size may potentially limit the access to nutrients, which may explain the superior performance of the constructs with the larger pores. On the other hand, decreasing the pore size improved the retention of the synthesized matrix molecules. Chemical modification of the polymer may further promote matrix retention. The effect of embedding the cells into a fibrin gel before seeding them into the scaffolds and the long term effect of mechanical stimulation using a specific bioreactor system is currently investigated.

**REFERENCES:** [1] Grad S et al., *Biomaterials* 24:5163, 2003. [2] Gorna K et al., *MRS 2004 Spring Meeting*, San Francisco.

# Synthetic Biomolecular Hydrogels for the Conduction of Tissue Regeneration

M.P. Lutolf[1] and J.A. Hubbell[2]

*[1] ETH Zurich, Zurich, Switzerland. [2] EPF Lausanne, Lausanne, Switzerland.*

**INTRODUCTION:** New challenges in tissue engineering call for the development of designer extracellular microenvironments (ECM) that can interact with cells to control their fate, enabling spatially and temporally complex morphogenetic processes of tissue formation and regeneration. Materials derived from natural ECMs such as collagen are advantageous because of their inherent biological characteristics (e.g. integrin signaling and susceptibility to proteolytic remodeling). Despite of this, many problems associated with their purification, biocompatibility, physicochemical properties, and the difficulty of adapting matrix properties to a specific biological situation, have spurred the development of synthetic tissue-inducing biomaterials. Here we present such a family of synthetic ECMs: Poly(ethylene glycol)-(PEG) based hydrogels containing a combination of bioactive peptides, namely adhesion ligands (RGDSP) providing traction for cell migration, and substrates of cell-secreted matrix metallo-proteases (MMPs), allowing gels to undergo cell-mediated remodeling. The potential of these materials in regenerating critical size bone defects in the rat cranium is discussed.

**METHODS:** Hydrogels were formed at physiologic conditions by a conjugate addition reaction as described previously [1]. Cell-induced proteolytic invasion of gels was analyzed as a function of time by measuring the radial distance that human foreskin fibroblasts (HFFs) migrated through the networks from an embedded cell cluster. Gels with different network architecture, variable adhesion peptide density and enzymatic activity were tested. Gel formulations were also analyzed in vivo as carriers of recombinant bone morphogenetic protein-2 (BMP-2). Disks were implanted in critical size (8mm ∅) calvarial defects in rats (n=5). After 5 wk implantation, animals were sacrificed, and the defect regions explanted, radiographed, and histologically processed.

**RESULTS:** HFFs cultured within adhesive and MMP-sensitive hydrogels migrated over large distances (Fig. 1A). Cell invasion completely stopped (Fig. 1B) when non-degradable peptides were incorporated, non-adhesive peptides (RDGSP) were used, or in the presence of a broad MMP inhibitor. Cell invasion rate responded to the protease substrate activity, the network architecture and the adhesion site density.

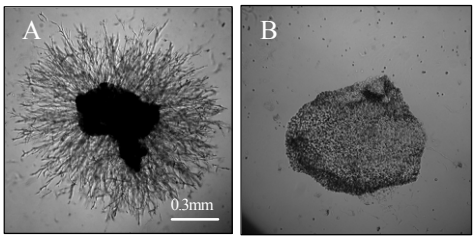


*Fig. 1: 3-D HFF invasion into adhesive and MMP-sensitive synthetic hydrogels (A). The lack of either one of these peptide signals completely impaired invasion (B).*

Bone formation in rat cranium defects. Materials containing RGDSP and MMP-sensitive peptides were fully resorbed, new bone covering the original defect area (Fig. 2B). MMP-insensitive control materials containing rhBMP-2 showed no cell infiltration and significantly less bone formation around the still intact gel implants (Fig. 2A).

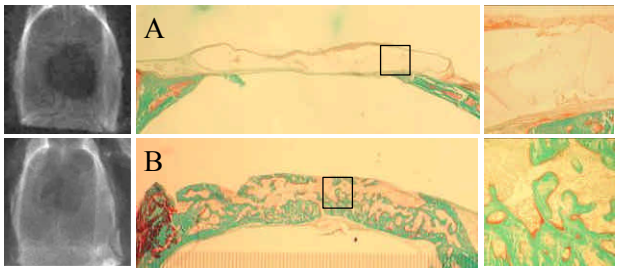


*Fig. 2: Radiographic (left) and histological (right) analysis of bone formation (green: calcium phosphate) in rat calvarial defects. Degradable and adhesive gels are completely remodeled and new bone formed at the site of the original defect (B), whereas non-degradable matrices show no cell infiltration and consequently little bone formation (A).*

**DISCUSSION & CONCLUSIONS:** We show that is possible to molecularly engineer synthetic hydrogels to render them cell-adhesive and responsive to cell-secreted proteases. This basic set of biomimetic characteristics allows the matrices to participate in pathways of morphogenesis during tissue regeneration. This new class of synthetic biomaterials may become an alternative to existing natural matrices for the reconstruction of various tissues.

**REFERENCES:** [1] M.P. Lutolf and J.A. Hubbell (2003) *Biomacromolecules* **4**: 713-722

# Osteogenesis of Human Mesenchymal Stem Cells Cultured on Silk Biomaterials: Comparison of Adenoviral Gene and Protein Delivery of Bmp2

L. Meinel[1-3], S. Hofmann[1,2], O. Betz[4], R. Fajardo[5], HP. Merkle[1], G. Vunjak-Novakovic[2], R. Langer[2], D. Kaplan[2]

*[1] Galenische Pharmazie, ETH Zürich, Winterthurerstrasse 190, CH-8057 Zurich, meinel@mit.edu, [2]Department of Biomedical Engineering, Tufts University, Medford, MA, [3]Division of Health Sciences and Technology, M.I.T. Cambridge, MA, [4]Center for Molecular Orthopaedics, Harvard University, Boston, MA [5]Orthopaedic Biomechanics Laboratory, Harvard University, Boston, MA.*

**INTRODUCTION:** Bone morphogenetic proteins (BMP) are known to drive differentiation of human mesenchymal stem cells (MSC) along the osteogenic lineage. Bone tissue engineering and gene therapy based on MSC and a silk biomaterial were combined to study osteogenesis *in vitro*. The objective of this study was the comparison of hMSC differentiation in response to locally produced BMP2 as compared to BMP2 protein supplemented to the culture medium.

**METHODS:** Cells were infected with 25 MOI of virus, encoding for BMP2 (Ad-BMP2 group). Upon seeding on 3D silk scaffolds constructs were cultured for 4 weeks and BMP2 released into the culture medium was measured by ELISA. The experiment was repeated with uninfected hMSCs (BMP2 protein group) adding the same concentrations of protein as measured in the Ad-BMP2 group.

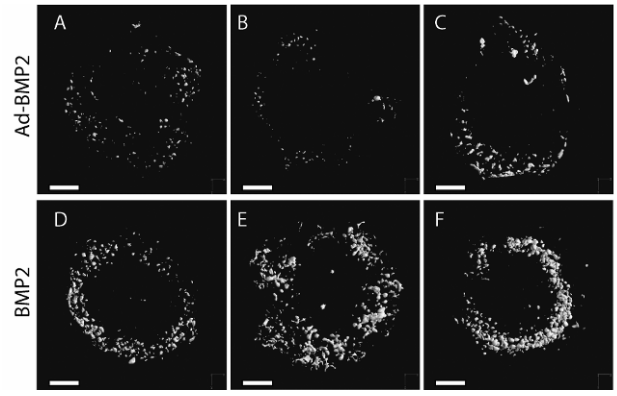


*Fig. 1: CT-images from three representative constructs with MSC transfected with Ad-BMP2 (A – C) or untransfected MSC exposed to BMP2 supplemented medium*

**RESULTS:** Infected cells displayed a transient expression of BMP2 and a transient production of BMP2 over three weeks, with peak concentrations of 40 ng/ml at day 7 of culture. Both the Ad-BMP2 MSC group and the protein BMP2 group had strong over-expression of osteopontin and bone sialoprotein. AP activity was significantly higher after week 1 in the Ad-BMP2 group as compared to the BMP2 protein group. Mineralization was significantly higher by untransfected MSC exposed to BMP2 supplemented medium as for Ad-BMP2 transfected cells (**Figure 1**).

**DISCUSSION & CONCLUSIONS:** The results of the study demonstrate that the generation of bone-like tissue in cultures of human MSC on silk scaffolds can be achieved by providing BMP2 either by adenoviral gene transfer or by direct supplementation of BMP2 protein. The tissue engineering system studied can be used as a model to study stem cell differentiation in response to growth factors in adenoviral or protein based approaches. In conclusion, viral transfer of BMP2 resulted in increased expression levels of matrix components but the quantity and distribution of mineralization was significantly less as by cells exposed to BMP2 protein directly supplemented to the medium.

European Cells and Materials Vol. 7. Suppl. 2, 2004 (pages 6-7) ISSN 1473-2262

# Lipid coating supports osteogenic differentiation of human mesenchymal stem cells

F. Feyerabend[1], M. Schossig[1], A. Slobodianski[2], P. Adamietz[2], H. Clemens[3], R. Willumeit[1]

*[1] GKSS Research Centre, Geesthacht, Germany. [2] University Hospital Eppendorf, University of Hamburg, Hamburg, Germany. [3] University of Leoben, Leoben, Austria.*

**INTRODUCTION:** The use of human mesenchymal stem cells (hmsc) is a promising approach in tissue engineering. Still there are many difficulties to overcome especially in cultivation and differentiation into different tissues. One task is the triggering of bone tissue production which should occur for bone regeneration or substitution preferably at metal implant surfaces. For a better acceptance of the implant, coating of the implant surface is one of the main interests. A promising but so far not thoroughly investigated approach is the covering of the surface by lipids. By mimicking the surface to which the cells adhere with a model membrane, the artificial character of the implant is hidden and the implant recognition by the surrounding tissue avoided [1].

The combination of implant surface modification with biological model membranes and hmsc has a high potential for bone tissue engineering. In our approach we studied the proliferation and differentiation of hmsc directly on a metal carrier with and without lipid coating. This method will be suitable for *in vitro* engineering of biohybrid bone substitution material.

**METHODS:** We used porous Ti-6Al-4V (composition in mass percent) plates as metal carrier. Covering of the surfaces was done with lipid layers, by applying 30 µl of palmitoyl-oleoyl-phosphatidyl-ethanolamine (POPE) in chloroform:methanol (80:20) on the surface of the plates and evaporation of the solvent. The characterization of the lipid layers was done by epifluorescence microscopy and scanning electron microscopy (SEM; Leo Gemini 1550 VP).

Hmsc were proliferated up to three passages in DMEM with 10 % tested FCS. 2 x $10^5$ cells were applied on the carrier and proliferated for ten days. For visualization of cell adhesion after 3 hours, 3 and 7 days by SEMthe samples were fixed in 2.5 % glutaraldehyde over night, stained with 1 % osmium tetroxide for two hours and dehydrated in aequous alcohol series. Afterwards they were critical point dried (Baltec CPD 30). The osteogenic differentiation of hmsc was induced by the addition of 10mM β-glycerolphosphat, 5mM ascorbic acid-2-phosphate, $10^{-7}$M dexamethasone and $10^{-7}$M 1α,25-dihydroxyvitamin $D_3$ for three weeks. Samples were analysed by epifluorescence microscopy using DAPI- and osteocalcin-staining on a Leica CTR MIC.

**RESULTS:** Cell adhesion on coated and uncoated carriers showed no differences. After three hours the adhered cells displayed a rounded phenotype. Afterwards the cells spread to a large extent on the carrier. Already after three days the carrier was completely covered with a dense layer of large hmsc, which did not change after seven days (*Figure 1*).

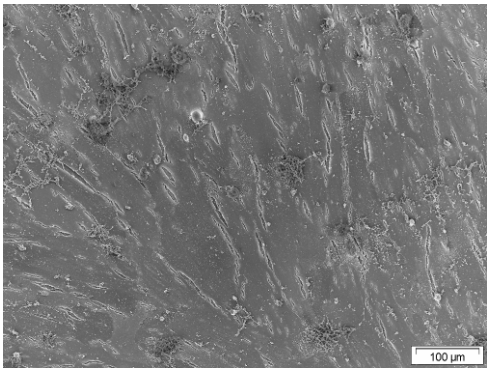


*Fig. 1: Example for cell adhesion after three days of proliferation on the porous Ti-6Al-4V-carrier. SEM-image, 1000x magnification.*

In spite of proliferation, were no differences were visible, the osteogenic differentiation of hmsc showed clear differences. On the uncoated carriers the cells were equally distributed and showed no signs of osteogenic differentiation (*Figure 2*). On carriers coated with POPE the cells accumulated and bone formation, measured by osteocalcin, was visible (*Figure 3*).

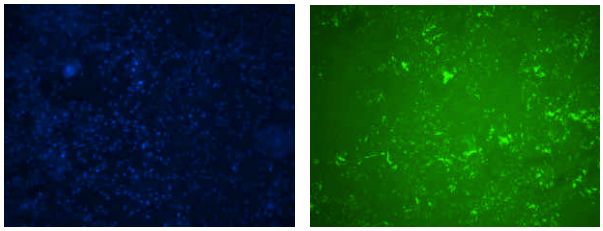

*Fig. 2: DAPI- (left) and osteocalcin- (right) immunostaining of hmsc after three weeks on*

*native carriers. Cells are equally distributed, no bone formation is visible. 400x magnification.*

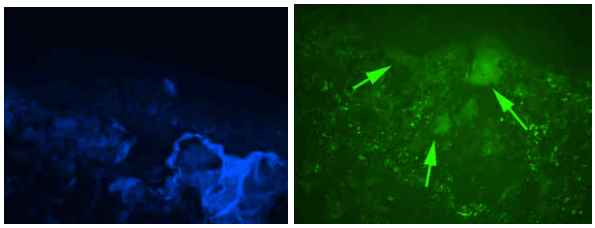

*Fig.3: DAPI- (left) and osteocalcin- (right) immunostaining of hmsc after three weeks on POPE-coated carriers. Cells are accumulated and show bone formation (arrows). 400x magnification.*

**DISCUSSION & CONCLUSIONS:** We used a simple system to modify implant surfaces with lipid layers. The combination of this coating with the culturing of hmsc on the carrier shows a support of osteogenic differentiation, in contrast to native carriers. Despite of other studies, in which a higher surface roughness (0,8-1,9µm) of cpTi-materials increased bone nodule formation [2,3], we found no osteogenic differentiation on the porous Ti-6Al-4V. We suggest that this difference is caused by an influence of the carrier material on the adhered cells, which can be excluded by application of the lipid. Influences of wear debris on hmsc were already described [4] and the possible cytotoxicity of vanadium and aluminium can also be a reason for this observation [5]. So we found a promising approach of ossification on artificial surfaces.

Further studies will concentrate on the quantification of bone formation and on the biochemical characterization of human mesenchymal stem cells during proliferation.

**REFERENCES:** [1] R. Willumeit, F. Feyerabend, H. Kamusewitz, M. Schossig and H. Clemens (2003) *Mat.-wiss. u. Werkstofftech.* **34**:1084-93. [2] A.L. Rosa and M.M. Belotti (2003) *Braz Dent J* **14**(1): 16-21. [3] L. Postiglione, G. Di Domenico, L. Ramaglia, S. Montagnani, S. Salzano, F. Di Meglio, L. Sbordone, M. Vitale, and G. Rossi (2003) *J Dent Res* **82**(9):692-696. [4] M.L. Wang, L.J. Nesti, R. Tuli, J. Lazatin, K.G. Danielson, P.F. Sharkey, R.S. Tuan (2002) *J. Orth. Res.* **20**: 1175–1184. [5] Y. Okazaki, S. Rao, Y. Ito, T. Tateishi (1998): *Biomaterials* **19**(13):1197-215.

**ACKNOWLEDGEMENTS:** The authors wish to thank the group of Andreas Guse, Department of medical biochemistry and molecular biology, University Hospital Eppendorf and Reinhard Bredehorst, Department of Biochemistry and Molecular Biology, University of Hamburg for expert technical assistance and helpful discussions.

# Effect of biochemical factors on the neogenesis of ligament tissue.

Fawzi-Grancher S, Slimani S, Vaquette C, Wang X, Muller S

*Group Mechanics and Cell and Tissue Engineering, LEMTA-UMR 7563 CNRS, Faculté de Médecine, Plateau de Brabois, 54500 Vandoeuvre-lès-Nancy, France.*

## INTRODUCTION

Ligament healing is a complicated process which consists of cell proliferation and migration, together with the synthesis and deposition of ligament components. Its seems to be affected by both ligament specific and environmental factors. Ligament–specific factors include cell properties responses to growth factors and proliferation, (1-3) and environmental factors include biomechanical forces. The aim of our work was to define the biochemical conditions for *in vitro* reconstruction of ligament tissue. Different growth factors are known to affect biological responses such as cell proliferation, chemotaxis, matrix synthesis (4) and the ecretion of other growth factors. In the present study, we analysed the effects of two growth factors (PDGF-AB, TGF-β1) on the proliferation and the collagen synthesis of fibroblast *in vitro.*

## MATERIALS AND METHODES

Two types of cells were used: CRL.2703 fibroblast cell line (ATTC N°.2584882), and human anterior cruciate ligament (ACL), grown in DMEM with 10% foetal bovine serum. Cells were seeded on different surfaces (glass, silicone membrane, coated or not with 1% gelatin), and treated with one of the following growth factors: PDGF-AB at (1, 5, 10, 50 ng/ml), or TGF-β1 at (0.1, 0.5, 1, 5, 10ng/ml). After 3 days culture, cell viability was performed using the MTT colorimetric assay (tetrazolium salt 3-(4,5-dimethyl-2-thiazolyl)-2,5-diphenyltetrazolium bromide). Absorbance at 570nm was measured. Cell proliferation was detected by labelling cells with propidium iodide (nucleus dye). Cell cycle based on DNA content was analyzed by flow cytometer (FACscan Becton- Dickinson, USA). Synthesis of type I and III collagen was observed by confocal microscopy (SP2-Leica, D) and quantified by western blotting. For immunofluorescence assay the cells were labeled with a primary antibody (rabbit anti-collagen I or III) followed by a second antibody (Alexa Fluor-488 conjugated goat anti-rabbit, Molecular Probes, USA).

## RESULTS – DISCUSSION

**PDGF-AB and cell proliferation**

Our experiments show that PDGF-AB had the maximal stimulatory effect on cell proliferation at 10ng/ml on different surfaces. Higher concentration (50ng/ml) of this growth factor had almost the same effect. As shown in Fig.1, the percentage of cells in S-phase and G2/M phase increased when the cells were treated with 10ng/ml PDGF-AB in comparison with the control.

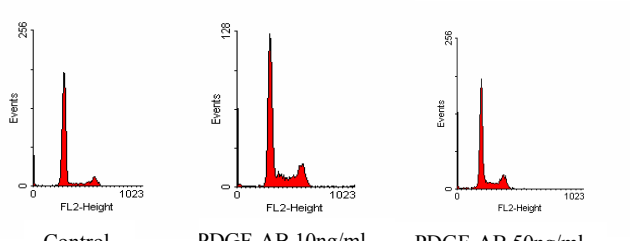


Control PDGF-AB 10ng/ml PDGF-AB 50ng/ml

Fig.1: Flow cytometric analysis of cell cycle, after 72 hours of PDGF-AB treatment.

**TGF-B1 and collagen synthesis**

Collagen synthesis increased when the cells were treated with TGF-β1 at 10ng/ml in comparison with the control.

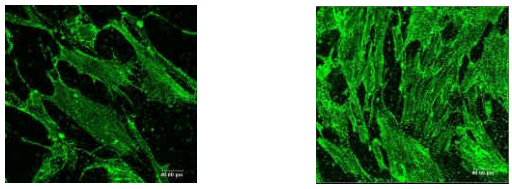

Control TGF-β1, 10ng/ml

Fig.2: Three dimensional image of collagen type III matrix by confocal microscopy.

## CONCLUSIONS

These results allow us to optimise the biochemical conditions for in vitro culture of ligament tissues. Actually we are studying the effect of cyclic stretching (5-20%) on the cells with the help of a device developed in our laboratory.

## REFERENCES

[1] Clark RAF (1995): Collagen matrices attenuate the collagen- synthetic response of cultured fibroblasts to TGF-β. *J cell Sci 108*: 1251-61.

[2].Murphy PG (1994): Influence of exogenous growth factors on the synthesis and secretion of collagen type I and III by explants of normal and healing rabbit ligaments. *Biochem Cell Biol 72*: 403-9

[3].McGee GS, Davidson JM (1988): Recombinant basic fibroblast growth factors accelerates wound healing. *J Surg Res 45*: 145-53.

[4].Mustoe TA, Pierce GF (1987) Accelerate healing of incisional wounds in rats induced by TGF-β.*Science237:* 1333.

# Peptide-functionalized Protein-resistant Adlayers on Titanium Surfaces: An Approach for Producing Cell-selective Biomaterial Surfaces

M. Schuler[1], G.R. Owen[2] S. Tosatti[1], D.M. Brunette[2] and M. Textor[1]

*[1]Dept. of Materials, Federal Institute of Technology (ETH), Zurich, Switzerland. [2]Dept. of Oral Biological & Medical Sciences, University of British Columbia, Vancouver, BC, Canada.*

**INTRODUCTION:** Osteoblasts are sensitive to surface microtopography, exhibiting a more differentiated morphology on rougher surfaces. Surface effects are mediated through cell surface receptors (e.g. integrins or transmembrane proteoglycans) that recognize and bind to a specific motif in cell attachment proteins. Thus, not only the topography but also the (bio)chemistry of a surface plays an important role. Recently, we demonstrated that the assembly of peptide-functionalized poly-L-lysine-*g*-poly(ethylene glycol) (PLL-*g*-PEG) polymers on titanium surfaces is a promising approach for manufacturing protein-resistant surfaces presenting peptide moieties at controlled surface density to interact directly with integrin cell receptors[1].

**METHODS:** We investigated osteoblast cell response (morphology and motility) to smooth and rough titanium surfaces that were modified with different amounts of RGD-functionalized PLL-*g*-PEG adlayers. Both rough SLA dental implant surfaces (sand-blasted, large-grit, acid etched; from Institut Straumann AG, Switzerland) and smooth Si wafer coated with a thin film of $TiO_2$ were used to study the effect of topography.

**RESULTS & DISCUSSION:** Investigations of cell attachment and adhesion indicated that osteoblasts adhere preferentially to rough compared to smooth surfaces. SLA surfaces coated with PLL-*g*-PEG showed reduced cell numbers but a high degree of osteoblast differentiation[1].

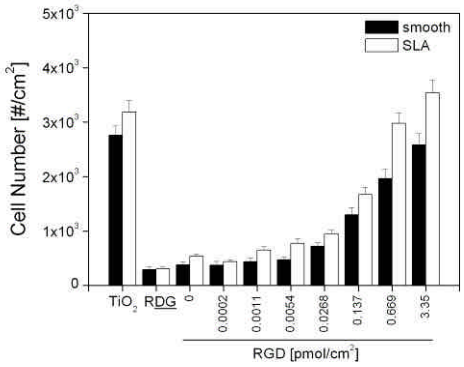


*Fig. 1: Average cell number (cells per cm²) as a function of peptide surface density for three independent series of smooth and SLA (rough) titanium topographies. Titanium ($TiO_2$), RDG (inactive peptide) and 0 pmol/cm² RGD-peptide surface concentration (= non-functionalized PLL-g-PEG polymer) served as controls.*

An increase of the amount of RGD-peptide modulates osteoblast response, resulting in increased cell attachment, spreading (increase of footprint area) and proliferation, but decreased differentiation (e.g. reduced TGF-β1 expression)[1].

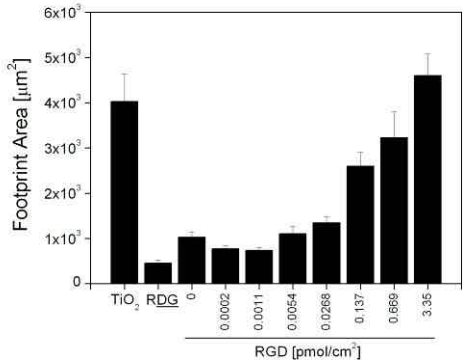


*Fig. 2: Footprint area per cell (average of 21 single cells) on smooth titanium surfaces as a function of RGD-peptide surface density. Titanium ($TiO_2$), RDG (inactive peptide) and 0 pmol/cm² RGD-peptide surface concentration (= non-functionalized PLL-g-PEG polymer) were used as control surfaces.*

These results suggest that cell shape and cell differentiation are strongly correlated.

**OUTLOOK:** New PLL-*g*-PEG polymers with covalently linked heparin-binding peptides (KRSR[2] and FHRRIKA[3]) have been synthesized. Preliminary experiments on cell proliferation (WST-1 assay) with MG63 osteoblast - like cells suggest that these peptides increase the rate of proliferation.

**REFERENCES:** [1]S. Tosatti, *et al*., *J Biomed Mater Res*, 68(3): 458-472, 2004. [2]K.C. Dee *et al*., *J Biomed Mater Res.*, 40(3): 371-77, 1998. [3]K. E. Healy *et al*., *Biomaterials*, 17(2):195–208, 1996.

**ACKNOWLEDGEMENT:** This project was supported by a grant from the ITI Foundation for the Promotion of Oral Implantology, Switzerland.

# Maintenance of cancellous bone explants *ex vivo*

CM. Davies, P. Jäggi, RG. Richards

*AO Research Institute, Davos, Switzerland.*

**INTRODUCTION:** The Zetos culture system[1] has potential to keep cancellous bone tissue viable *ex vivo*[2] through the use of unique chambers and a loading device that allows the tissue to remain in its natural 3D milieu. Bone and marrow cells constantly interact with each other and with migratory cells and the extracellular matrix. This type of niche has never been reproduced *in vitro*. Tissue engineering methods have been aimed towards recreating this microenvironment in order to produce a possible means to fill bone defects caused by tissue trauma or disease. This culture system may be used as a means of maintaining tissue for re-implantation into patients or with different bone substitutes to evaluate their potential as bone replacements, reducing the amount of animal experimentation conducted.

**METHODS:** Human femoral heads (Ethic Commission Graubünden (18/02) approval), distal ovine femora or distal bovine metacarpals were excised and cut into 9mm thick sections with the use of an Exakt 300 band saw. Cores 10mm in diameter were bored from the sections with a specially produced fluted, hollow diamond-tipped drill and cut parallel to 5mm with a Leica annular saw. Bone cores were inserted inside the diffusion chambers and left to settle at 37°C for 24 hours. Bone cores were loaded daily in the loading device for 300 cycles at 1Hz with a walking or jumping waveform, giving each core the equivalent of 4,000 µstrain (maximum and minimum compression of 20 µm and 5 µm respectively). Both fresh (at explantation) and bone cores from the Zetos culture chambers (day 15) were fixed in 70% ethanol, before being dehydrated through an ethanol series. Samples were embedded in Technovit 9100, polymerised at –20°C for histological and immunohistochemical evaluation[3]. $^{3}$H-glycine was placed in the media for 24 h allowing incorporation into newly synthesised proteins. Media and tissue proteins were harvested and analysed for radioactivity.

**RESULTS:** $^{3}$H-glycine was detected in protein through SDS-page and Western blot analysis as well as autoradiography of embedded sections, demonstrating cell viability after 15 days in culture. Histological sections showed osteoblasts had laid down collagen fibres to produce osteoid seams; living osteoclasts in Howship's lacunae were also seen. Bone marrow and osteocytes appeared well preserved. Very little necrotic tissue was observed. Noncollagenous proteins such as osteopontin, osteonectin and osteocalcein, as well as procollagen Type I and RankL were localised through immunohistochemical labelling of sections.

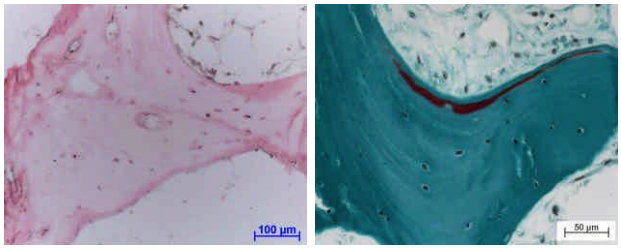


***Fig. 1:*** *Left image- protein production in osteocytes and soft tissue 15 days post-explantation; right - osteoid seam from bovine tissue 30 days post-explantation.*

**DISCUSSION & CONCLUSIONS:** Culture of cancellous bone explants within the loaded Zetos system maintains bone cells viable for at least 15 days. Conventional organ culture techniques usually suffer from extremes of too much oxygen at the surface and too little oxygen in the centre causing tissue necrosis. By allowing the bone cells to be cultured in its near to natural microenvironment this system could overcome the barriers of homogeneous cell seeding and scaffold composition associated with tissue engineering and other bioreactor systems. The system also has potential for studying bone remodeling in normal and osteoporotic animal or human bone, bone bio-mechanics, and the effects of drugs, hormones or growth factors on cancellous bone, making it an essential laboratory aid in the future.

**REFERENCES:** [1]Jones D.B., Broeckmann E., Pohl T., and Smith E.L. (2003). Development of a Mechanical Testing and Loading System for Trabecular Bone Studies for Long Term Culture. *Eur Cell Mater* **5**: 48-60 [2]Clarke M.C.H., Savil J., Jones D.B., Nobel B.S., Brown S.B. (2003). *J. Cell Biol.* **160**:4 577-587. [3]Yang R. et al., (2003) Immunohistochemistry of matrix markers in Technovit 9100 New®-embedded undecalcified bone sections. *Eur Cell Mater* (**6**) 57-71.

**ACKNOWLEDGEMENTS:** Funded by the 3R Foundation grant # 78/01. The authors wish to thank to Dr Thomas Perren for supplying human tissue

European Cells and Materials Vol. 7. Suppl. 2, 2004 (pages 11-12) ISSN 1473-2262

# Chitosan Coated Plga-Microspheres - A Modular System for Targeted Drug Delivery

S. Fischer, C. Foerg, H.P. Merkle, B. Gander

*Institute of Pharmaceutical Sciences, ETH Zürich, Switzerland*

**INTRODUCTION:** Microparticulate drug and antigen delivery systems are of considerable therapeutic interest. Currently, this field is dominated by the use of poly(lactide-*co*-glycolide) (PLGA) type microspheres (PLGA MS). However, because of the deficiency of suitable functional groups on their surface, conventional PLGA MS lack the possibility of surface modifications for specialized targeting or biomimetic purposes. Such modifications are thought to improve greatly the effectiveness of microparticulate delivery systems.

To solve this problem, we propose a solvent extraction process to coat conventional PLGA particles by means of a biocompatible cationic polyelectrolyte, e.g. chitosan, using a static micromixer. This one-step procedure can easily be performed aseptically. In a second step the functional groups of the hydrocolloidal chitosan shell provide the possibility to bioconjugate various bioactive ligands, e.g. sugars, antibodies or peptides, to the surface via covalent coupling. Such modular synthetic carriers may pave the way to targeted delivery of microparticulate drug delivery systems to specialised cells, e.g. phagocytic antigen-presenting cells[1].

**METHODS:** PLGA microspheres were prepared by solvent extraction using a static micromixer[2]. The polyelectrolyte shell was formed by incorporating chitosan of different molecular weights into the $W_2$-phase. The surface charge of the resulting particles was assessed by zeta potential measurements. The particle size distribution was determined by laser light scattering using a Fraunhofer diffraction model. N-hydroxysuccinimidyl-poly(ethylene glycol)-biotin (NHS-PEG-biotin) served as model ligand and was covalently linked to the chitosan's free amino groups on the particle surface under mild conditions. To assess the presence of PEG-biotin on the particles´ surface, particles were incubated with a fluorescent streptavidin conjugate and visualized by confocal laser scanning microscopy (CLSM). To account for false-positive results due to adsorption of the fluorescent marker, chitosan-free PLGA particles were treated the same way and compared to chitosan-coated particles. Particle morphology was analysed by scanning electron microscopy (SEM).

**RESULTS:** The zeta potential of the microparticles increased with higher chitosan concentrations in the external aqueous $W_2$ phase (***Fig. 1***). The mean diameter was well reproducible and adjustable within the range of approx. 1 to 10 µm.

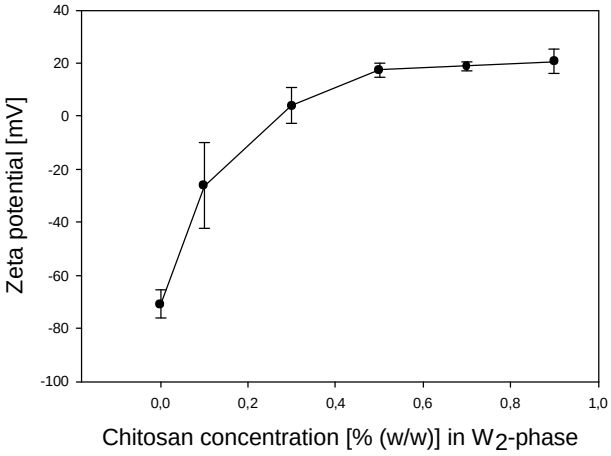


*Fig. 1: Zeta potential [mV] of chitosan-modified microspheres in 1 mM KCl as a function of chitosan concentration [% (w/w)] in the $W_2$ phase.*

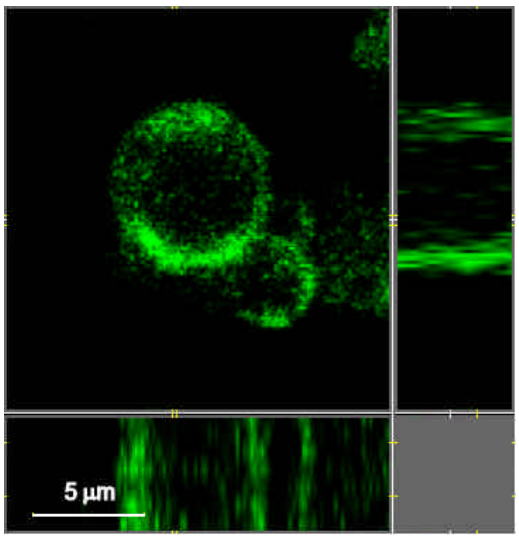


*Fig. 2: Confocal laser scanning micrograph of chitosan coated PLGA microparticles after coupling with PEG-biotin and incubation with fluorescent streptavidin*

As proof-of-concept for the accessibility of the primary amino groups of the chitosan coatings for covalent conjugation purposes, PEG-biotin was coupled to the surface. Subsequent incubation with fluorescent streptavidin and inspection of the particles by CLSM demonstrated the fluorescent character of the surface modification and the principal proof-of-concept of our approach (***Fig. 2***). The chitosan coated microparticles were spherical and showed smooth surfaces without pores as assessed by SEM (not shown).

**DISCUSSION & CONCLUSIONS:** The increase in zeta potential from –70.8 mV (chitosan-free PLGA particles) to +20.5 mV with increasing chitosan concentrations in the $W_2$-phase used for particle preparation strongly suggests that the polycationic chitosan was firmly adsorbed to the particle surface. This finding was confirmed by X-ray photoelectron spectroscopy (data not shown). The coupling of biotin via a NHS-PEG-linker showed that the amino groups of chitosan represent suitable sites for covalent bioconjugation of different ligands. The process allows the production of particles with a mean diameter between 1 and 10 μm, a useful size range for the phagocytosis by phagocytes like dendritic cells or macrophages.

Preparation of these novel modular micro-particulate delivery systems is straightforward. Particle size and surface characteristics can be easily adjusted and controlled, and drugs and antigens can be readily embedded. Thus, these novel carriers may serve as multifunctional delivery system for various applications. Its applicability as a modular delivery platform will be further investigated.

**REFERENCES:** [1] S. Faraasen, J. Vörös, G. Csúcs, M. Textor, H.P. Merkle, E. Walter (2003) *Pharm Res* **20**:237-246. [2] S. Freitas, A. Walz, H.P. Merkle and B. Gander (2003) *J Micro-encapsulation* **20**:67-85

**ACKNOWLEDGEMENTS:** The authors would like to thank Dr. Christina Haerdi-Landerer for the preparation of the scanning electron micrographs. We also thank Sabine Ellenberger for her valuable technical assistance.

# Engineering Cartilage-Like Tissue from Human Mesenchymal Stem Cells on Silk Scaffolds

S. Hofmann[1,2], D. Kaplan[2], G. Vunjak-Novakovic[3], HP. Merkle[1], R. Langer[3], L. Meinel[1-3]

*[1] Galenische Pharmazie, ETH Zürich, Winterthurerstrasse 190, CH-8057 Zurich, meinel@mit.edu, [2]Department of Biomedical Engineering, Tufts University, Medford, MA, [3]Division of Health Sciences and Technology, M.I.T. Cambridge, MA.*

**INTRODUCTION:** Scaffold geometry and stability critically determine the quality of engineered tissues. Silks have unique mechanical properties, rivaling synthetic fibers such as Kevlar in tensile strength. This study evaluates the quality of engineered cartilage from human mesenchymal stem cells (MSC) cultured on silk scaffolds as compared to other established protein substrates.

**METHODS:** MSCs were seeded on silk, collagen, and crosslinked collagen scaffolds, and cell proliferation (PicoGreen DNA Assay), sulphated glycosaminoglycan (GAG) deposition (spectrophotometrically by dimethylmethylene blue dye binding) and gene expression of aggrecan and collagen 2 (RT-PCR) were analyzed every third day for a period of 3 weeks. Samples were further analyzed histologically (H&E, safranin O) and immunohistochemically (collagen 2).

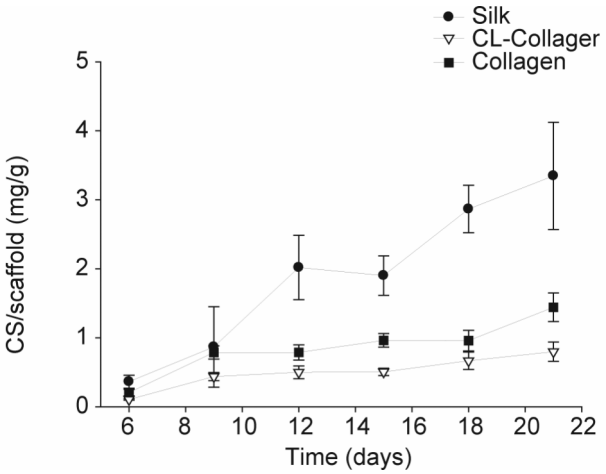


*Fig. 1: Deposition of glycosaminoglycan on silk, cross-linked collagen and collagen scaffolds*

**RESULTS:** GAG deposition was significantly higher on silk scaffolds (3 µg/mg wet weight) as compared to collagen scaffolds (1 µg/mg) after 3 weeks, with a substantial degradation of the non-crosslinked collagen scaffold (**Figures 1, 2 A-C**). The cartilage matrix was rich in collagen 2 (**Figure 2 D-F**), a finding corroborated on the transcriptome levels for all scaffolds. Aggrecan over-expression was observed over time, peaking at day 8, particularly on silk scaffolds (80 fold as compared to MSC prior to seeding).

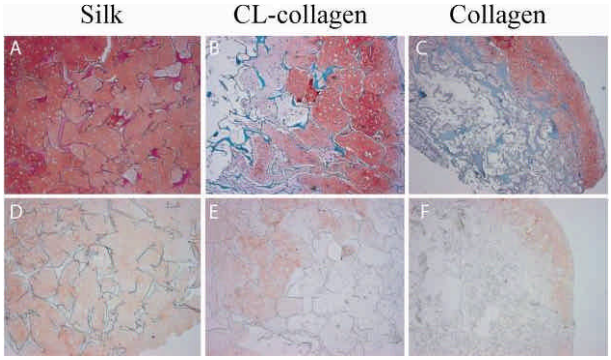


*Fig. 2: Cartilage-like tissue deposition on silk (left), cross-linked collagen (center), and collagen (right) scaffolds. Upper panels (A–C) stained with Safranin O, lower panels (D-F) show deposition of type 2 collagen by immunohistochemistry*

**DISCUSSION & CONCLUSIONS:** In conclusion, the engineering of cartilage-like tissue from human MSC on silk scaffolds was superior to collagen materials. Together with their unique mechanical properties, silks are excellent biomaterials for cartilage tissue engineering.

European Cells and Materials Vol. 7. Suppl. 2, 2004 (pages 14-15) ISSN 1473-2262

# Regulating Myoblast Phenotype through Controlled Alginate Scaffold Degradation: A Delivery Vehicle for Skeletal Muscle Tissue Engineering

T. Boontheekul[1], and D.J. Mooney[1,2,3]

*[1]Department of Chemical Engineering, [2] Biomedical Engineering, [3]Biologic & Material Science, Ann Arbor, MI, 48109, USA*

**INTRODUCTION:** Skeletal muscle tissue engineering is a new therapeutic strategy for treatment of muscle loss or deficiency (e.g. muscular dystrophies). In general, skeletal muscle develops by proliferation and differentiation of mononucleated muscle precursor cells (myoblasts), followed by fusion of these cells into multinucleated myotubes, and finally alignment of tubes into fibers [1]. Tissue engineering aims to mimic this process by transplanting myoblasts using appropriate carriers.

A key issue in tissue engineering is to mimic specific functions of the native ECM to guide new tissue formation. Biomaterial vehicles are being designed to present signaling molecules, and regulate cell phenotype [2]. It is widely believed that these materials should degrade over time to provide new space for tissue development; however, the role of material degradation on cellular function has not been extensively investigated [3].

This study addressed the hypothesis that the degradation rate of materials will control myoblast phenotype. Alginate, a naturally derived copolymer, has been utilized as a scaffold for skeletal muscle tissue engineering due to its biocompatibility and ability to form gels with a gentle gellation process. Coupling adhesive peptide sequence to alginate chains has provided a direct linkage between myoblasts and the alginate. This peptide-modified alginate has shown an ability to regulate myoblast proliferation and differentiation in 2-dimensional cell culture [4]. Recently, combining partial oxidation on alginate chains prior to gel formation with the utilization of a bimodal molecular weight distribution (binary system) has provided a means to control the degradation of alginate gels. We propose to utilize this material system to study the effect of alginate degradation on myoblast phenotype in 3-dimensional culture.

## METHODS

**Alginate modification:** Sodium alginate powder rich in GG-blocks ($M_w$ = 2.7 × $10^5$ g/mol,) was used as the high molecular weight component (HMW) to form gels. Low molecular weight alginate ($M_w$ = 5.3 × $10^4$ g/mol, LMW) was obtained by gamma (γ)-irradiating HMW with a cobalt-60 source for 4 hours at a γ-dose of 5.0 Mrad. Alginates (both HMW and LMW) were partially oxidized to a theoretical extent of 1% of sugar residues with sodium periodate, and an oligopeptide ($G_4$RGDSP) was subsequently coupled at an average density of 3.4 mM peptide/mole of alginate monomer, using carbodiimide chemistry.

**Cell culture and cell immobilization:** C2C12 mouse myoblasts were cultured in growth media (DMEM supplemented with 10% FBS and 1% penicillin/streptomycin) and maintained subconfluent prior to experiments. Myoblasts were then harvested and mixed with the 3 alginate gel types described below. Alginate/cell mixtures (at the density of 20×$10^6$ cells/ml alginate) were mixed with $CaSO_4$ slurry, cast between two glass plates separated with 1 mm spacers, and allowed to gel 30 or 40 minutes for unary and binary systems, respectively. Following gelling, alginate/cell disks were punched out using a 4.5 mm puncher, and cultured with growth medium in spinner flasks.

**Assays:** Alginate disks were harvested and stained with a tetrazolium salt (MTT) to determine myoblast viability. Cell proliferation was assessed by incubating with $^3$H-thymidine overnight, dissolving the gels with EDTA/PBS and counting the cell-associated radioactivity using a scintillation counter. Cell counts were performed by dissolving the gels with EDTA/PBS, incubating with trypsin, and counting cells using a Coulter counter. In addition, myoblasts were visualized by staining the actin cytoskeletal with Oregon Green Phaloidin. The alginate disks were mounted onto coverslips and imaged with a BioRad Radiance 2000 confocal system.

**RESULTS:** C2C12 myoblasts were encapsulated in three different gels: 1. partially oxidized binary gels (LMW: HMW = 1:1, fastest degradation rate), 2. partially oxidized unary gels (HMW, intermediate degradation rate), and 3. non-oxidized unary gels (HMW, no degradation) to investigate the effect of degradation on cell phenotype.

Cell viability was first determined following cell encapsulation and culture. Alginate modification and gelling did not lead to cytotoxicity, and the chosen culture conditions provided sufficient oxygen and nutrient transportation up to 3 weeks in all three gel types, as shown by dark purple crystal produced by mitochondria of viable cells with the MTT assay (data not shown). Next, $^{3}$H-thymidine incorporation illustrated that cells could proliferate in all gel types (Fig. 1). The proliferation was highest in non-oxidized unary gels, followed by partially oxidized unary, and partially oxidized binary gels, respectively. The reliability of thymidine incorporation assay in this culturing system was confirmed by examining myoblasts in differentiation medium. As expected, the thymidine incorporatation was arrested in all gel types (Fig. 1), as myoblasts typically withdraw from cell cycle when cultured in low serum containing medium. The thymidine incorporation data was consistent with cell count data (not shown), as the cell numbers increased in the order of non- oxidized unary gels, partially oxidized unary, and partially oxidized binary gels, respectively. In fact, the cell number in partially oxidized binary gels on day 5 decreased from the initial values.

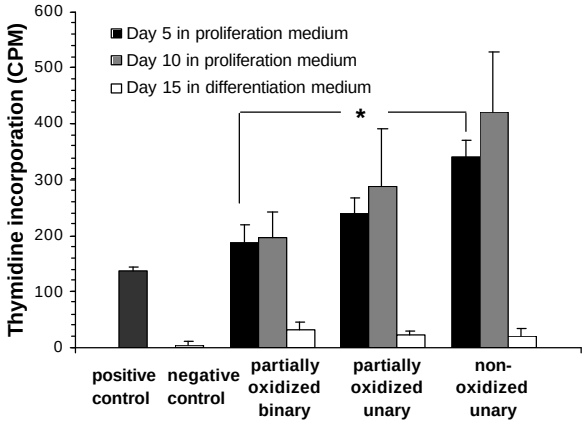


*Fig. 1: Thymidine incorporation of myoblasts encapsulated in three different alginate gels. Positive and negative control represent proliferating myoblasts cultured on 2-dimensional alginate gels and blank alginate, respectively. Experimental values are reported as means ± SD. * denotes a statistically significant difference (p-value < 0.05).*

Myoblast morphology was visualized by staining the actin cytoskeleton to determine if cells differentiated by fusion into multinucleated myofibers. Myoblasts cultured in degradable gels (partially oxidized binary and unary gels) spread and fused on the top of the gel surface by day 7 (Fig.2). This result indicates the decrease in cell number at day 5 resulted from this cell fusion. On the contrary, the cells in non-oxidized gels maintained a round morphology throughout the gel volume. No spread or fused cells were observed in these non-degradable gels.

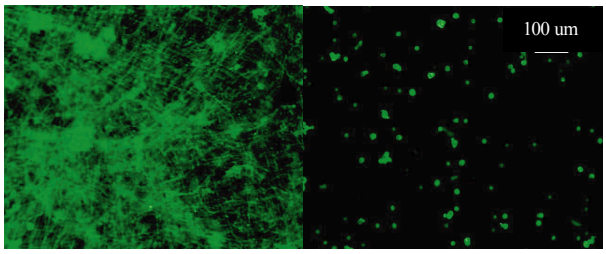


*Fig. 2: Actin visualization (green) highlights fusing myoblasts on partially oxidized binary and unary gels (left) and round-shaped myoblasts in non-oxidized gels (right).*

**DISCUSSION & CONCLUSIONS:** The results of this study indicate the degradation rate of the encapsulation material dramatically influenced myoblast phenotype. Cells immobilized in degradable gels (partially oxidized binary and unary gels) illustrated lower proliferation than those in non-degradable gels (Fig.1). Cells in these degradable gels exited the cell cycle, committed to the differentiation pathway, and fused (Fig. 2). This response may be due to the mechanical stiffness reduction upon gel degradation, which allows the cells to spread, migrate, and fuse. In contrast, the non-degradable gels maintained a high stiffness over time, and this likely prevented cell spreading and cell-cell interaction. The cells still proliferated in these gels, likely due to the high proliferative nature of these C2C12 cells.

This study provides a cell-delivery vehicle for skeletal muscle tissue engineering, and emphasizes the critical role of material degradation in regulating cellular behaviour. This latter result may be applied to a broad range of other tissue/cell types as well.

**REFERENCES:** [1] M.D Grounds, J.D White, N. Rosenthal et al (2002) *J Histochem Cytochem* **50:** 589-610 [2] M.P Lutolf, F.E Weber, H.G Schmoeker, et al (2003) *Nat Biotechnol* **21**:513-8 [3] E. Alsberg, H.J Kong, Y. Hirano, et al (2003) *J Dent Res* **82**: 903-8 [4] J.A Rowley, D.J Mooney (2002) *J Biomed Mat Res*, **60**: 217-23

**ACKNOWLEDGEMENTS:** The authors gratefully acknowledge NIDCR/NIH for financial support (RO1 DE13349), as well as Royal King Anandamahidol foundation (Thailand) for a graduate fellowship to TB.

European Cells and Materials Vol. 7. Suppl. 2, 2004 (pages 16-17) ISSN 1473-2262

# Novel Biodegradable Nerve Conduits for Peripheral Nerve Regeneration

L.A.Pfister[1], T.Christen[2], H.P.Merkle[1], M.Papaloïzos[3], B.Gander[1]

*[1] ETH Zurich, Zurich, Switzerland. [2] CHUV, Lausanne, Switzerland.*
*[3] Center for Hand Surgery and Therapy, CH8, Geneva, Switzerland.*

**INTRODUCTION:** Regeneration of peripheral nerves after axotomy remains a clinical challenge, and functional outcome is often disappointing, especially when there is a gap between the nerve stumps. Nerve conduits (NC) that guide the axons into the distal nerve stump are a promising alternative to improve this situation, obviating the need to harvest autologous nerve grafts with potential neuroma formation and morbidity at the donor site. Furthermore, the properties of NC can be tailored to provide an optimal environment for peripheral nerve regeneration. An ideal NC should 1) be biocompatible, 2) maintain its structure for at least 3 months *in vivo*, 3) degrade after healing to prevent long term irritation, 4) be flexible, i.e., having a modulus in the range of nerve tissue to prevent compression on the regenerating nerve, and 5) be porous to ensure nutrients supply.

In this study, novel biodegradable NC were developed that meet the above mentioned requirements. The NC were made of polyelectrolyte complexes of the natural occurring polysaccarides alginate and chitosan, which form physically cross-linked hydrogels due to their opposite charges in aqueous solution. *In vivo*, the complexes slowly degrade by ion substitution and enzymatic degradation.

**METHODS:** NC were produced by spinning mandrel technology. Suspensions of 1% polyelectrolyte complex of alginate and chitosan were deposited onto a spinning steel mandrel from a syringe. The solvent was evaporated under a stream of air. Swelling behaviour was assessed by placing dry NC in PBS and measuring the inner and outer diameters from successively taken micrographs. Porosity was confirmed by scanning electron microscopy (SEM) and confocal laser scanning microscopy (CLSM), and the mechanical properties measured on films by oscillating shear rheology. The *in vivo* behaviour of the NC was tested in a 3 mm gap in the rat peroneal nerve, which was bridged with a 6 mm long NC. NC biocompatibility and integrity were assessed after 2 and 4 weeks.

**RESULTS:** The NC swell rapidly and water uptake was up to 90 % by weight. Interestingly, swelling proceeded almost exclusively towards the outside, and the inner diameter was maintained at approx. 1.2 mm, the dimension of the mandrel onto which the suspension was molded. This advantageous swelling assured an open lumen of the NC (Fig 1). CLMS and SEM microscopy showed a high, open porosity favourable for nutrients and growth factor supply.

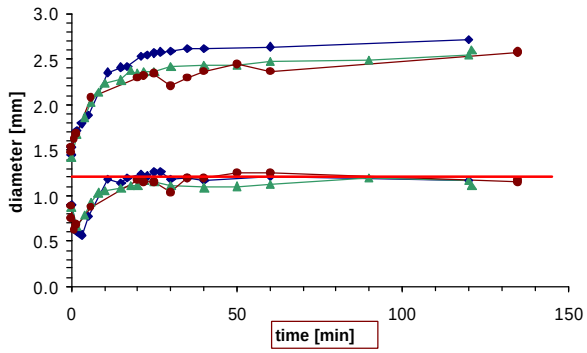


*Fig. 1: Inner (lower curves) and outer diameter (upper curves) of the NC upon swelling in PBS. The horizontal red line denotes the initial diameter of the mandrel.*

Rheology of alginate/chitosan films revealed a storage modulus of 52 kPa, which is below values reported in literature for nerve tissue[1] (66 to 266 kPa, calculated from the Young's modulus) (Fig. 2). However, preliminary *in vivo* data after 4 weeks demonstrate that the NC possess sufficient mechanical stability to maintain their shape. In addition, only slight inflammation was seen. The lumen of the conduit was seeded with inflammatory cells, and a small fibrous capsule surrounded the NC.

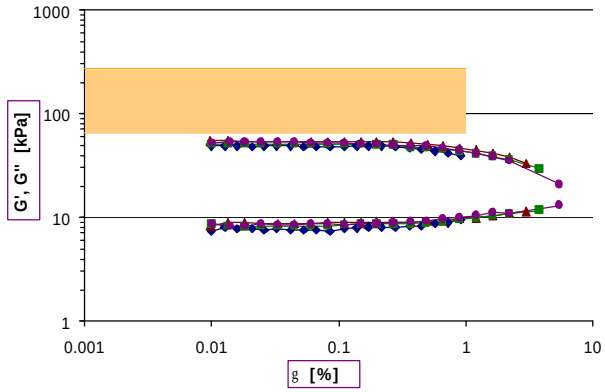


*Fig. 2: Storage (upper curves) and loss modulus (lower curves) of alginate/chitosan films at 37°C and 10 Hz. For comparison, the orange bar denotes values from literature for the storage modulus of soft nerve tissue.*

**DISCUSSION & CONCLUSIONS:** The developed biodegradable NC exhibited high swelling and water uptake, which created a porous scaffold with open porosity that should ensure exchange of nutrients. The swollen material of the conduits also possessed low stiffness, thereby eliminating the risk of nerve compression observed from NC made of stiffer materials (e.g. silicone[2]). Combined with sufficient strength and an adequate immune response, as observed *in vivo*, the alginate/chitosan NC should be a promising alternative to conventional treatments and the more frequently described silicone or collagen conduits. In our future work, we will combine the NC with a delivery system for controlled localized release of growth factors. We expect that the combination of nerve guidance and stimulation of nerve growth will improve substantially the functional regeneration of severed nerves.

**REFERENCES:** [1] F.A. Grieshaber, et al (1992) *Biomed Tech (Berl)* **37**:278-86. [2] J.S. Belkas, et al (2004) *Neurol Res* **26**:151-61.

**ACKNOWLEDGEMENTS:** We thank the Gerbert-Rüf Stiftung, SUVA and ETH Zurich for financial support, and ISP Alginate (represented by Staerkle & Nagler AG) for provision of materials

.

# Scaffolds and Cells for Bone Engineering

J.E. Davies
Institute of Biomaterials and Biomedical Engineering and
Faculty of Dentistry, University of Toronto

**INTRODUCTION:** Functional scaffolds are essential for some bone tissue engineering approaches. In many cases the ideal scaffold should be biodegradable at a rate which compliments the ingrowth of host tissue. Specifically, bone engineering scaffolds should also be osteoconductive so that, as the scaffold degrades, the structural integrity of the composite will be maintained. Our approach has been to develop a polymeric based biodegradable material with a macroporous, interconnecting, structure which mimics the dimensional scale ranges found in human trabecular bone. This scaffold has evolved in an iterative manner to respond to the biological reactions to the scaffold. These biologically-driven design criteria have resulted in a novel 3-phase biodegradable, anti-inflammatory, and osteoconductive scaffold material, on which we can seed human osteoprogenitors. We source the latter from either adult marrow – mesenchymal progenitor cells (MPC) or by extraction of perivascular cells from human umbilical cord (HUCPV), to provide both autogeneous and potentially allogenic tissue engineering strategies.

**METHODS:** Macroporous, biodegradable poly(lactide-co-glycolide) (PLGA) scaffolds containing an osteoclast-resorbable calcium phosphate particulate phase were fabricated by a salt-leaching phase inversion technique which we have described in detail elsewhere (1). In some cases these scaffolds were coated with a thin film of CaP by immersion in 5 x simulated body fluid (SBF) for 5days.

Adult human marrow cells were obtained from marrow discarded from marrow transplant donors. The harvest was elutriated using a Ficoll-Paque™ (Sigma) density gradient to recover the mononuclear cell fraction. The cells were inoculated (~1 x $10^6$ cells/ml) into siliconized stirred suspension spinner flasks with medium containing 2 ng/ml and 10 ng/ml of highly purified recombinant human IL-3 and SCF respectively (2). The cell population expanded in these non-contact conditions was then plated on culture substrates to conduct bone nodule (CFU-O) assays. Some cells were seeded directly, from suspension, into scaffolds.

HUCPV were obtained from consenting full-term caesarian section patients. The umbilical cord was sectioned and the amniotic epithelium opened to reveal the vessels which were removed together with their peri-vascular tissue. These vessel fragments were then looped and the perivascular tissue enzymatically digested in 0.5mg/ml collagenase in PBS. The resulting cell harvest was cultured in both non-osteogenic and osteogenic (dexamethasone-containing) culture conditions.

**RESULTS & DISCUSSION:** The 3-phase biodegradable scaffold has evolved, in an iterative manner, to address several problems associated with the biological response to such compliant materials. The mechanical properties of the native PLGA geometry are insufficient to withstand the contractile forces of high densities of seeded cells. This is overcome by including a calcium phosphate particulate phase. The resulting scaffold has sufficient mechanical strength but is still not osteoconductive. The latter is achieved by the second calcium phosphate coating phase.
The cell sources provide, in the case of MPC, a rapidly expanding mesenchymal progenitor population which maintains a functional phenotype when finally seeded on a solid substrate and produces morphologically identifiable bone matrix. The HUCPV cells represent a rapidly expanding population of adherent cells which contain a subpopulation that exhibits osteogenic potential even in non-osteogenic culture conditions. Furthermore these cells, upon storage and passage, show an increasing population of MHC-/- cells, as determined by flow cytometry, and thus represent a potential allogeneic source of human cells for tissue engineering and other cell-based therapeutic strategies.

**Acknowledgements:** ORDCF grant.

**References:** (1) Holy CE et al. (2003) J Biomed Mater Res. 65A(4): 447-53. and Guan L and Davies JE (2004) Preparation and characterization of a highly macroporous biodedgradable composite tissue engineering scaffold. *Submitted* (2) Baksh D, Davies JE, Zandstra PW 2003 Exp. Hematol. 31:723-732. and Baksh D, Zandstra PW, Davies JE, (2004) Osteogenic development from long-term, non-adherent, suspension cultures of adult human bone marrow-derived cells *Submitted*

European Cells and Materials Vol. 7. Suppl. 2, 2004 (pages 22-23) ISSN 1473-2262

# Update on Multifunctional Materials (Mfm): Bioabsorbable Osteoconductive Drug-Releasing Hard Tissue Fixation Screws

N.Ashammakhi[1,3], M.Veiranto[1], P.Viitanen[1], K.Knuutila[1], E.Suokas[2], J.Tiainen[3], S.Leinonen[3], S-M. Niemelä[3], H.Syrjälä[4], T.Waris[3], P.Törmälä[1]

[1] *Institute of Biomaterials, Tampere University of Technology, Tampere, Finland.*
[2] *Linvatec Biomaterials Ltd., Tampere, Finland.*
[3] *Department of Surgery, University of Oulu, Oulu, Finland.*
[4] *Department of Infection Control, Oulu University Hospital, Oulu, Finland.*

**INTRODUCTION:** Further to achievement of reliable biocompatible hard reliable tissue bioabsorbable fixation devices, development of next generation was envisaged. There has been also an extensive research in development of slow-releasing drug systems. These two technologies thus were brought together, to develop devices, e.g. with dual function, hence the name "multifunctional" devices. For additional function, to address the problem of replacement of the bioabrorbale screw tracks with fibrous tissue, osteoconductivite agent was added.

**MATERIALS AND METHODS:** Bioaborbable polyesteric polymers (PLGA 80/20 or PLDLA 70/30) were used as the matrix material. Bioactive glass (BG) 93/13 was included to confer the osteoconductive function. In MFM-1, for infection-resistance function, ciprofloxacin (CF) was included in the implant. CF is bacteriocidal and it has a wide range of activity against osteomyelitis-causing bacteria, with good penetration to compact bone. In MFM-2, for the function of modification of tissue-reaction, agent-x1 was used. The composite was made into rods which were subsequently self-reinforced (SR), then machined into screws, and granules and sterilized using g-irradiation. Drug release, changes in molecular weight, *in vitro* degradation profiles, mechanical properties, and microstructure were evaluated. Effects of MFMs *in vitro* cell models were study the effect of the devices (on S. epidermides bacterial culture, attachment and biofilm formation; on chondrocytes, and on osteoblasts). *In vivo* models included the implantation in cranial bone of rabbits to assess tissue reactions, biodegradation and drug bone concentration. Biomechanical testing was also carried out using human cadaver bones (pull out tests). In an osteomyelitis model in rabbits, MFM granules were used.

**RESULTS:**

MFM-1**:**
CF was **released** from the studied screws after 44 weeks (P/L/DL)LA) and 23 weeks (PLGA) in vitro.

During this time drug release remained in range of 0.06 – 8.7 µg/ml/d (for P(L/DL)LA) and 0.6 - 11.6 µg/ml/d (for PLGA) after the start burst peak. The maximum release occurred in the 15th week (for P(L/DL)LA) and 8th week (for PLGA). CF remained bioactive throughout the *in vitro* drug release study. Initial mechanical properties of the screws are high and their application is easy. Measured initial shear strengths of the studied ciprofloxacin-releasing screws were 152 MPa (P/L/DL)LA) and 172 MPa (PLGA). Studied screws retain their mechanical properties at least 12 weeks (P(L/DL)LA) and 9 weeks (PLGA) *in vitro* at the level that ensures their fixation properties.

**Histology** did not show much difference from the control plain PLGA screws except for some increased giant cells at some areas of the implantation site. **Pull-out tests** indicated that the early version of the MFM-1 type of screws have lower values as compared to controls. The inclusion of the bioactive glass leads to further drop in mechanical properties. Inhibition of bacterial growth, attachment and biofilm formation was significantly different than controls. In rabbit osteomyelitis model, healing was observed using MFM-1 antibiotic releasing devices.

MFM-2:
Over 60 d, release The mode of the release curve followed close trend to that seen with MFM-1. A Peak was observed during the 1st 6h. SR has enhanced the release process as also didi g-sterilization further. SEM microstructure showed highly oriented SR structure and proper distribution of the drug agent. Study of mechanical properties is going on.

**COMMENTS:** These are the first reliable MFM antibiotic-releasing screws in the world, that can add to surgeon's tools to combat against bone infection and its costly consequences. During degradation, MFM-1 screws progressively released the drug and retained sufficient mechanical

properties over 2-3 months. For MFM-2, therapeutic levels were achieved and maintained for the time passed so far (61 d).

**CONCLUSIONS:** SR-P(L/DL)LA and SR-PLGA MF screws with appropriate drug release, structural, mechanical and biocompatibility properties can be produced. Clinical studies will be started in near future (MFM-1).

**ACKNOWLEDGEMENTS:** Research funds from the Technology Development Center in Finland (TEKES, Biowaffle Project 40274/03 and MFM Project 424/31/04), the European Commission (EU Spare Parts Project QLK6-CT-2000-00487), the Academy of Finland (Project 73948) and the Ministry of Education (Graduate School of Biomaterials and Tissue Engineering) are greatly appreciated.

European Cells and Materials Vol. 7. Suppl. 2, 2004 (pages 24-25) ISSN 1473-2262

# The Influence of Steam Sterilization on Retrieved UHMW-PE Parts

Y.Dirix[1], H. Gellner[2], H. Schmotzer[1]

[1]*PI Precision Implants AG,. Schachenallee 29, 5001 Aarau, Switzerland;*
[2]*Helios Klinik Blankenhain, Wirthstrasse 5, 99444 Blankenhain, Germany*

## INTRODUCTION:

Ultra high molecular weight polyethylene is an important material for the construction of bearing surfaces in hip or knee implants. However it is also a contributing factor to the failure of total joint replacements. For example aseptic loosening due to wear particles or fatigue damage causing fracture of polyethylene parts has been observed in hip and knee replacements, respectively. The explanted polyethylene parts can provide valuable information on the reason for revision, whether it was related to the raw material, the design of the implant, the sterilization procedure etc. Usually the complete explanted joint system is autoclaved in the clinic using hot steam (134°C). The goal of this research was to investigate the influence of this steam sterilization on the properties the polyethylene. Therefore a revised hip inlay was split into two parts, one half was cleaned without a thermal treatment, and the other half was sterilized using hot steam. On both parts, the chemical properties were analyzed using infrared spectroscopy.

## METHODS:

A hip inlay (ABG, Benoist Girard France) which was articulating against a 32 mm zirkonium ball head, was revised after 9 years. This cup was γ-sterilized in air [1]. The hip cup was split into two parts. One half was desinfected for 15 minutes in an ultrasonic cleaning bath using a 5% Stammopur DR2 solution. The other half was sterilized in a unisteri 446-steam sterilisator (MMM, Germany) at 134°C. The sterilisation time was 20 minutes, however the whole cycle, (heating–evacuation–sterilization–cooling) takes approximately 3 hours. After the sterilization or cleaning, the oxidation index of the polyethylene was measured using Fourier transform infrared spectroscopy (FTIR). Thin (150 microns) microsections were cut from the inlay in the non-loaded regions from both halfs of the cup (which used to be connected to each other). The microsections were cut as a function of the distance from the surface of the inlay and were used with and without extraction of the components that diffused into the polyethylene. The microsections were extracted for 48hrs in cyclohexane at 80°C to extract the absorbed body fluids. All microsections were scanned in the FTIR spectrometer with a resolution of 4 cm-1. The oxidation index was measured by deviding the area of the carbonyl peaks at 1720 cm-1 by the area of the internal reference peak at 1370 cm-1 [2].

## RESULTS AND DISCUSSION:

A photograph of the retrieved hip cup is shown in Figure 1. The part of the inlay which was subjected to the hot steam (right), does not fit anymore to its cleaned counterpart (left). During clinical use, there is wear and plastic deformation (creep) of the polyethylene. Heating the polyethylene in the autoclave close-to, but below the melting temperature (137°C) results in partial recovery of this plastic deformation.

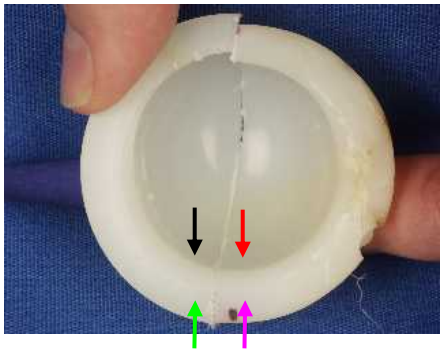

*Figure 1: Top view of retrieved hip inlay after 9 yrs implantation. One half as received (left) and one half after steam sterilization (right). Arrows indicate the locations where the oxidation indices were measured.*

The oxidation indices (OI) as a function of the depth in the material are shown in Figure 2.

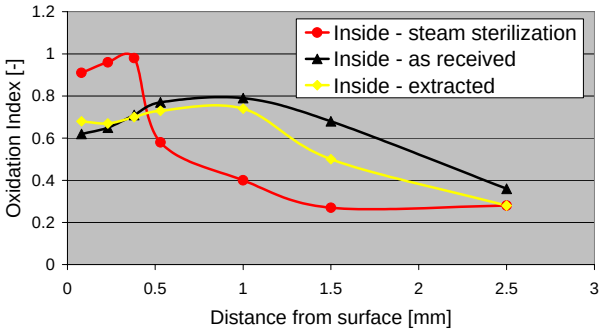


*Figure 2: Oxidation index profile (OI in the non loaded zone on the inside of the cup (see Figure 1)*

The oxidation index in the non-loaded zone of the inlay after cleaning (black curve) shows a maximum at 1 mm below the surface of the inlay.

This subsurface maximum is typical for γ-sterilized polyethylene parts, aged on the shelf and during clinical use [3]. The oxidation is a result of oxygen which reacts with the free radicals present in the polyethylene. The free radicals are formed during the γ-sterilization and the oxygen difuses into the polyethylene surface, either on the shelf or via the body fluids during clinical use.

These body fluids difusing into the surface also have carbonyl groups and therefore might lead to erroneous (high) oxidation values. However a comparison of the the oxidation profile before (black curve) and after extraction (yellow curve) shows that there are only minor differences, i.e., the oxidation is dominated by reactions between oxygen and free radicals and not strongly influenced by the absorbed body fluids.

Steam sterilization of the same area has a strong influence on the oxidation level and on the profile (red curve versus black curve). The oxidation maximum shifts towards the surface and to higher values (OI ~ 1). The heat during the sterilization activates both chemical reactions and difusion processes. The differences in oxidation index are probably the result of oxidative reactions occuring of free radicals still present in the material and/or due to diffusion of oxidized species towards the surface. The latter is possible due to the increased mobility at 134°C in combination with a vacuum of 65 mbar in the autoclave.

The influence of steam sterilization on the oxidation index curves measured on the OUTSIDE of the inlay is even more pronounced (see green and violett arrows in Figure 1):

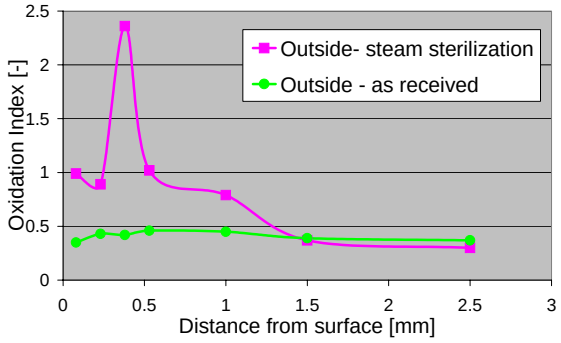


*Figure 3:Oxidation index profile in the non-loaded zone on the outside of the cup (see Figure 1)*

Also on the outside, the steam sterilization shifts the oxidation maximum towards the surface. However, there is a very sharp subsurface maximum which was not observed on the inside of the inlay. An explanation might be that on the outside more residual free radicals are present which then react very fast due to the thermal activation during autoclaving.

## CONCLUSIONS:

- The steam sterilization procedure affects the dimensions of explanted polyethylene parts due to partial release of stresses built-up in the material during use.
- The heat, vacuum and steam adversely affect the oxidation index present directly after explantation which might lead to erroneous conclusions.
- Chemical analysis and dimensional measurements on revised PE parts are virtually impossible after steam sterilization.
- Attention should be paid when comparing oxidation values from literature of retrieved UHMW-PE implants.

## REFERENCES:

[1] MDA /2004/011
[2] oxidation index was measured after ASTM F21002-01
[3] “The UHMW-PE Handbook”, ed. S. Kurtz, Chapter 11, Elseviers Academic Press, 2004

European Cells and Materials Vol. 7. Suppl. 2, 2004 (page 26) ISSN 1473-2262

# Microfabricated Cell Culture System for Single Cell Analysis in 2.5 Dimensions

M.R. Dusseiller[1], M. Koch[1], D. Schlaepfer[2], R. Kroschewski[2], M. Textor[1]

*[1] Laboratory for Surface Science and Technology, Department of Materials, [2] Institute of Biochemistry, Department of Biology, Swiss Federal Institute of Technology (ETH) Zurich, CH-8092 Zurich, Switzerland*

**INTRODUCTION:** In the last decade a number of techniques have been developed to generate microscopic patterns of biomolecules on different materials surfaces. Such chemical patterns have been successfully used as model surfaces for biorelated studies and applied to the field of biosensors, cell-surface interactions and tissue engineering. Due to the inherent complexity of cellular systems great care has to be taken to control the microenvironment of the cells[1].

It is the goal of this work to create a new type of array system to study single cells in a 2.5-dimensional microenvironment, where both topography and surface chemistry can be tailored accordingly. It is well known that the shape and adhesion state of a cell has great influence on its fate and behavior[2], but model systems to have a more complete control of the cell shape in 3-dimensions are still missing[3].

**METHODS:** Here we present a route to fabricate polystyrene (PS) chips with wells of 5 to 50 µm size and adjustable depth, which have been hot-embossed using a silicon rubber (PDMS) as the master. This master was replicated from a microstructured Si mold (Fig 1), produced by standard photolithography and dry etching using inductive coupled plasma (ICP). To further tailor the surface topography of the wells a simple heat treatment was used to flatten out the scalloping effect inherent in the dRIE-process. By the use of a self-assembling graft-co-polymer, poly-L-lysine *grafted* poly(ethylene glycol) (PLL-g-PEG)[4], the surface of oxygen plasma treated PS can be functionalized to be either protein repelling, thus resistant to cell adhesion, or carry a specific biofunctionality, such as cell binding peptide sequences (e.g. RGD) in any desired concentration[4]. Different routes to selectively functionalize the surface inside the wells and the surrounding plateau were investigated. Cell experiments were performed using fibroblasts (HFFs) and epithelial cells (MDCKs).

**RESULTS:** Some selected results are shown in the following figures. A high-throughput method to produce large quantities of structured PS films could be established (Fig 1). Preliminary results demonstrate the feasibility of creating surfaces that combine topographical features and area-selective chemical contrast (Fig 2).

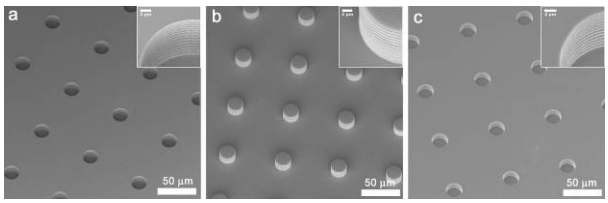


*Fig 1: SEM images of a) dRIE structured Si showing an array of wells; b) replicated PDMS structures; c) hot-embossed wells in PS. Tilt angle: 30°. All structures are approximately 13 µm in depth.*

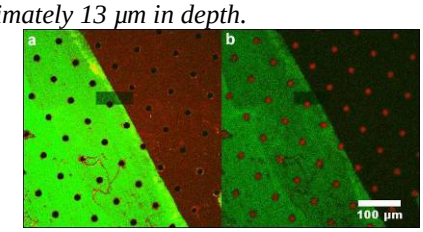


*Fig 2: CLSM image of stamped border of the PS surface after µCP of PAH, adsorption of PLL-g-PEG/biotin, finbinogen488 (green channel) and streptavidin633 (red channel). a) focused on top; b) focused on the bottom of the wells.*

**DISCUSSION & CONCLUSIONS:** The combination of cheap replication techniques, biocompatible polymers and designated surface chemistries is demonstrated to be a promising approach to produce low-cost biochips for investigating cell function and response, e.g. in the context of drug screening and development, or to create model tissues for *in-vitro* analysis. Furthermore, microstructures with optimized geometries will allow for the analysis of single cells or small clusters of cells in a controlled microenvironment, taking into account the 3-dimensional nature of cellular adhesion and mimicking more closely the *in-vivo* situation.

**REFERENCES:** [1]Bhadriraju, K. and C.S. Chen, *Drug Discovery Today*, 2002, 7(11), 612-620. [2]Cukierman, E., R. Pankov, and K.M. Yamada, *Current Opinion in Cell Biology*, 2002. 14(5), 633-640. [3]Chen, C.S., J. Tan, and J. Tien, Annu. *Rev. Biomed. Eng.*, in press, 6(1). [4]VandeVondele, S., J. Voros, and J.A. Hubbell, *Biotechnol Bioeng*, 2003, 82(7), 784-90.

**ACKNOWLEDGEMENTS:** The authors would like to thank Dr. S. Blunier, IMES, ETHZ, for the use of their clean room facilities; M. Gössi, Polymer Technology, ETHZ, for help with the polymer processing.

European Cells and Materials Vol. 7. Suppl. 2, 2004 (page 27) ISSN 1473-2262

# Synthesis of Poly(Propylene Sulfide)-*Block*-Poly(Ethylene Glycol), (Pps-Peg), and its Application to Surfaces

*L. Feller[1], S. Tosatti[1], S. Cerritelli[2] , M. Textor[1], J. A. Hubbel1[2],*

*[1]Dept. of Materials, ETHZ, Zürich, Switzerland. [2]Séction des sciences de la vie. EPFL, Lausanne, Switzerland*

**INTRODUCTION:** Poly(ethylene glycol) (PEG) has been used in numerous biomedical systems to reduce protein adsorption and cell adhesion. PEG can be attached to surfaces through a variety of different approaches including silanization, self-assembly of thiols, and plasma polymerization. In our approach series of block copolymers containing one (di-block) or two (tri-block) PEG chains separated by a poly(propylene sulfide) (PPS) part were used. Adsorbed to gold surfaces, a stable linkage between the sulfur atoms of the PPS thioether and the metal surface was observed. The hydrophilic PEG part forms a dense layer of biocompatible PEG chains, which is exposed to the aqueous environment.

**METHODS:** Various architectures of di- and tri-block PPS-PEG copolymers were synthesized[2], characterized, and adsorbed on gold substrates from methanol based solutions. While the PPS part was kept constant (goal: MW 4000), the PEG part was varied between 1100 and 5000 Da molecular weight. Adsorption of the polymer to the gold surface was characterized by *ex situ* ellipsometry, X-ray photoelectron spectroscopy (XPS), and *in situ* surface plasmon resonance (SPR). SPR was used to determine the resistance of the PPS-PEG adlayer upon human serum albumin (HSA) as well as full serum exposure.

50nm gold adlayers were deposited on glass substrates by using reactive magnetron sputtering techniques (PSI, Villigen, Switzerland) with an adhesive layer of 5nm Cr in between. SPR chips were purchased by Ssens (Hengelo, Netherlands)

The polymers were dissolved in methanol (1mg/ml) at room temperature and the substrates were dipped for 45 min and subsequently rinsed in pure methanol and dried with nitrogen. Protein resistance was tested with human serum albumin (1mg/ml in Hepes II) and full human serum. Uncoated substrates served as controls.

**RESULTS:** Both XPS intensities normalised to gold and *ex situ* ellipsometry thickness measurements are in good agreement and show the chemisorption of PPS-PEG on gold.

Fig. 1 shows an SPR plot of polymer adsorption and subsequent HSA and serum exposure.

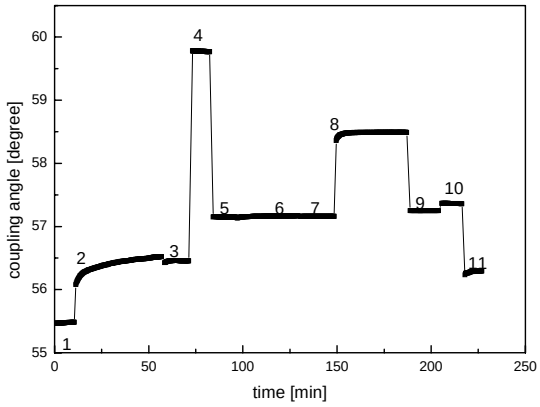


*Fig.1: PPS-PEG Triblock (5000/2101/5000 Da) adsorbed on gold shows good resistance to HSA and serum. 1) Methanol baseline 2) PPS-PEG adsorption 3) Methanol rinse 4) change to ethanol 5) Hepes II baseline 6) Exposure to HSA 7) rinse with Hepes II 8) Exposure to serum 9) Hepes II rinse 10) Cleaner 11) Methanol.*

**DISCUSSION & CONCLUSIONS:** PPS-PEG chemisorbs from methanol on gold surfaces. By variation of the PPS-PEG architecture it was possible to tailor the degree against protein adsorption of the surfaces till a maximum of 90% reduction upon serum exposure.

**REFERENCES:** [1] J. P. Bearinger et al (2003) Nature Materials 2:259-264

[2] A. Napoli et al (2001) Macromolecules 34:8913-8917

**ACKNOWLEDGEMENTS:** We would like to thank Dr. S. Terrattaz (EPFL) for his help and make the SPR available to us. Thanks to Dr. J. Vörös for the helpful discussions.

# A Fast and Simple Method for Producing Biodegradable Nanospheres

S. Freitas[1], G. Hielscher[2], H. P. Merkle[1], B. Gander[1]

[1] *Institute of Pharmaceutical Sciences, ETH Zürich, Switzerland.*
[2] *Dr. Hielscher GmbH, Teltow, Germany.*

**INTRODUCTION:** Biodegradable micro- and nanospheres (MS, NS) made of poly(lactide-co-glycolide) (PLGA) or other materials are very potent drug and antigen delivery systems with inherent potential for drug and antigen targeting. Present methods to produce PLGA NS are typical batch processes and suffer from difficulties of scaling-up under sterile conditions. Here, we present a novel and elegant method to produce PLGA NS in a continuous, contact- and contamination-free process that can be readily run under sterile conditions. During the entire manufacturing process, the product is in direct contact only with sterile glass and Teflon® tubes. The process can be run in a closed system to prevent any environmental contamination.

**METHODS:** PLGA50:50 (Resomer® RG503H, Boehringer Ingelheim) nanoparticles were produced using a modified solvent extraction/ evaporation process [1]. PLGA dissolved in dichloromethane (2 or 5%, w/w) was dispersed in aqueous 0.5% (w/w) PVA-solution by means of the novel experimental set-up involving a contact-free flow-through ultrasonication cell (Figs 1 & 2) [2, 3]. A coarse O/W-dispersion was first prepared through a magnetically stirrered micro-cell, and then homogenized in the ultrasonic flow-through cell (flow rates of O- and W-phases were at 1:8). The initially formed PLGA-solvent nanodroplets gradually solidified during the passage in the tubes to become PLGA nanoparticles. Final hardening of the particles was achieved in a larger volume of 0.5% PVA solution.

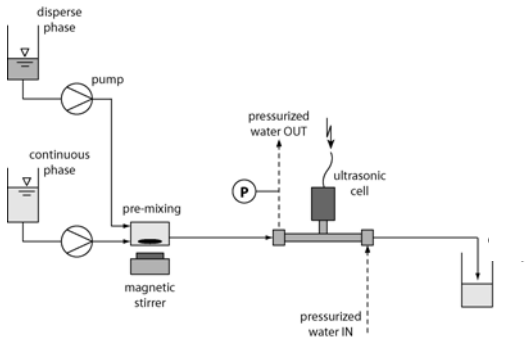


*Fig. 1: Experimental set-up for the production of PLGA nanospheres.*

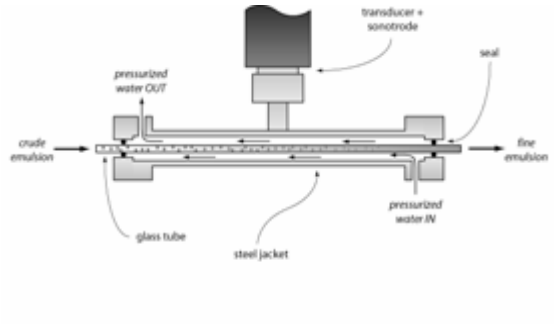


*Fig. 2: Design of the ultrasonic flow-through cell.*

**RESULTS:** Nanoparticles with a mean diameter of 485 nm were readily prepared from a 2% PLGA solution in DCM at 32 W sonication power (Tab. 1). The size distribution was mono-modal with a slight tailing (Fig. 3A). Nanoparticle sizes extended from 175 to 755 nm according to the 10 and 90% percentiles. Repeatability of the production process was consistently good, as reflected by only minor variability in the mean particle diameter. Lowering the emulsion's residence time in the sonic field from 14 to 7 s had only a minor impact on the nanoparticle size. A reduction of the sonication power from 32 to 25 W, however, resulted in a significant increase of the mean particle size from 485 to 700 nm, caused by a more pronounced tailing of the size distribution curve (Fig. 3A). A less prominent, though significant increase in the mean particle size from 485 to 600 nm was found when using a 5% instead of a 2% PLGA solution. Finally, the more hydrophilic PLGA was exchanged for a more hydrophobic and lower molecular weight PLA without noticeable changes in particle mean size and size distribution (not shown).

No differences were observed in the morphology of the different batches of particles prepared from 2% polymer solutions. They all exhibited perfectly spherical shapes and smooth surfaces (Fig. 7B). The particles made from the 5% PLGA solution, however, were less spherical, showed slightly wrinkly surfaces, and fusions of two or sometimes more particles (Fig. 3C).

*Table 1. Mean diameter of PLGA50:50 nanospheres prepared under different conditions. Mean of two batches ± absolute deviation.*

| Polymer conc. (w/w, %) | Sonication power (W) | Residence time (s) | Mean particle diameter D[4,3] (nm) |
|---|---|---|---|
| 2 | 32 | 14 | 485 ± 15 |
| 2 | 32 | 7 | 500 ± 20 |
| 2 | 25 | 14 | 700 ± 20 |
| 5 | 32 | 14 | 600 ± 10 |

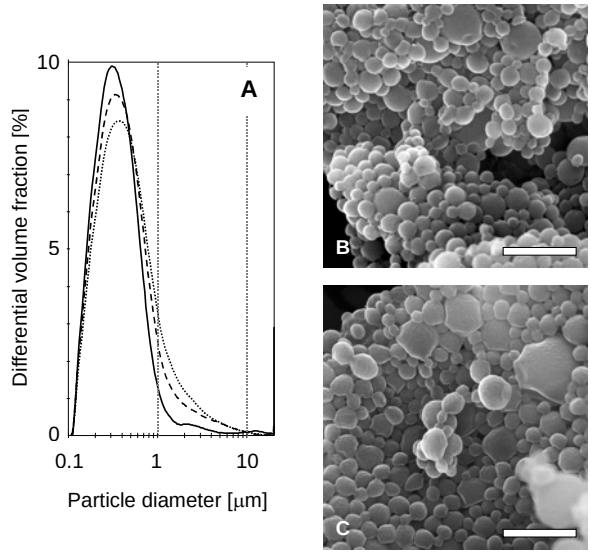


*Fig. 3: PLGA nanoparticles. (A): Size distribution of particles prepared at polymer concentration/ sonication power of 2%/ 32 W (—), 5%/ 32 W (---), and 2%/ 25 W% (●●●●); residence time = 14 s. (B),(C): SEM pictures of particles prepared from 2 and 5% polymer solutions, respectively. Residence time = 14 s; sonication power = 32 W. Bars represent 1 μm.*

**DISCUSSION & CONCLUSIONS:** The ultrasonic flow-through cell was found to be well suited for emulsion-solvent extraction/evaporation based production of biodegradable polymeric nanospheres. The design of the cell avoids direct contact between the sound-emitting sonotrode and the emulsion and, thereby, prevents particle contamination of the product. Future research will be directed towards scaling-up the process and increasing the power input to yield even finer emulsions. In addition, the suitability of the cell for the preparation of water-in-oil emulsions, e.g. for further processing into drug-loaded microspheres, will be studied.

**REFERENCES:** [1] Hoffart V. et al. (2002), *Drug Dev Ind Pharm* **28**: 1091-9. [2] Freitas S. et al. (2003), *Deutsche Patentanmeldung*. [3] Freitas S. et al. (2004), *Ultrasonics Sonochem.* (submitted).

**ACKNOWLEDGEMENTS:** Dr. E. Wehrli, Laboratory of Electron Microscopy, ETH Zürich for the preparation of the SEM-micrographs.

European Cells and Materials Vol. 7. Suppl. 2, 2004 (pages 30-31) ISSN 1473-2262

# Towards medium-chain-length polyhydroxyalkanoate for medical applications

P. Furrer[1,2], M. Schmid[1], A. Hinz[1], E. Pletscher[1], S. Panke[2] and M. Zinn[1]

*[1]Swiss Federal Laboratories for Materials Testing and Research EMPA, Laboratory for Biopolymers, Lerchenfeldstr. 5, 9014 St. Gallen, Switzerland*

*[2]Swiss Federal Institute of Technology Zürich ETHZ, Institute of Process Engineering, Bioprocess Laboratory, Sonneggstrasse 3, 8092 Zürich, Switzerland*

**INTRODUCTION:** Medium-chain-length poly-hydroxyalkanoate (mclPHA, monomers from $C_6$-$C_{14}$) is a water insoluble, biodegradable, and biocompatible elastomer and hence it is well suited for medical applications [1]. It is a promising material for the production of porous scaffolds like recent publications of PHA copolymers indicate [4, 5].

PHA is intracellularly accumulated in Gram negative production strains and is currently extracted by chlorinated solvents. However, it has been observed that PHA is contaminated by lipopolysaccharides (lps) from the outer cell membrane during recovery. For medical purposes the polymer needs to be highly pure, especially with respect to pyrogenic compounds. Lps are considered to be the main source of pyrogenic contamination.

Unfortunately only few methods for the depyrogenation of PHA have been described in literature, for instance the treatment with ozone, peroxides or NaOH [2, 3]. Generally the molecular weight of PHA is decreased by using lps-degrading agents. Therefore another non-PHA degrading approach for depyrogenation is required. It is known that appropriate extraction steps may minimize the co-extraction of lps.

**METHODS:** MclPHA produced with *Pseudomonas putida* GPo1 was recovered as follows: The fermentation broth was centrifuged (10'000xg) and the resulting wet biomass was freeze dried. The dry biomass was grinded and extracted with various organic solvents at room temperature for 24 h. The suspension was filtrated (1µm reg. cellulose filter) to obtain a clear PHA solution. One third of the solution was evaporated and finally dried under vacuum at 40°C for 48h to obtain the rough PHA. The remaining parts were concentrated and precipitated in water and methanol, respectively.

Test-tubes (10 ml) were coated by rotation with about 200 mg mclPHA, dried and exposed to endotoxin-free water for 36 h at 37°C. The endotoxin-containing water was removed and diluted 1:100. The chromogenic *Limulus* amebocyte lysate (LAL) test (Cambrex QCL-1000) was applied to determine the amount of endotoxins in these solutions. For calibration a 29 EU standard (strain 0111:B4) was used. The final values were expressed as endotoxin units (EU) per gram PHA.

The molecular weights were determined by GPC–RALS (Viscotek, TDA 302).

**RESULTS:** The capacity to extract mclPHA from freeze-dried *P. Putida* GPo1 was investigated for various solvents as shown in Fig. 1.

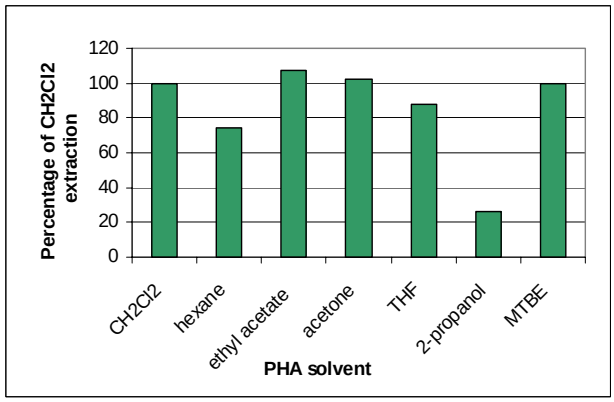


*Fig. 1: Efficiency of PHA extraction from biomass for various solvents in comparison to standard extraction (methylene chloride).*

GPC measurements revealed that the molecular weight was equal for all extracts ($M_w$=170 kDa, $M_n$= 75 kDa) within the measurement uncertainty (<10%), except for the 2-propanol extract ($M_w$=92 kDa, $M_n$=55 kDa).

Significant differences in endotoxicity could be observed (Fig. 2). Ethyl acetate, acetone, tetra-hydrofuran (THF), 2-propanol and *tert.*-butyl-methyl ether (MTBE) extracts showed a much lower endotoxin content than the extracts with methylene chloride ($CH_2Cl_2$) and hexane.

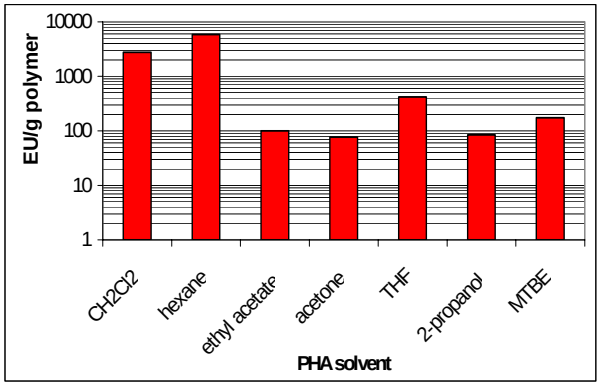


*Fig. 2: Endotoxicity of differently extracted PHA. The exposure time of PHA samples to water was 36 h.*

Whether the precipitation of solubilized PHA has an influence on the endotoxicity was assessed for methanol and water (Fig. 3).

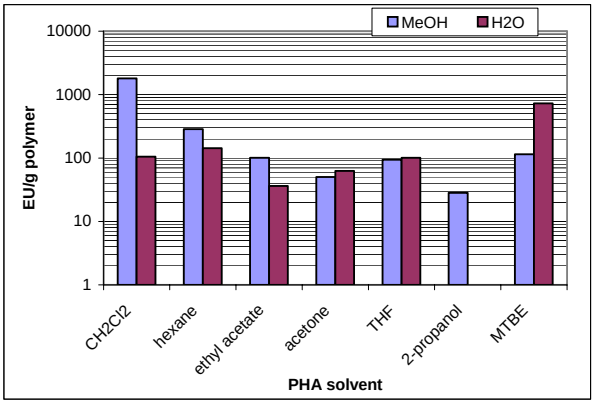


*Fig. 3: Endotoxicity of PHA precipitated in either methanol or water.*

**DISCUSSION & CONCLUSIONS:** The standard extraction solvent ($CH_2Cl_2$) has to be replaced by a more environmentally friendly one. All solvents except hexane and 2-propanol showed similar extraction yields like methylene chloride. A significant decrease in the molecular weight could only be seen for 2-propanol. Based on these criteria ethyl acetate, acetone, THF and MTBE are valid alternatives.

However, ethyl acetate and acetone extracts contain the lowest amount of endotoxin and will be considered for further, more detailed analysis.

Finally, precipitation with water or methanol strongly decreased the endotoxicity of nearly all extracts.

It has to be noted that special attention has to be paid to the test methods for samples of mclPHA, because lps may still be enclosed in the polymer matrix. Therefore the porosity and the surface roughness of PHA and the extraction time with water are crucial for analysis.

**REFERENCES:** [1]B. Witholt and B. Kessler (1999) *Curr. Opin. Biotechnol.* **10:**279-285. [2]S.F. Williams et al. (1999) *Int. J. Biol. Macromol.* **25:**111-121. [3]S.Y. Lee et al. (1999) *Appl. Environ. Microbiol.* **65:**2762-2764. [4]Y. Deng et al. (2003) *Biomaterials* **24**:4273-4281. [5]Y.-W. Wang et al. (2004) *Biomaterials* **25**:669-675.

**ACKNOWLEDGEMENTS:** The authors thank P. Manser (EMPA) for supporting the endotoxin measurements and Dr. S. Wunderli (EMPA) for constructive discussions.

European Cells and Materials Vol. 7. Suppl. 2, 2004 (pages 32-33) ISSN 1473-2262

# Cuspal Deformation During Light-Curing of Resin-Based Restorative Materials Measured by ESPI ( Electronic Speckle Pattern Interferometry)

J. Gamba [1], J. Forchelet [1], M. Cattani-Lorente [2], V. Chatelain [2], I. Krejci[2], S. Bouillaguet [2]

*[1] EIVD, Yverdon-les-bains, Switzerland. [2] Dental School, Geneva, Switzerland.*

**INTRODUCTION:** Polymerization shrinkage that occurs during light-curing of resin-based restorative materials inside a cavity may result in cuspal deformation [1], enamel crack propagation [2] or debonding of the restoration [3]. The amount of stress generated depends on the bulk of the composite and the rate at which it polymerizes. In recent years, a curing protocol called exponential curing has been introduced with the hope of reducing stress from polymerization shrinkage and improving composite properties. Exponential curing relies on the concept that an initial, low energy of curing light will start the polymerization reaction and will allow stress to be dissipated by flow of the material before a higher energy light is applied to complete the polymerization. However, the benefits of this curing concept in terms of stress concentration and tooth deformation has always been controversial.

Although different methods have been proposed to measure the polymerization shrinkage of resin composite materials [4-6], none of these has been able to measure the deformation of teeth during the in situ polymerization of the resin. Because Speckle interferometry has the capability to perform contactless, real time and high-sensitivity measurements of displacement on the surface of an object, we have used ESPI to measure the cuspal deformation of teeth during in situ polymerization of the restorative material. Our hypothesis was that the exponential curing mode would cause less stress and deformation during polymerization than the standard curing mode, without reducing the mechanical properties of the cured material.

**MATERIALS & METHODS:** MOD cavities with average dimensions of 2x3.5x2 mm were prepared in 24 extracted human molars. The adhesive system (AdheSE, Vivadent) was then applied to the cavity walls and the specimen glued onto a heavy metal base used to maximize stability. This also allowed specimens to be accurately mounted in a Michelson speckle interferometer constructed for the measurement of out-of-plane displacement. Briefly, this device illuminates the the tooth surface with a 10 mW He-Ne laser, creating a granular pattern of speckles on the tooth surface. Images of the speckles were captured with a CCD camera with an image array of 756x581 pixels. The displacement of the teeth due to the polymerization shrinkage was calculated by multiplying the total number of observed fringes by d.

$$d = \lambda/2 \qquad (1)$$

where $\lambda$ is the wavelength of the laser light.

The resin composite material (Tetric Ceram, Vivadent) was inserted into the cavity and bulk cured using either the LED Elipar Freelight 2 (3M-ESPE) or the halogen Swiss Master Light (EMS). For each light source, two curing modes were selected: standard (STD) or time dependent (EXP). For the STD conditions, irradiation times were 20 s at 800 mW/cm$^2$ for the Freelight 2 and 10 s at 2000 mW/cm$^2$ for the Swiss Master Light. For the EXP conditions preset programs with intensities increasing exponentially during the first seconds were used. Tooth deformation during light curing was measured in real time for 60s.

For polymerization control, each tooth was sectioned in two halves, and the Vickers hardness of the resin-composite was measured at eight different locations inside the restoration. The indentations were made by applying a 0.5 Kg load with a Hauser micro-indenter. The results were compared with a multifactor analysis of variance followed by a LSD multiple range test ( $P< 0.05$)

**RESULTS:** The mean displacement of the teeth during the polymerization reaction is given as a function of time in the Figures 1 and 2. The Vickers hardness $VH_{0.5}$ is given in the Table 1.

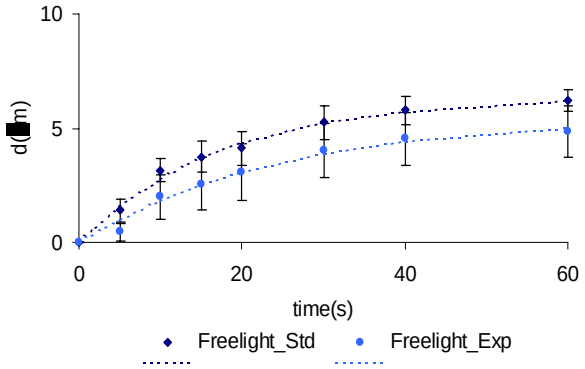


*Fig. 1: Mean displacements (µm) of the teeth during the setting reaction obtained with the LED Freelight 2.*

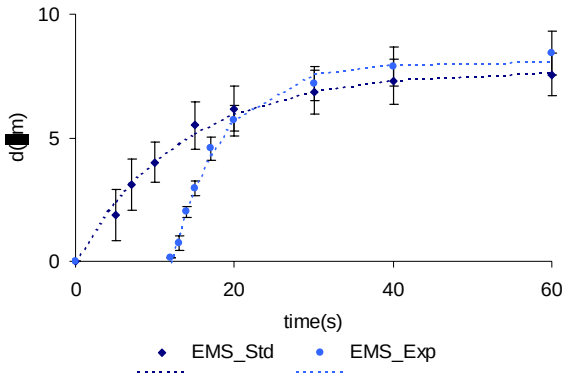


*Fig. 2: Mean displacements (µm) of the teeth during the setting reaction obtained with the halogen Swiss Master Light.*

A two-factor analysis of variance showed that only the type of light source had a statistical significant effect upon the displacement of the teeth during the polymerization reaction ($p<0.0001$). For both light sources, the use of a continuous or time dependent irradiance output did not significantly affect the displacement ($p=0.5625$)

*Table 1. Mean $VH_{0.5}$ hardness and standard deviation at different locations in the restoration for the different illumination conditions .*

| | Freelight2 | | EMS | |
|---|---|---|---|---|
| Position | STD | EXP | STD | EXP |
| bottom | 56±32 | 49±16 | 69±18 | 54±24 |
| bottom | 62±28 | 51±28 | 60±26 | 74±32 |
| middle | 98±10 | 90±17 | 87±12 | 96±20 |
| middle | 101±8 | 100±9 | 97±4 | 98±11 |
| middle | 99±5 | 98±5 | 96±7 | 99±15 |
| middle | 95±5 | 88±18 | 79±28 | 100±13 |
| top | 111±8 | 110±7 | 96±4 | 102±9 |
| top | 106±8 | 109±6 | 100±4 | 108±4 |

A multifactor analysis of variance showed that there was no significant effect from neither the type of source ($p=0.8895$) nor the illumination conditions used ($p=0.7414$) on the hardness of the material. However, significant differences were found ($p<0.0001$) between the hardness values measured at the top, the middle and the bottom of the cavities.

**DISCUSSION & CONCLUSIONS:** The curing contraction of the resin composite material will cause deformation of the surrounding tooth structure only through a bonded interface. The bond strength between the resin composite and dentin was determined in a pilot experiment in order to ensure that a good adhesion was obtained.

Tooth deformation will be also influenced by the the extent of the polymerization reaction. In the present study, the polymerization extent was assessed indirectly by measuring the Vickers hardness of the set resin composite. The hardness values indicated that comparable polymerization degrees were obtained with both light sources for both irradiaton modes. However, the hardness significantly decreased from the top to the bottom of the restoration. This result could be explained by the thickness of the composite layer which was slightly greater than ususally recommended.

For both light sources, the final teeth displacements were not influenced by the illumination mode. With the EXP mode of the Swiss Master Light an initial displacement delay was observed, which could be related to a shift of the gel point of the polymerization reaction. A significant lower displacement was obtained with the Freelight 2. As this effect can not be related to a lower extent of the setting reaction, it is probably due to a slower reaction rate induced by a lower irradiance output, which allowed greater flow of the resin composite.

In conclusion, the exponential curing modes tested in this study did not offer any advantage over conventional curing modes in term of tooth deformation. Therefore our working hypothesis has to be rejected.

**REFERENCES:**

[1] N Meredith, DJ Setchell. (1997), *J Dent* **25**:331-337.
[2] K Okuda et al. (2002), *Oper Dent* **27**:289-296.
[3] L Han et al. (1992), *Dent Mater J* **11**:26-37.
[4] DC Watts, AJ Cash (1991), *Dent Mater* **7**:281-287.
[5] AJ DeGee et al.(1993), *Dent Mater* **9**:11-14.
[6] T Attin et al.(1995), *Dent Mater* **11**:359-362.

**ACKNOWLEDGEMENTS:** We gratefully acknowledge 3M-ESPE, EMS and Vivadent for kindly furnishing the light sources and the resin composite used in this study.

European Cells and Materials Vol. 7. Suppl. 2, 2004 (pages 34-35) ISSN 1473-2262

# Calcium-Phosphate – Calcium-Sulphate Bone Cements Strucutre and Compression Strength after Setting

A.Gisep, B.Rahn

*AO Research Institute, Davos, Switzerland*

**INTRODUCTION**: Ceramic bone cements represent a group of bone substitute materials, which are used in many different kinds of fractures of the musculo-skeletal system in humans. Advantages of these materials over the autologous transplantation of cortical or cancellous bone are – among others – the reduction of post-operative pain, donor site morbidity, the avoidance of a second intervention and the unlimited supply of the materials.

A few products of ceramic injectable materials are out on the market: Norian SRS, BoneSource, Biopex, α-BSM etc. All these materials have hydroxyapatite (HA) as a final setting product and most of them have very long resorption times.

An experimental biphasic cement consisting of a dicalcium-phosphate dihydrate (DCPD) matrix filled with β-tricalcium-phosphate (β-TCP) granules has shown to have a faster resorption than the above mentioned HA-cements1. Mixtures of the DCPD matrix with calcium-sulphate could even enhance the resorption rate, which could be useful in i.e. pediatric or other high-turnover applications.

The aim of this study was to investigate an injectable cement consisting of calcium-sulphate dihydrate (CSD) and DCPD. Setting times with different mixing solutions were measured and the resulting materials characterized.

**METHODS:** The following materials were used as a basis for the ceramic cements:

β-TCP, calcium-sulphate hemidydrate CSH, and monocalcium-phosphate monohydrate MCPM in powder form. MCPM and β-TCP were mixed in a 1:1 molar ratio, then mixed in a 1:4 molar ratio with CSH powder.

Mixing solutions were different concentrations of sodium-citrate (SC), glucose (GL) and sodium-pyrophosphate (SP) in distilled water (0.1 and 0.01 molar). Mixing was done in a Degussa vacuum-mixer for 30 sec. Afterwards, the paste was filled in an aluminium vial, where the measurements were done.

For the setting time measurements, a modified automated Vicat needle test was done. An universal testing machine (Instron 4302) was used with a 3.0 mm plunger to carry out the indentation tests. Crosshead speed was 20 mm/min, maximum load was 26.4 N. Initial and final set were calculated. Data evaluation was done with Microsoft Excel.

Mechanical tests were done on an Instron 4302 universal testing machine with a 10 kN load cell and 1 mm/min crosshead speed. Compression strength was calculated with Microsoft Excel.

Structural investigations were carried out with an Hitachi S-4100 field emission scanning electron microscope (SEM).

**RESULTS:** Setting times (initial set) of the ceramic powders varied from 12 minutes (distilled water) up to 86 minutes (0.1M SC). Except for the glucose containing solutions, the effect of setting time prolongation was bigger with 0.1M solutions as compared to 0.01M solutions. SC had the biggest effect on setting times, SP as a retarder for DCPD only had the lowest impact on setting times. The cement mixture with 0.1M SP solution induced such an extensive gas formation in the setting cement that a measurement was no more possible. Table 1 shows the values of setting times of all mixtures.

*Table 1: setting times in minutes of MCPM - β-TCP – CSH powders with different aqueous solutions*

| | 0.01M | 0.1M |
|---|---|---|
| SC | 69 | 86 |
| SP | 24 | - |
| GL | 74 | 37 |
| Dist. H2O | 12 | |

Compression strength of the samples was 3.4±1.7 MPa for the cement with distilled water, 5.3±1.7 MPa for 0.01M SC, 5.9±1.5 MPa for 0.01M GL and 4.5±1.8 MPa for the SP solution.

Upon structural characterisation, a two-phase material was found with backscattered electron imaging at 20 kV. Globular structures, sometimes not entirely filled, were found to be surrounded by a less dense crystalline structure.

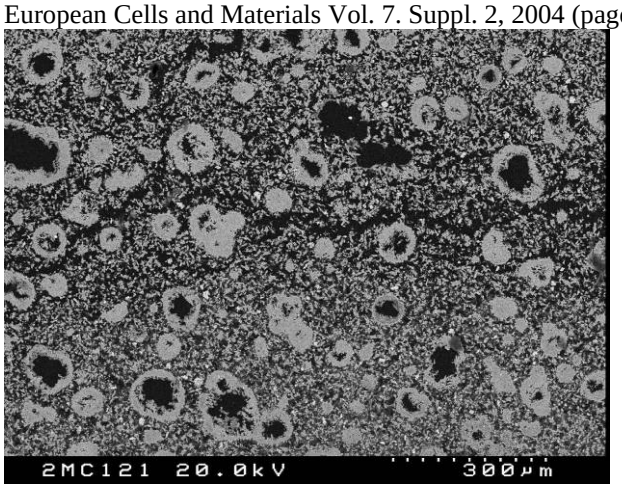


*Fig. 1: Backscattered electron micrograph of the two-phase material. Bright globular structures surrounded by less dense matrix.*

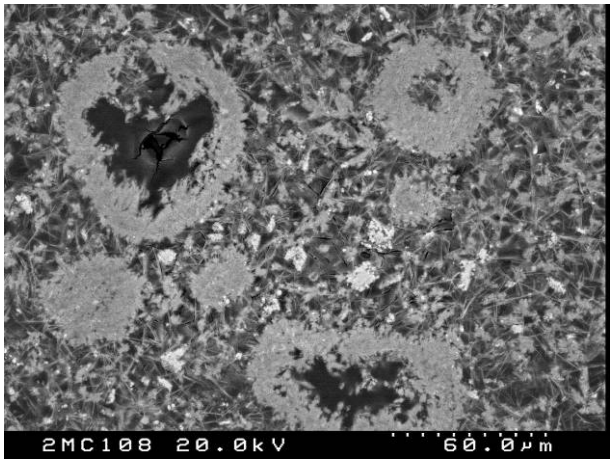


*Fig. 2: Magnification of figure 1. The crystalline structures can be seen in more detail.*

**DISCUSSION & CONCLUSIONS**: SC, known to be a retarder for both the CSD and DCPD setting reaction, had the biggest effect on the setting time of the new mixture of MCPM - β-TCP – CSH powders. The compression strength of all samples still is in a low range. However, Gisep et al.1 has shown that even high strength ceramic cements were not able to withstand high loads in a highly loaded defect model in the sheep. Ceramic bone cement therefore have to be used in stable or stabilized fracture situation only. New cements of the above mentioned mixtures could therefore have a wide range of applications in high-turnover and fast bone remodelling areas. Long initial setting times are not considered to be a major problem for these cements, as this value is reached long after the viscosity of the material gets too high for liquid-state modifications in the defect or leaking.

The two that are building up during immersion of the material in phosphate buffered saline solution could be different in their resorption speed in vivo. This would have to be justified first by XRD or TEM investigations and later certainly in vivo.

**ACKNOWLEDGEMENTS:** Thanks to Marc Bohner, Robert Mathys Foundation, for his scientific contribution to this study.

European Cells and Materials Vol. 7. Suppl. 2, 2004 (page 36) ISSN 1473-2262

# Degradation *in vitro* of New Bioresorbable Terpolymers of Lactides

M. Glarner, S. Gogolewski
Polymer Research, AO Research Institute, CH-7270 Davos, Switzerland

**Introduction:** Times to complete resorption of bioresorbable implants from lactide copolymers with a molecular weight of 200.000 dalton or higher often exceed 3 years. For implants from poly(L-lactide) the time to complete resorption may exceed 15 years in human patients.[1] This may raise the question whether there is any advantage in using resorbable implants with this type of degradation pattern, especially for maxillofacial and/or paediatric applications. With this in mind we recently designed new terpolymers consisting of lactides, glycolide and ε-caprolactone, assuming that the time to complete resorption of these terpolymers will be significantly shortened due to the disturbed chain regularity. The foreseen application of these new terpolymers is for internal fixation devices and microporous membranes for guided bone regeneration.

The purpose of the present study was to evaluate the *in vitro* degradation of one these new terpolymers.

**Materials and methods:** Resorbable pins (3.2 x 50.0 mm) produced by injection-moulding from poly(L-lactide-co-DL-lactide-co-glycolide) 80-10-10%. The viscosity-average molecular weights were 255.000 dalton and 55.000 dalton for the raw polymer and the pins, respectively. *Degradation in vitro:* Phosphate buffer solution, pH=7.4, 37ºC, 4, 8, 12, 16, 20, 24 28, 32 and 36 weeks. "Static" mode, the pH of the ageing medium was not adjusted over the whole test period. "Pseudodynamic" mode, the ageing medium was replaced if the pH dropped more than 0.5. *Samples evaluation:* Molecular weights and the polydispersity index Q estimated from viscosity measurements and size exclusion chromatography; mechanical properties of wet samples (bending strengths and moduli) measured in 4-point-bending mode (ASTM D790M); crystallinity changes assessed from the heat of melting (DSC, heating rate 10ºC/min); the samples appearance observed under SEM.

**Results and Discussion:** Injection-moulding of the polymer caused an extensive thermo-oxidative degradation of the material (75%). This significantly affected the behaviour of the polymeric implants during *in vitro* degradation. From the first week of the experiment there was a progressive drop in the molecular weight which at 4 weeks was 40% and at 16 weeks 15% of the initial value. At 28 weeks the remnants of the implant were powderlike.

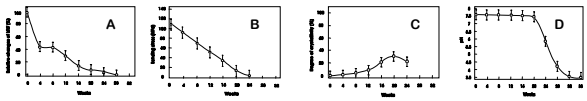


Fig. 1. Changes of molecular weight (A); bending strength (B); crystallinity (C) and pH (D) upon degradation of the samples.

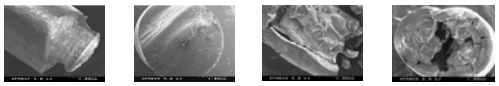

Fig. 2. SEM images of the pins before (A and B) and after 28 weeks in vitro degradation (C and D).

There was a progressive drop in mechanical properties of the samples from the first week of ageing. At 16 weeks the pins retained 31% of the initial strength, but at 24 weeks it was not possible to measure the strength due to pin fragmentation.

The crystallinity of the polymer used in the study increased during the first few weeks of the experiment from an initial value of 0.0% to 10% at 12 weeks, 21 at 16 weeks and 30% at 20 weeks. At 24 weeks the crystallinity was reduced to 22%. Similar behaviour has already been reported for other polyhydroxyacids. There was no change in the pH of the medium upon *in vitro* degradation of the samples in the pseudodynamic mode, and there was a decrease in the pH from week 20 through 36 from 7.5 to 3.5 in the static mode.

The polymer could be transformed into microporous membranes for guided bone regeneration using a phase-inverse process.

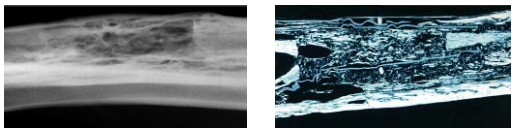

Fig. 2. Bone regeneration in critical-size defects in the rabbit radius covered with a microporous polylactide membrane.

**Conclusions**: Experimental implants produced from the new bioresorbable terpolymer show much higher susceptibility to degradation *in vitro* than implants from commonly used polyhydroxyacids. This is not only due to the chemical composition of the polymer, but also results from the low initial molecular weight of the samples used in the study. It is prerequisite that thermo-oxidative degradation of the polymer upon processing is avoided if the melt-processed implants are used *in vivo* for bone fracture fixation. The polymer can, however, be used for the preparation of the microporous bone regeneration membranes as solution-processing does not degrade the material.

References: Bos RRM, Presentation at the AO Maxillofacial Course, Davos, December 2003.

European Cells and Materials Vol. 7. Suppl. 2, 2004 (page 37) ISSN 1473-2262

# Cytocompatibility of biodegradable polyurethanes to cells and bacteria

LG Harris, K Gorna, S. Gogolewski, RG.Richards
*AO Research Institute, Davos, Switzerland.*

**INTRODUCTION:** Biodegradable polyurethanes have potential for use as implantable devices (orthopedic, maxillofacial, cardiovascular, wound dressing and plastic surgery) due to their elasticity, and the possibility of changing their chemistry and structure[1]. Studying bacterial and cell adhesion help determine surface cytocompatibility and suitability for *in vivo* trials. To determine the cytocompatibility of experimental polyurethanes (PUs) with different hydrophobic:hydrophilic (pho:phi) content ratios, the adhesion of hTERT (infinity telomerase-immortalised) human fibroblast cells, *Staphylococcus aureus* and *Staphylococcus epidermidis* to these surfaces were studied.

**METHODS:** Materials used in the study (Table 1) were characterised using laser profilometry for roughness, contact angle for wettability, and scanning electron microscopy (SEM) for morphology. The surfaces were either coated with 5µg/ml human plasma fibronectin (Fn) or left uncoated. To quantify the amount of cell spreading on each surface, approx. 20,000 hTERT fibroblasts were cultured in DMEM with 10% FCS at 37ºC onto each surface for 2 and 4 days, before fixation and imaging with an SEM using a backscattered electron detector (BSE)[2]. The area of spread cells were analysed using an image analysis package. *S. aureus* (SA) and *S. epidermidis* (SE) were cultured on the test surfaces (no Fn) in Brain Heart Infusion broth for 2 and 4 hours. Adherent bacteria were fixed and imaged with an SEM using BSE imaging[2], and the amount adhering quantified using a Partec PAS flow cytometer.

| Materials used | Code | Ra (µm) | Contact angle |
|---|---|---|---|
| 100% hydrophobic PU | 100% | 0.28 | 80 +/- 1 |
| 70/30 pho:phi PU | 70% | 0.16 | 73+/- 2.5 |
| 30/70 pho:phi PU | 30% | 1.93 | 77 +/- 2 |
| 70/30 poly(L-DL-lactide) | PLDL | 0.05 | 80 +/- 2 |
| Thermanox® (polyethylene tetraphtalate; cell culture plastic) | Therm | 0.04 | 64 +/- 2 |

*Table 1. Surfaces characterisation, including profilometry results and contact angle measurements*

**RESULTS:** The characterisation of the studied surfaces show that they have different roughness (Ra) and wettability (Table 1). 100% hydrophobic is the smoothest and 30% hydrophobic the roughest. hTERT cells showed the greatest degree of cell spreading on the 70% and Thermanox surfaces after 2 days with and without fibronectin (Fig 1). Only round cells were found on 100% and 30 % with and without fibronectin, therefore they were not analysed.

*Fig 1. Average cell area on each surface. A) without Fn after 2 and 4 days of culturing; B) with Fn after 2 days of culturing. Stars refer to samples not analysed because few spread cells were found on the surfaces.*

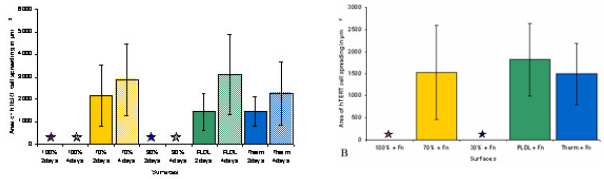

*S. aureus* and *S. epidermidis* were found on all surfaces to varying degrees when visualised with the SEM and counted with the flow cytometer (Fig. 2).

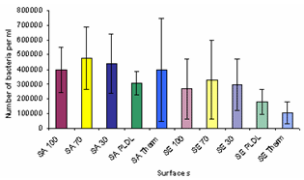

*Fig. 2. Differences in the amount of SA and SE adhering to each surface after 4h of culturing.*

**DISCUSSION & CONCLUSIONS:**
Surface characterisation have shown that the surfaces have different properties. On the 100% and 30% hydrophobic surfaces, hTERT cells spread less in comparison to the 70%, PLDL and Thermanox surfaces. The adsorption of fibronectin to the surfaces had no effect on the adhesion and spreading of hTERT cells when compared to the uncoated surfaces. A similar trend was observed in the adhesion of *S. aureus* and *S. epidermidis* to the surfaces. Slightly less *S. epidermidis* were seen in comparison to *S. aureus*.

**REFERENCES:** [1]Gorna K, Gogolewski S (2002) J Biomed Mater Res 60:592-606; [2]Richards RG, ap Gwynn I (1995) J Microsc 177:43-52.

**ACKNOWLEDGEMENTS:** Thanks to Markus Glarner for producing the PLDL surfaces.

European Cells and Materials Vol. 7. Suppl. 2, 2004 (pages 38-39) ISSN 1473-2262

# Measurement of pH near Fibroblast Cells on Stainless Steel and Titanium

S.Hiromoto[1], T.Hanawa[1]

[1] *Biomaterials Center, National Institute for Materials Science, Tsukuba, Japan.*

**INTRODUCTION:** The cells adhere to biomaterials through the points of contact with cell adhesive proteins. Around the cells, they generate extracellular matrix and various biomolecules and ions. Collagen and glycosaminoglycan in the extracellular matrix are long-chain molecules. They would raise the viscosity around the cells and mass transfer of molecules and ions around the cells would be prevented. The environmental change with cells affects the corrosion behavior of biometals. For example, when fibroblast cells are cultured on biometals, the precipitation of phosphate and calcium decreases and the electrochemical property of pure Ti changes [1-3]. Also, the redox potential at the interface is possibly modified because probably sulfate ion in the solution precipitates as sulfide/sulfite on stainless steel and pure Ti only when the fibroblast cells is cultured on the specimens [1,2].

In this study, pH near murine fibroblast L929 cells on 316L stainless steel and pure Ti was measured using a tungsten microelectrode to investigate the effect of cells on the chemical environment of the biometals.

**METHODS:** The surface of 316L stainless steel and commercially pure Ti (99.5%) disks was polished with #600 grid SiC paper (Buehler Ltd.). After autoclaving sterilization, the specimens were fixed on the base of polystyrene cell culture dish. The dish with specimen was sterilized again. The dish without specimens was also prepared. Murine fibroblasts L929 cells were cultured in the dish for 605 ks (7days) with MEM+FBS (Eagle's minimum essential medium with the addition of 10vol% of fetal bovine serum) in a 5% $CO_2$ incubator. The cells covered the base of dish after 605 ks. For comparison, the dish with the specimens and MEM+FBS was placed in the incubator for 605 ks. When pH was measured, the dish was moved inside a thermostatic unit at 310 K and 5% $CO_2$ gas was flown over the dish.

A saturated calomel electrode (SCE) and a tungsten (W) microelectrode with the tip with a diameter of 3 μm and a length of 5 μm were used as reference and pH sensor electrodes, respectively. The tip of the W electrode was placed at the intra-L929 cell adhesive layer (a few micrometer above the base) and 2-mm above the cell adhesive layer (*i.e.* extra-cell layer) on both specimen and polystyrene base as shown in *Fig. 1*. The tip was confirmed to be inside the cell layer under the observation by a stereoscopic microscope placed in the vertical line. In the case of the dish with only MEM+FBS, the tip of the W electrode was placed just over the base (a few micrometer above the base) and 2-mm above the base of the dish. The position just over the base is the same position of the intra-cell layer in the dish with cells. The measurement was performed on several dishes prepared in different experimental days and each dish was named alphabetically.

Open circuit potential ($E_{open}$) of the W electrode was monitored using a potentio-galvanostat. The $E_{open}$ was converted to pH using a pH-$E_{open}$ calibration curve measured in standard pH solutions.

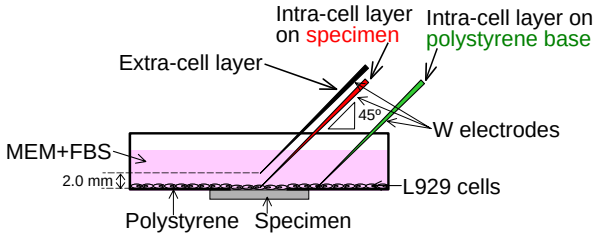


*Fig. 1: Measurement position of the W electrode in presence of cells.*

**RESULTS:** *Figure 2* shows the pH of the intra-adhesive layer on the specimens and polystyrene base. The pH of the extra-cell layer is shown as a dotted line in *Fig. 2*. The pH values of the intra-cell layer on 316L and Ti specimens were lower than those on polystyrene base and of the extra-cell layer. The pH of the intra-cell layer on 316L specimen was lower than that on Ti specimen. The pH of the intra-cell layer on polystyrene base was as same as that of the extra-cell layer.

*Figure 3* shows the pH just over the specimens and polystyrene base immersed in MEM+FBS without cells. The pH above the specimens and polystyrene base is shown as a dotted line in *Fig. 3*. The pH values just over 316L and Ti specimens were as same as those on polystyrene base, while the former was sometimes lower than

the latter. Also, the pH just over the specimens and polystyrene base were as same as that above the specimens and polystyrene base.

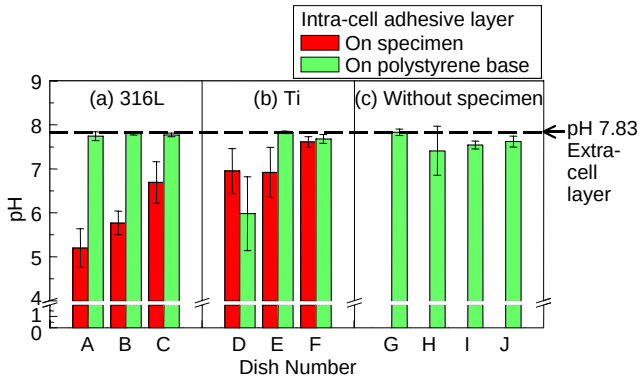


*Fig. 2: pH of the intra-cell adhesive layer on the specimens and polystyrene base.*

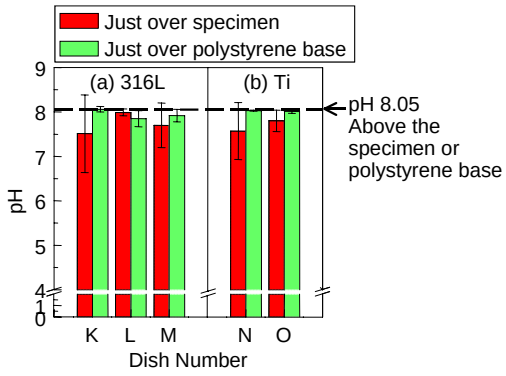


*Fig. 3: pH just over and 2-mm above the specimens and polystyrene base without cells.*

**DISCUSSION & CONCLUSIONS:** In presence of cells, only on the specimens, the pH of the intra-cell layer was lower than that of the extra-cell layer (*Fig. 1*). Without cells, the pH just over the specimen was also lower than that above the base (*Fig. 2*). These indicate that a certain interaction between the metallic materials and solution and cells causes the decrease of pH. The decrease of pH on 316L was larger than that on Ti, indicating that the corrosion reaction of the specimens is responsible for the decrease of pH because the corrosion resistance of 316L is generally lower than pure Ti. The decrease of pH at the intra-cell layer on the metallic materials is supposed to be caused by the acidifying effect of the dissolved metal ions. The dissolved metal ions are possibly accumulated at the interface between cells and materials due to the prevention of mass transfer by the extracellular matrix and cells.

The acidifying effect of metal ions depends on the concentration and the valence of the metal ions. The valence of the metal ions dissolved from 316L and Ti was not known, on the other hand, the concentration of the metal ions from 316L specimen is estimated to be higher than that from Ti specimen. According to this, the acidifying effect of dissolved metal ions on 316L specimen was larger than on Ti specimen. On the other hand, the molecules and ions generated by the cells against the dissolved metal ions are supposed to be another cause of the decrease of pH. Further investigation is necessary.

**REFERENCES:** [1] T. Hanawa et al (2002) *Mater. Trans* **43**:3088-3092. [2] S. Hiromoto et al (2004) *Biomaterials* **25**:979-986. [3] S. Hiromoto et al (2002) *Electrochim Acta* **48**:387396.

**ACKNOWLEDGEMENTS:** This work was supported by Japan Society for the Promotion of Science (JSPS), Young Scientists (B), Grants-in Aid for Scientific Research (15760545, 2003).

European Cells and Materials Vol. 7. Suppl. 2, 2004 (pages 40-41) ISSN 1473-2262

# Effect of Albumin on Fretting-Corrosion Mechanism of a Ti-Al-V Alloy

S.Hiromoto[1], S.Mischler[1]

[1] *Laboratory for Metallurgical Chemistry, Institute of Materials, EPFL, Lausanne, Switzerland.*

**INTRODUCTION:** Fretting is a kind of wear characterised by small amplitude displacement, typically less than 100 μm. It occurs often between screws and holes of bone plates and between the stem of artificial joints and bone. Acceleration of crack initiation, release of wear particles and enhanced corrosion of implants are consequences of fretting. The intracellular fluids surrounding implants contain various ions and molecules. The adsorption of species such as protein affects the wear behaviour of biometals. For example, the effect of protein on the sliding wear behaviour was investigated between polymers and biometals using pin-on-disk apparatuses [1,2]. It was observed that proteins may act as lubricant [1] or may increase the wear rate [2], and this depending on the experimental conditions. The effect of protein on the fretting behaviour of titanium alloys was not yet investigated.

In this study, the effect of albumin on the fretting behaviour of Ti-6Al-4V alloy was investigated using a previously developed tribo-electrochemical apparatus [3] allowing one to test metals under well-controlled mechanical and chemical conditions. The simultaneous acquisition of mechanical and electrochemical parameters during fretting permits a better insight into fretting mechanisms and the effect of proteins.

**METHODS:** 8 mm diameter Ti-6Al-4V alloy disks with a $R_a$ value of 0.6 μm and an $Al_2O_3$ ball with a diameter of 10 mm were employed as specimen and counter part, respectively. The specimen, $Al_2O_3$ counter part, electrolytic cell, and Pt counter and Ag/AgCl reference electrodes were mounted on the fretting apparatus as described elsewhere [3]. Phosphate buffer 0.9% NaCl solutions (PBS, pH 7.5) with and without 1.0 g/l bovine serum albumin were poured in the electrolytic cell and left for about 90 minutes. The temperature of the solution was kept at 310±1 K. A normal load of 10 N was applied to the specimens that were polarized at +0.5 V (Ag/AgCl). After 90 minutes polarization, the fretting oscillation with a displacement of 100 μm and a frequency of 1 Hz was applied for 60 minutes. After stopping fretting, the sample was removed from the cell and rinsed with ethanol. The worn surfaces were analyzed using scanning electron microscopy (SEM).

During the test, normal force, tangential force, and electric current were monitored. Each parameter was acquired at a sampling rate of 1000 points per second and, simultaneously, the mean value was calculated every second. Frictional coefficient was calculated by dividing the tangential force by the normal force.

**RESULTS:** *Figure 1* shows the evolution with fretting time of the mean values of frictional coefficient and current with and without albumin.

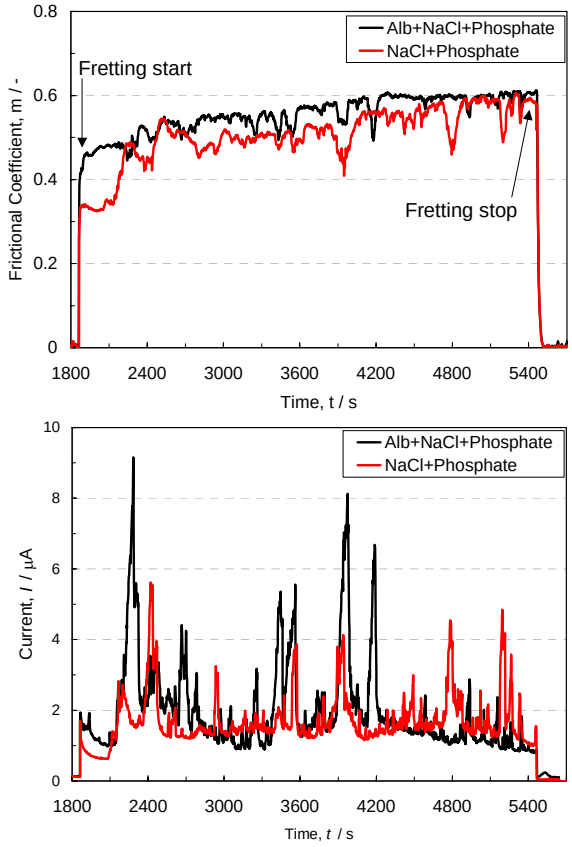


*Fig. 1: Mean value transients of frictional coefficient and current in phosphate buffer 0.9% NaCl solutions with and without albumin.*

The initial stage for 300 s showed smaller values of frictional coefficient and current than the latter stage characterised by large fluctuations. Interestingly, the fluctuations of the frictional coefficient and the current occurred in the same time. The intensity of current fluctuation with albumin was higher than that without albumin. On the other hand, there was not a significant

difference in average values of frictional coefficient and current with and without albumin.

SEM images of the wear trace are shown in *Fig. 2*. There were two regions in the wear trace: flat plateau region and abraded region. The relative ratio of abraded region to flat region with albumin was higher than that without albumin. High magnification images of the boundary between flat and abraded regions are shown in *Fig. 3*. The amount of wear particle accumulated in the abraded region with albumin was larger than that without albumin. The size of the wear particles varied from a few ten micrometers to finer sub-micrometer debris.

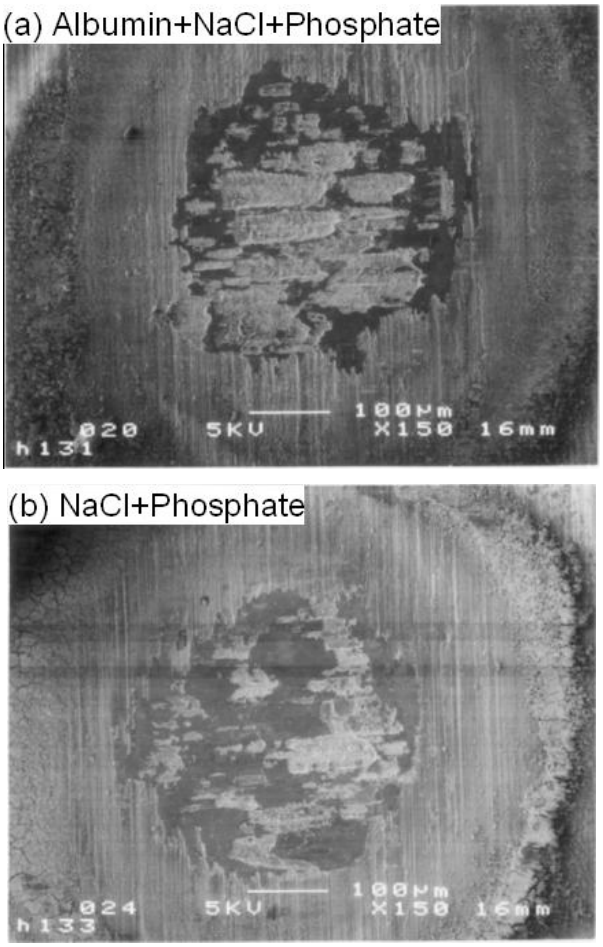


*Fig. 2: SEM images of the wear trace with and without albumin. (Low magnification)*

**DISCUSSION & CONCLUSIONS:** The fretting mechanism can be divided into two stages: the initial stage without fluctuation and the latter stage with fluctuations. The fluctuation of frictional coefficient and current was attributed to the formation of wear particles and to their ejection from the contact [3].

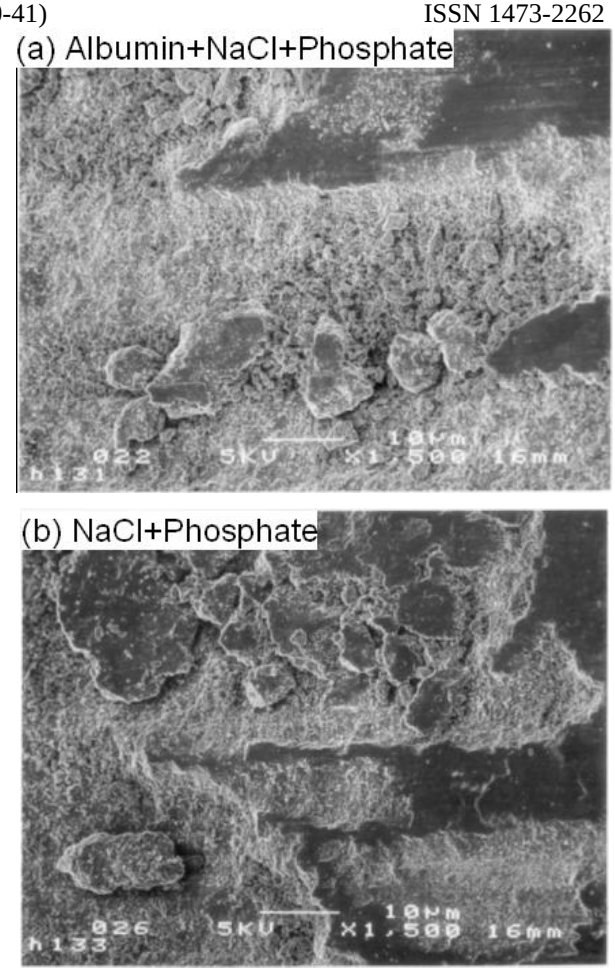


*Fig. 3: SEM images of the wear trace with and without albumin. (High magnification)*

Therefore, it is suggested that during the initial stage, the asperities of the surface are plastically deformed. The latter stage probably begins with the formation of large wear particles like the plates of a few ten micrometers shown in *Fig. 3*.

The intensity of current fluctuations (*Fig. 1*) and the relative ratio of abraded region in the wear trace (*Fig. 2*) increased with albumin. This indicates that albumin promotes the abrasion of the titanium alloy during fretting. Two mechanisms can explain this effect. First, the ductility of the asperities can be decreased by organic adsorbed species such as albumin (Rehbinder effect [4]). Another possible mechanism is that cohesion of the deformed layer is weakened by the albumin buried in it during plastic deformation.

**REFERENCES:** [1] J. Black (1992) Biological Performance of Materials, Marcel Dekker, Inc, pp 92. [2] M.R. Widmer et al (2001) *Tribology Lett* **10**:111-116. [3] S. Barril et al (2002) *Wear* **252**:744-754. [4] D.H. Buckley (1981) Surface Effects in Adhesion, Friction, Wear, and Lubrication, Elsevier Sci Pub, pp 553-567.

European Cells and Materials Vol. 7. Suppl. 2, 2004 (page 42) ISSN 1473-2262

# Monitoring of Cell Migration on Structured Surfaces

J.-P. Kaiser and A. Bruinink

*MaTisMed, Biocompatible Materials, Swiss Federal Laboratories for Material Testing and Research (EMPA), Lerchenfeldstrasse 5, CH-9014 St. Gallen*

**INTRODUCTION:** Cell migration is crucial to technological applications such as tissue engineering and implant surfaces [1]. Regarding bone related implants, like the hip prosthesis and dental implants, the correct interaction between bone marrow cells and implant materials is crucial for their clinical success. An optimal interaction consists in the colonization of the implant surface by the correct cell types and is among others determined by attachment and migration of latter cells. The observation of the cell migration and its analysis may be of key importance in order to understand the mechanisms [2]. In order to monitor cell behaviour over periods of several days, cells had been labelled with a fluorescent dye (DiI) [3]. The monitoring was done with a confocal laser scanning microscope combined with a computer-assisted image analysis software.

**METHODS**: For the observation of the mobility of the cells on the scaffolds, the cells were stained with a fluorescent lipophilic dye (DiI). For observing the movement of the cells on the scaffolds, the scaffold with the labelled cells was transferred in an incubation chamber, with a cover glass lid, which allowed the on-line observation of the cells on the scaffold. The monitoring was done with a confocal laser scanning microscope. With a heating chamber, which was installed around the microscope, it was possible to maintain a constant temperature of 36.7° C. The movement of the cells was monitored by using a Zeiss Axioplan 2 microscope with a LSM 510 scanning module. For the observation of the cell movement on the scaffolds the Zeiss LSM software Release 2.8 (12/2000) was used. During several days each 15 min. a picture was taken from several previously selected areas of interest. From the obtained pictures the migration pathway (trajectory), cell shape, migration direction and the migration velocity were estimated by special image analysis software developed by Visiometrics (Konstanz, D). Data were further analysed using MS Excel-macros.

**RESULTS and DISCUSSION:** Cells were seeded on a titanium scaffold with eleven different structures. By that consisting of grooves, and ridges of different width, depth and inter groove/ridge distances the observation of the cell migration could be monitored on all types of surfaces at the same time. On a plane, non-structured surface no guided migration was observed. The covered trails (trajectories) of the moving cells on the plane surface were random (Fig. 1a). The movement on the structured surfaces was different. The angles of the trajectories on grooved surfaces were quite well orientated along the axes of the grooves (Fig. 1b).

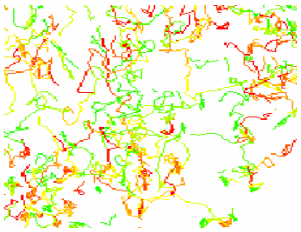

*Fig. 1a: The covered trails of moving cells on a plane surface were randomly distributed.*

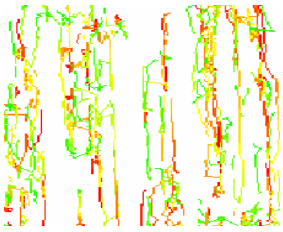

*Fig. 1b: The covered trails of migrating cells on a structured surface with deep grooves were following the direction of the grooves.*

The analysis of the cell shape revealed that the cells on the non-structured surface were randomly orientated. On grooved surfaces cells were better orientated. Depending from the depths of the grooves around 37 % to 53 % of the cells were orientated parallel to the axes of the grooves, within a variation in the latitude of ± 15 %. It was obvious that the topography on the scaffold surfaces influenced not only cell orientation and the direction of migration, but also the average velocity of the migrating cells in x and y direction. Even the cells on the structured surfaces migrated well orientated in the direction of the grooves, no significant differences in the frequency of the velocities were found between cells plated on the plane and cells plated on the structured surfaces.

**REFERENCES:** [1] D.A. Lauffenburger and A. Horwitz (1996) *Cell* **84**:359-369. [2] K. Webb, V. Hlady and P.A. Tresco (2000) *J. Biomed. Mat. Res.* **49**:362-368. [3] J.-P. Kaiser and A. Bruinink (2004) *J. Mater. Sci.: Mater. Med.* **15** 429-435.

European Cells and Materials Vol. 7. Suppl. 2, 2004 (page 43) ISSN 1473-2262

# Unexpected Tissue Engineering: Cartilage neoformation in long-term HydroCoil®- occluded experimental aneurysms

M. Killer[1], B. Richling[1], B. Minnich[2], A. Lametschwandtner[2], & H. Plenk Jr.[3]

[1] *Dept. Neurosurgery, Christian Doppler Medical Center, Paracelsus Medical University Salzburg,*

[2] *Institute for Organismal Biology, University of Salzburg,*

[3] *Bone &Biomaterials Research, Intitute of Histology and Embryology, Medical University Vienna, AUSTRIA*

**INTRODUCTION:** The long-term stability of coil-occluded aneurysms, especially in wide-necked aneurysms is rather poor. To minimize the recanalization rate mutiple coil modifications were introduced. In the new HydroCoils®(1), a hydrogel coating expands up to nine times by volume after deployment and is able to create a better filling volume of the aneurysm than with pure platinum coils. In our HydroCoil®-studies, the in vivo stability of occlusion in flow exposed aneurysms was evaluated angiographically, and the aneurysm healing and foreign body responses to this new endovascular tool were assessed histologically. We present the unexpected occurence of cartilage neoformation in these aneurysms one year after coiling.

**MATERIAL & METHODS:** In 42 rabbits wide-necked flow exposed carotid bifurcation aneurysms were constructed microsurgically. After a minimum healing of 3 weeks 21 aneurysms were treated with ComplexCoils® as basket coils, and HydroCoils® (MicroVention Inc., Aliso Viejo, CA, USA) as filling coils. In the other 21 cases HydroCoils® alone were used. After 6, 9 and 12 month the rabbits were again angiographed before sacrification. The aneurysm – parent artery – complexes were embedded into methyl-methacrylate, diamond saw-sections cut and ground to a thickness of 100 µm, surface-stained and evaluated by light microscopy.

**RESULTS:** Angiographically, the amount of filling of the aneurysms was dramatically increased, compared to pure platinum coils. Histologically, vascularized granulation tissue of varying density was growing from the walls of the aneurysms towards the center of the sac, and was also observed in the clefts between HydroCoils®. Especially in the long-term results after one year, neoformation of cartilage was observed there in 5 of 12 cases (Fig.1). The successful healing of the aneurysm was confirmed by the formation of an endothelium-covered new vessel wall at the aneurysm orifice.

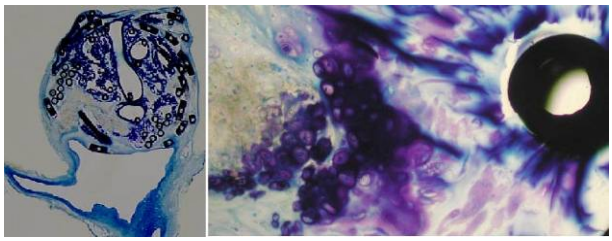

*Fig. 1: Ground section of a 1 year HydroCoil® – occluded aneurysm with the coils in-situ (left), and cartilage neoformation in the hydrogel-coating at higher magnification (right).*

**DISCUSSION & CONCLUSIONS:** The healing of embolized aneurysms is largely dependend on the nature and amount of the embolizing material. Aneurysms coiled with pure platinum coils are filled only with a small amount of material. Recanalization of the organized thrombus is caused mainly by hemodynamic factors. Blood pulsation pushes away coils placed at the aneurysm neck, and leads to compaction of coils and consecutive recanalization. The hydrogel coil works by expanding during the treatment session to fill spaces between coils and better obliterate the aneurysm. The mechanical forces of the blood flow, and the hydrogel as flow absorber, but also potential trigger of stem cells to form cartilage (2,3) may have resulted in this unexpected neoformation of cartilage in HydroCoil®-occluded aneurysms. This seems to represent better thrombus stabilization and healing with so far reduced chances for recanalization.

**REFERENCES:**

[1]Kallmes DF et al. (2002) New Expandable Hydrogel-Platinum Coil Hybrid Device for Aneurysm Embolization. *Am J Neuroradiol* **23**: 1580-88. [2]Archer CW et al.(2003) The chondrocyte. *Int J Biochem Cell Biol* **35**: 401-4. [3]Williams CG et al. (2003) In vitro chondrogenesis of bone marrow-derived mesenchymal stem cells in a photopolymerizing hydrogel. *Tissue Eng* **9**: 679-88.

**ACKNOWLEDGEMENTS:** These studies were supported by *MicroVention Inc*.

European Cells and Materials Vol. 7. Suppl. 2, 2004 (page 44) ISSN 1473-2262

# Early Cell and Tissue Reactions in a HydroCoil®–occluded Human Aneurysm

M. Killer[1], B. Richling[1], & H.Plenk Jr.[2]

[1] *Dept. Neurosurgery, Christian Doppler Medical Center, Paracelsus Medical University Salzburg,*
[2] *Bone &Biomaterials Research, Intitute of Histology and Embryology, Medical University Vienna, AUSTRIA*

**INTRODUCTION:** The HydroCoil®, a new device for endovascular aneurysm occlusion, has recently been described in animal studies (1). The coil's hydrogel coating expands up to nine times by volume after deployment and is able to create a better filling volume of the aneurysm than with pure platinum coils. We present the first histological evaluation of this coil in a deceased human subject. Our own previous human and animal studies serve as the basis for this histological evaluation (2,3).

**CASE REPORT:** A 52-year-old male presented with headache since ten days and was subsequently found to have a subarachnoid hemorrage from an aneurysm of the anterior communicating artery. The patient maintained in good neurological status (Hunt-Hess Grade II). Because of vasospasm, seen in the diagnostic angiogram, the patient underwent an embolization using HydroCoils® with additional pure platinum coils (MicroVention Inc., Aliso Viejo, CA, USA). Despite a wide-necked shape, the hydrogel coils could be deployed in optimal position. Subsequent hydrogel expansion obliterated the aneurysmal space, and complete occlusion of the aneurysm on angiograms(DSA) could be achieved (Fig.1). Due to severe vasospasm, which worsened despite extensive treatment, the patient developed multiple infarcts and died 26 days after treatment. The aneurysm-parent artery-complex was retrieved for histological evaluation of plastic-embedded, surface stained ground sections.

**RESULTS:** Histological evaluation showed the beginning of healing in the aneurysm sac, and the formation of a new vessel wall at the aneurysm orifice 3 weeks after coiling with HydroCoils®. Near the aneurysm wall, where uncoated coils could be seen, and in the center of the aneurysm, where HydroCoils® were placed, different stages of blood clot organization were found within a framework of fibrin. At the aneurysm orifice multiple fibrin layers were seen on both, uncoated and hydrogel-coated coils. Starting from the parent vessel wall, new cell layers had grown over the fibrin covered coils (Fig.2). These cell layers seem to be the beginning of a new vessel wall, covering the aneurysm orifice with a neointima.

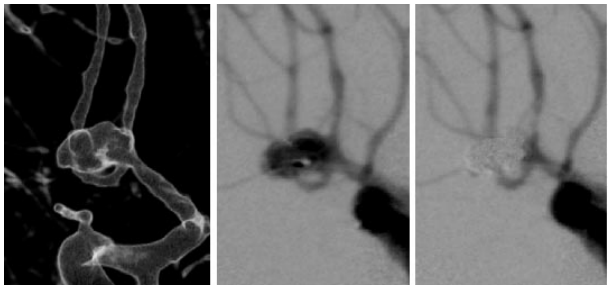

*Fig. 1: Working projection of the aneurysm in 3D-DSA reconstruction (left), and DSAs of the aneurysm before coiling (middle) and after 100 % occlusion without compromising the parent arteries (right).*

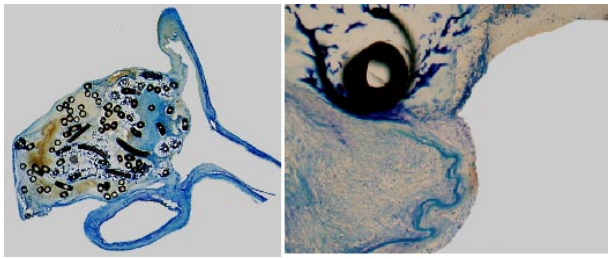

*Fig. 2: Histological overview of the aneurysm ground section with the coils in situ (left), and the cell layers from the parent artery forming a neointima.*

**DISCUSSION & CONCLUSIONS:** Hydrogel-coated coils represent a significant improvement of the aneurysm coil occlusion paradigm. As opposed to other reported coil modifications, HydroCoils® work by expanding during the treatment session to fill spaces between coils and obliterate the aneurysm. Thus thrombus stabilization and healing can occur better, and recanalization should be minimized.

**REFERENCES:** [1]Kallmes DF et al. (2002) New Expandable Hydrogel-Platinum Coil Hybrid Device for Aneurysm Embolization. *Am J Neuroradiol* **23**:1580-88. [2]Bavinzski G et al. (1999) Microscopic Histopathologic Findings in Aneurysms of the Human Brain Treated with Guglielmi Detachable Coils, *J Neurosurg* **91**:284-293. [3]Bavinzski G et al. (1999) Histopathological Findings in Experimental Aneurysms Embolized with Conventional and Thrombogenic/ Antithrombolytic Guglielmi Coils. *Minim Invasive Neurosurg* **42**:167-174.

European Cells and Materials Vol. 7. Suppl. 2, 2004 (pages 45-46) ISSN 1473-2262

# Experimental Verification of Viscoelastic Properties of Spongy Bone Tissue

L. Mezerová
*Czech Technical University, Faculty of Civil Engineering, Laboratory of Biomechanics and Biomaterial Engineering, CZ,* melzerov@fsv.cvut.cz

**ABSTRACT:** The viscoelastic properties of most biological materials are significant for the distribution and redistribution of the fields of deformation through the periods of time. The values of viscoelastic constants are not exactly defined for greater number of biomaterials. They are dependent on the age of a human being, on the intensity of loading, and on the period of time through which the loading acts. This research work has been aimed at the experimental and analytical determination of the coefficient of viscosity **λ**, and the modulus of elasticity of the time-dependent viscoelastic strain **E** in the spongy bone of human femurs.

It is Poynting-Thompson model that belongs to the most relevant mechanical models which enable us to determine the material rheological constants in the spongy bone tissue as precisely as possible. This model is made up of an elastic element characterized by the modulus of elasticity $E_0$, and of the Kelvin-Voight viscoelastic member that consists of an elastic element of the time-dependent viscoelastic strain E and the coefficient of viscosity λ.

In the order to determine the rheological constants, the total number of 3 male femurs and 3 female femurs were used.

**KEY WORDS:** spongy bone, viscoelastic properties, rheological constants

**INTRODUCTION:** This research work has been aimed at the experimental and analytical determination of the coefficient of viscosity **λ**, and the modulus of elasticity of the time-dependent viscoelastic strain **E** in the compact bone of human femurs.

It is Poynting-Thompson model that belongs to the most relevant mechanical models which enable us to determine the material rheological constants in the spongy bone tissue as precisely as possible.

The influence of viscoelasticity on the value of relative strains of the spongy bone tissue of the femur diaphyses is a comparatively small. After a eight minute loading of the bone tissue through a load, the strains increase by about 1- 2 %.

**METHODS:** In the order to determine the rheological constants, the total number of 3 male femurs and 3 female femurs were used.

| Samples | Sex | Age | Height (m) | Weight (kg) |
|---|---|---|---|---|
| 1 | Man | 27 | 1,8 | 80 |
| 1 | Man | 27 | 1,8 | 80 |
| 2 | Woman | 30 | 1,58 | 75 |
| 2 | Woman | 30 | 1,58 | 75 |
| 3 | Man | 35 | 1,72 | 80 |
| 3 | Man | 35 | 1,72 | 80 |
| 4 | Woman | 36 | 1,72 | 80 |
| 4 | Woman | 36 | 1,72 | 80 |
| 5 | Man | 47 | 1,78 | 72 |
| 5 | Man | 47 | 1,78 | 72 |
| 6 | Woman | 47 | 1,74 | 72 |
| 6 | Woman | 47 | 1,74 | 72 |

Table 1: Samples of spongy bone

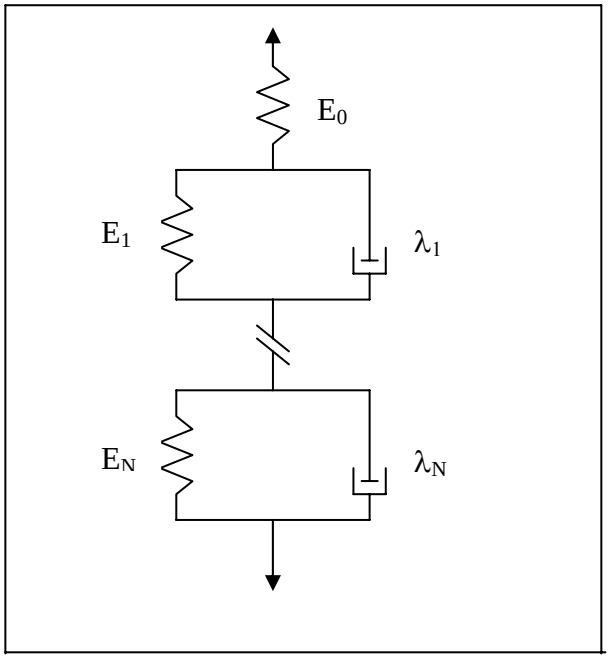


It is Poynting-Thompson model that belongs to the most relevant mechanical models which enable us to determine the material rheological constants in the spongy bone tissue as precisely as possible. This model is made up of an elastic element characterized by the modulus of elasticity $E_0$, and of the Kelvin-Voight viscoelastic member that consists of an elastic element of the time-dependent viscoelastic strain E and the coefficient

of viscosity λ. For the resultant bone tissue relative strain, the following equation applies:

$$\varepsilon = \varepsilon_1 + \varepsilon_2 = \frac{\sigma}{\varepsilon_0} + e^{\frac{-E^*t}{\lambda}}\left[\frac{1}{\lambda}\int_0^t \sigma(\tau)^* e^{\frac{E^*\tau}{\lambda}} d\tau + \left(\varepsilon_0 - \frac{\sigma_0}{E_0}\right) e^{\frac{E^*t_0}{\lambda}}\right]$$

in witch $E_0$ is the modulus of elasticity given by the stress ratio σ and the immediate elastic strain ε, E is the modulus of elasticity of the time-dependent viscoelastic strain, λ is the coefficient of viscosity, $\sigma_0$, $\varepsilon_0$ are stresses and strains in the initiate time $t_0$.

In the order to determine the rheological constants, the total number of 3 male femurs and 3 female femurs were used. The miniature beams of 10 x 10 x 15 mm were taken out of the femurs. Then the beams were placed into a loading device and exposed to stress. Strains in the damp bone tissue (that was extracted from human beings not later than twelve hours after their death) were being detected for load during the period of 10 minutes.

**RESULTS:** On the basis of experimental measuring and analytical solution, the following conclusions can be made: moduli of elasticity $E_0$ = 4,18 MPa , the modulus of elasticity of the time-dependent viscoelastic strain, and the coefficient of viscosity were verified at a value of 32 GPa, and 6,7 GPa.min respectively.

**CONCLUSION:** Presented results of the experimental measurements proved that:

The influence of viscoelasticity on the value of relative strains of the spongy bone tissue in the femur is a comparatively small.

After a ten-minutes loading of the bone tissue through a load, the strains increase by about 1-2 % only (!!!).

The influence of viscoelastic properties of the spongy bone tissue on the value of relative strains during the normal process of walking is insignificant and practically negligible. It becomes fully evident only after long-term loading, approximately after five minutes at the earliest.

**ACKNOWLEDGEMENT:** This research has been supported by the research project of GACR No. 106/02/D104

European Cells and Materials Vol. 7. Suppl. 2, 2004 (page 47) ISSN 1473-2262

# β-TCP/PLGA open porous scaffolds for the prevention of alveolar bone loss after tooth extraction: Evaluation in a mini-pig model

Nair PNR [1], Luder HU [1], Maspero FA [2], Ruffieux, K [2], Fischer JH [3], Schug J [1]

[1] Centre of Dental and Oral Medicine, University Zurich, Zurich, Switzerland
[2] Degradable Solutions AG, Schlieren, Switzerland
[3] Institute of Experimental Medicine, University of Köln, Köln, Germany

## Introduction

The major consequence of human tooth extraction is the loss of alveolar bone during remodelling of the jaw. During the first 6 months after the extraction, the height and volume of the alveolar process decrease substantially. Consequently, therapeutic reconstruction of the alveolar process requires considerable operative efforts and financial in puts.

A resorbable β-TCP/PLGA scaffold was developed in order to maintain the dimensions of the alveolar process. Using a moulding technique, the scaffold can be exactly shaped into the form of the root of an extracted tooth. This scaffold had an interconnected open porosity (55%) and a medium pore diameter of 280µm. Its degradation happens without the release of large amounts of acidic products. These features tend to favour tissue in-growth and the formation of bone in the extraction site so as to prevent atrophy of the alveolar bone.

In order to evaluate the biocompatibility and resorbability of the β-TCP/PLGA scaffold, an *in vivo* study was carried out using a mini-pig model. The aim of this communication is to present the results of the animal experiments.

## Materials and Methods

The suitability of β-TCP/PLGA scaffold for the preservation of alveolar bone was investigated in a mini-pig model. Using the root of the mandibular third incisor, a polyvinylsiloxane mould was prepared in order to exactly reproduce the shape of the root. The cavity of the mould was then filled with β-TCP granules (ø: 500-800µm) coated with a PLGA thin layer (about 15 µm). The mould with the granules was then heated at 80°C for 2 min. Due to this thermal treatment the granules fused together and formed a mechanical stable copy of the root.

A total of six left mandibular third incisor-sockets were treated with the scaffolds and four contra-lateral sites were used as non-treated controls. Animals were killed after 20, 40 and 60 weeks. Tissue reaction and the last stages of resorption of the scaffold-material were investigated by means of correlative histological and ultrastructural methods.

## Results

The proposed β-TCP/PLGA scaffold could be rapidly prepared using a moulding technique.

The fusion of the granules resulted in an open porous scaffold, which represented the exact copy of the root (Figure 1).

**Figure 1**: β-TCP/PLGA open porous copy of the root of a mandibular third incisor of a mini-pig. The open porosity of the scaffold allows the absorption of autologous blood.

The mechanical stability of the scaffold allowed easy handling and insertion of the replica into the extraction site.

The scaffolds implanted into the extraction sockets of the mini-pigs did not affect a satisfactory healing of the wound. No signs of microbial infection, exudation or dehiscence could be observed 10 days after the operation. No scaffolds were lost.

Macroscopically, the dimensions of alveolar process could be maintained as confirmed by standardized photographic and radiographic means.

Histological and fine structural investigations confirmed the biocompatibility and resorbability of the scaffolds. The β-TCP/PLGA granules were completely resorbed, showing at 60 weeks only clinically insignificant traces of calcium phosphate in multinucleated giants cells.

## Conclusions

The use of β-TCP/PLGA scaffolds seems to be a suitable therapeutic innovation for the prevention of alveolar bone loss after tooth extraction. They are completely resorbable and are replaced by newly formed bone tissue. The resulting bony bed will offer stable anchorage of a titanium dental implant.

# Thermo-explantation. A novel approach to remove osseointegrated implants

G. Massei [1], S. Szmukler-Moncler [2]

[1] *Private Practice in Torino, Italy,* [2]*Consulting in Implantology, Basel, Switzerland.*

**INTRODUCTION:** Explantation of osseo-integrated implants is indicated in case of implant fracture or because of revision. In addition, orthodontic dental implants have to be removed after being used as a stable anchor to mobilize teeth on the mandibular or the maxillary arcade. Implant removal is usually performed with trephines or with bone chisels. These mechanical methods are invasive and large bone defects are left behind. In some cases, the bone defect is too large to permit further implant replacement. In the present paper, we present a non-invasive method to remove osseointegrated implants.
Bone drilling for the preparation of an implant bed is performed with profuse irrigation, in order to avoid thermo-necrosis of the surrounding bone. To remove osseointegrated implants, we induced a localized thermo-necrosis at the bone-implant interface. The localized thermo-necrosis proved to weaken the bone-implant interface; the osseointegrated implants could be easily removed. We report here on the first 20 dental implants removed with this method.

**METHODS:** An Ultra-High Frequency (UHF) electrosurgical device (XO-ODONTOSURGE, XO-CARE, Hørsholm, DK) working at 27 MHz was used. A 3 seconds impulse was delivered by contacting the surgical wire to the metallic titanium implants. Anesthesia of the patients was not needed. After 2 weeks, the implants were reverse-torqued with a left-rotating device that was jammed in the broken part of the implants. The device was attached to a dynamometric key (Straumann AG, Waldenburg, CH) delivering torques in the 15-50 Ncm range. After implant removal, the sites were curetted and left to heal for 2 months. After 2 months, implants were placed if necessary. Seven fractured Screw-Vent (Screw-Vent, Encino, CA) implants and 13 osseointegrated TPS-coated implants of Ø 3.25 mm (Oraltronics, Bremen, D) used for an orthodontic purpose were removed. A biopsy was gained from one patient after removal of a fractured dental implant. The aim was to evaluate the extension of the induced bone thermo-necrosis. Three transversal histological sections were obtained, one from the apical end, one from the coronal portion and one from the middle. The sections were stained with Paragon and observed under the light microscope at a 1-200 x magnification.

**RESULTS:** The implants to be removed were submitted to a reverse-torque of 50 Ncm before treatment. All were clinically stable. Two weeks after delivery of the UHF impulse, the implants were reverse-torqued. All implants could be removed with a torque < 30 Ncm. After implant removal, the bone defect was minimal, gingiva suturing was even not necessary. The histological sections showed partial bone necrosis only. Bone necrosis was localised within 50 microns of the bone-implant interface.

**DISCUSSION & CONCLUSIONS:** This method prove to be efficient in the 20 treated cases. The retrieved biopsy suggests that bone-necrosis is limited to the interface, provided that the present impulse delivery conditions are respected. The thermal shock delivered by the UHF device is limited in time, temperature returns back to the initial temperature within 15 seconds (non published data) because the UHF impulse has no inertia. With this method, all osseointegrated implants, machined or TPS-coated, were easily removed without trephining. This non-invasive method, permitted successful replacement of implants of similar diameter, shortly after implant removal. Thermo-explantation should replace advantageously the trephine explantation method. Further studies should indicate if this method can be relevant to ease the removal of orthopaedic implants.

**REFERENCES:** [1] CW. Wilcox, TM Wilderling, P. Watson, JT Morris. (2001). Use of electrosurgery and lasers in the presence of dental implants. *Intern J Oral Maxillofac Implants* **16**:578-582.

Correspondence : ssm@bluewin.ch

# Effect of Ciprofloxacin-Releasing Bioabsorbable Polymer on Prevention of *Staphylococcus Epidermidis* Attachment and Biofilm Formation *in vitro*.

S-M.Niemelä[1], I.Ikäheimo[2], M.Koskela[2], M.Veiranto[3], E.Suokas[4], P.Törmälä[3], N.Ashammakhi[1,3], H.Syrjälä[5]

[1] *Department of Surgery, Oulu University Hospital, Oulu, Finland.*
[2] *Clinical Microbiology Laboratory of Oulu University Hospital, Oulu, Finland.*
[3] *Institute of Biomaterials, Tampere University of Technology, Tampere, Finland.*
[4] *Linvatec Biomaterials Ltd., Tampere, Finland.*
[5] *Department of Infection Control, Oulu University Hospital, Oulu, Finland.*

**INTRODUCTION:** Antibiotic coating systems have been successfully used to prevent bacterial attachment and biofilm formation. Our purpose was to evaluate whether bioabsorbable polylactide-co-glycolide (PLGA) 80/20 on its own, and PLGA together with ciprofloxacin (PLGA+AB) have any advantages over titanium in preventing *Staphylococcus epidermidis* attachment and biofilm formation in vitro.

**MATERIALS AND METHODS:** Cylindrical specimens of titanium, PLGA and PLGA+AB in triplicate were examined for *S. epidermidis* ATCC 35989 attachment and biofilm formation after incubation with a bacterial suspension of *ca.* $10^5$ cfu/ml for 1, 3, 7, 14 and 21 days, using scanning electron microscopy. Growth inhibition properties of PLGA and PLGA + AB cylinders were tested on agar plates.

**RESULTS:** On days 1, 3 and 21, no bacterial attachment was seen in 19.5%, 9.2% and 41.4% of the titanium specimens, in 18.4%, 28.7% and 34.5% of the PLGA specimens and in 57.5%, 62.1% and 57.5% of the PLGA + AB specimens, respectively. During the whole study period no biofilm was observed on 74%–93% of the titanium specimens, 58%–78% of the PLGA specimens and 93%–100% of the PLGA+AB specimens. PLGA + AB showed clear bacterial growth inhibition on agar plates while PLGA and titanium did not show any inhibition.

**CONCLUSIONS:** PLGA + AB bioabsorbable material was superior to titanium in preventing bacterial attachment and biofilm formation and may have clinical applicability, for example, in prevention of infection in trauma surgery or in the treatment of chronic osteomyelitis.

*Figure 1. Growth inhibition of S. epidermidis ATCC 35989 on agar plates. A) titanium, B) polylactide-co-glycolide (PLGA) 80/20, C) PLGA 80/20 containing ciprofloxacin.*

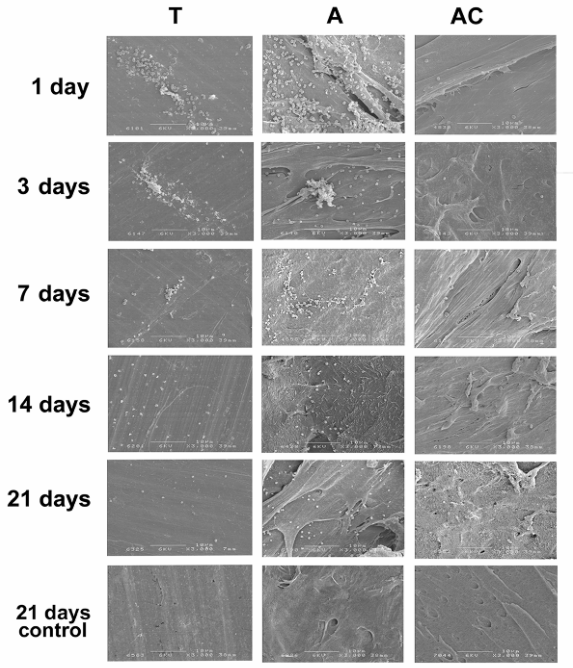


*Figure 2. Scanning electron micrographs of materials incubated with S. epidermidis ATCC 35989 for 1, 3, 7, 14 and 21 days, and control cylinders after 21 days of incubation in TSB medium without bacteria. Tested materials were titanium (T), polylactide-co-glycolide (PLGA) 80/20 (A) and PLGA 80/20 containing ciprofloxacin (AC).*

**ACKNOWLEDGEMENTS:** Research funds from the Technology Development Center in Finland (TEKES, Biowaffle Project 40274/03 and MFM Project 424/31/04), the European Commission (EU Spare Parts Project QLK6-CT-2000-00487), the Academy of Finland (Project 73948) and the Ministry of Education (Graduate School of Biomaterials and Tissue Engineering) are greatly appreciated.

European Cells and Materials Vol. 7. Suppl. 2, 2004 (page 50) ISSN 1473-2262

# Generation of Cartilage using Prefabricated Microvascularied Perichondrial Bioabsorbable Polylactide Nonwoven Scaffolds

H.Penttilä[1], R-M.Tulamo[2], T.Waris[3], V.Ellä[4], M.Kellomäki[4], P.Törmälä[4], N.Ashammakhi[3,4]

[1] *Department of Maxillofacial Surgery, Helsinki University Hospital, Helsinki, Finland.*
[2] *Department of Veterinary Medicine, University of Helsinki, Helsinki, Finland.*
[3] *Department of Surgery, Division of Plastic Surgery, Oulu University Hospital, Oulu, Finland.*
[4] *Institute of Biomaterials, Tampere University of Technology, Tampere, Finland.*

**INTRODUCTION:** It has been demonstrated that cartilage can be grown by using free perichondrial transfers in muscle tissue. The size of such grown cartilage pieces is, however, limited by the ability of nutrients and oxygen diffusion into the growing tissue because of the lack of vascularity. Growth factors have been tried to improve the outcome but none have been successful so far to induce permanent vascularity to the constructed tissue.

**AIM**: The aim of this experiment is to demonstrate whether it is possible to grow definitely larger and eventually thicker constructs of cartilage by using a composite of prefabricated grafts. These would provide vascularity and favourable environment for the chondrocytes to migrate into and grow.

**MATERIALS AND METHODS:** We used rabbits as experimental animals. As the source of perichondrium we used dorsal ear perichondrium with central artery and vein. As scaffold we used non-woven PLDLA 96/4 (poly-L/D-lactic acid 96/4) 1 mm thick 80 x 30 x1 mm sized pieces. The perichondrial flaps were raised and the pedicular vessels were dissected free and separated. Each scaffold was cut to the size of the flap and rounded at the corners. The flaps were placed under the ventral skin of each rabbit. The pedicular vessels were anastomosed to the femoral vessels, as end-to-end for arteries and side-to-end for veins. The ear skin was closed over the existing cartilage and the inguinal incision over the anastomosis area. The follow-up groups were 1 month, 3 months and five months. As controls we used three animals, one with biodegradable scaffold only, one with perichondrial flap and scaffold without microvascular method and one with microvascular pericohndrial flap without biodegradable scaffold. All controls were in the 5-month follow-up group.

**RESULTS:** It is feasible and the animals as well as the flaps have survived the procedure. Cartilage formation varied between animals and it was not time dependent. There was an invasion of the

scaffolds by fibroblasts led to fibrous tissue formation instead of cartilage inside the scaffolds.

**CONCLUSIONS:** Microvacularised perichondrial flaps combined with biodegradable scaffolds can be used to tissue-engineer cartilage constructs in a rabbit model. This may have an impact in staged clinical cartilage reconstruction in human.

**KEYWORDS:** Biodegradable scaffolds, cartilage, microsurgery, tissue engineering

**ACKNOWLEDGEMENTS:** Research funds from the Technology Development Center in Finland (TEKES, Biowaffle Project 40274/03 and MFM Project 424/31/04), the European Commission (EU Spare Parts Project QLK6-CT-2000-00487), the Academy of Finland (Project 73948) and the Ministry of Education (Graduate School of Biomaterials and Tissue Engineering) are greatly appreciated.

European Cells and Materials Vol. 7. Suppl. 2, 2004 (pages 51-52) ISSN 1473-2262

# Cobalt-Chromium Dental Alloys Enriched with Precious Metals

L. Reclaru[1], H. Lüthy[2], P.Y. Eschler[1], A. Blatter[1], O. Loeffel[2], M.H. Zurcher[3].
*PX Tech[1], La Chaux-de-Fonds; University of Zürich[2]; PX Dental[3], La Chaux-de-Fonds; Switzerland*

## INTRODUCTION

Non precious dental alloys (Co-Cr) compared to conventional gold alloys reveal generally an inferior corrosion resistance (pitting, crevice corrosion)[1]. A new generation of cobalt-chromium alloys enriched with precious metals (Au, Pt, Ru) are now coming on the market with the idea to improve the corrosion resistance.

The goal of this study was to verify this hypothesis.

## MATERIALS AND METHODS

The compositions of the commercial tested alloys and of a "classical" Co-Cr alloy are listed in Table I.

| *Chemical composition (wt %)* | | | | | |
|---|---|---|---|---|---|
| **Element** | **Co-Cr** | **#1** | **#2** | **#3** | **#4** |
| Co | 63.7 | 63.5 | 52.0 | 50.6 | 59.3 |
| Cr | 28.9 | 21.0 | 25.0 | 18.5 | 25.0 |
| Mo | 5.3 | | 4.5 | 3.0 | 5.0 |
| Ga | | 4.5 | 6.0 | | 2.5 |
| In | | trace | 5.0 | | 1.2 |
| Au | | 2.0 | 2.0 | | 2.0 |
| Pt | | trace | 2.0 | 15.0 | |
| Ru | | | | 10.0 | |
| Sn | | | 1.0 | | |
| Mn | 0.8 | 6.5 | 0.5 | 1.0 | |
| Si | | | 2.0 | 0.75 | |
| W | 0.1 | | | 0.5 | 4.0 |
| Nb | | | | 0.5 | |
| Al | | 2.5 | | | |
| Ti | | | | trace | |
| Fe | 0.4 | | | | |

**Table I**. Composition of the tested alloys (wt %).

Before electrochemical testing the alloys were analyzed micrographically and the phases identified by EDX (polishing of the specimens with SiC paper grit 320/500/1200/2400 then with polycrystallised diamond spray 6 µm/ 3 µm/ 1 µm (Struers, Copenhague, DK). The electrolytic etching was done in a bath of 100 ml $H_2O$ dest., 10 ml HCl conc. and 5 g chromium(VI)-oxide under 0.4 V / 0.3 A during 5 sec.[2]

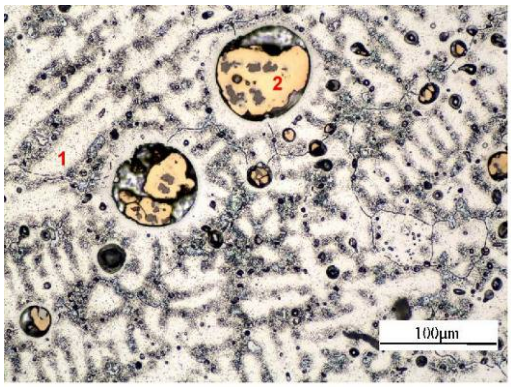


| | Co | Cr | Mo | Si | Mn | Ga | In | Fe | Pt | Au |
|---|---|---|---|---|---|---|---|---|---|---|
| **1** | 60.15 | 28.42 | 4.39 | 1.06 | 0.50 | 4.89 | | 0.58 | | |
| **2** | 1.30 | 0.62 | | | | | 42.77 | | 28.31 | 27.01 |

**Fig. 1**. Microstructure of alloy #1 and phases composition (wt %).

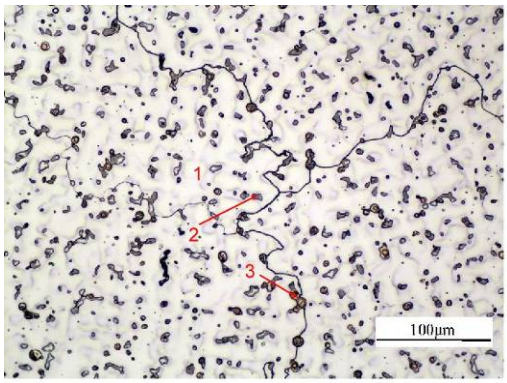


| | Co | Cr | Mo | Si | Ti | W | Ga | In | Pt | Au |
|---|---|---|---|---|---|---|---|---|---|---|
| **1** | 63.48 | 25.71 | 3.55 | | | 4.85 | 2.41 | | | |
| **2** | 28.46 | 32.83 | 22.98 | 1.74 | 0.95 | 11.31 | | | 1.73 | |
| **3** | 1.91 | 0.76 | | | | | | 13.52 | | 83.80 |

**Fig. 2**. Microstructure of alloy #2 and phases composition (wt %).

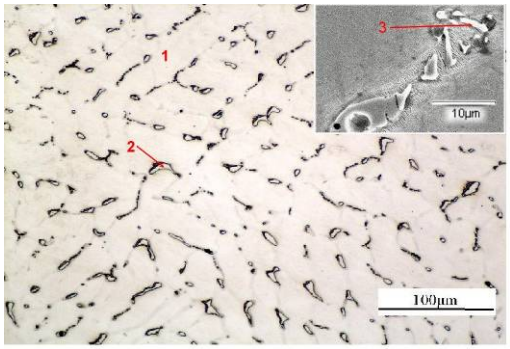


| | Co | Cr | Mo | Si | Mn | W | Ti | Nb | Pt | Ru |
|---|---|---|---|---|---|---|---|---|---|---|
| **1** | 48.96 | 17.48 | 3.44 | 1.02 | 0.70 | 1.25 | | | 16.44 | 10.72 |
| **2** | 42.75 | 19.51 | 11.76 | 4.36 | 0.88 | 1.56 | | | 8.25 | 10.93 |
| **3** | 15.33 | 9.47 | 10.70 | 1.01 | | 0.79 | 2.85 | 47.79 | 7.19 | 4.85 |

**Fig. 3**. Microstructure of alloy #3 and phases composition (wt %). Upper right: SEM picture.

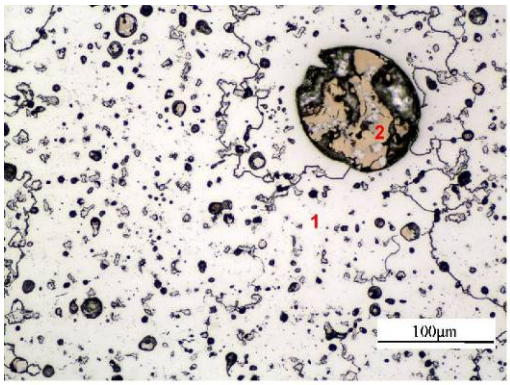


| | Co | Cr | Mo | Si | Ga | In | Pt | Au |
|---|---|---|---|---|---|---|---|---|
| **1** | 59.61 | 28.04 | 5.37 | 0.63 | 6.35 | | | |
| **2** | 1.44 | 0.76 | | | | 51.17 | 28.87 | 17.77 |

**Fig. 4**. Microstructure of alloy #4 and phases composition (wt %).

### *Electrochemical measurements*

The test samples had the form of discs of diameter 11 mm. They were metallographically polished with diamond paste (granulometry 1 µm).

Electrochemical measurements were conducted in artificial saliva of the Fusayama type (dearated with nitrogen, temperature 37°C, pH = 5) using the rotating electrode technique. The cathodic and anodic potentiodynamic polarisation curves were measured from - 1000 mV to + 1250 mV vs. SCE

## RESULTS

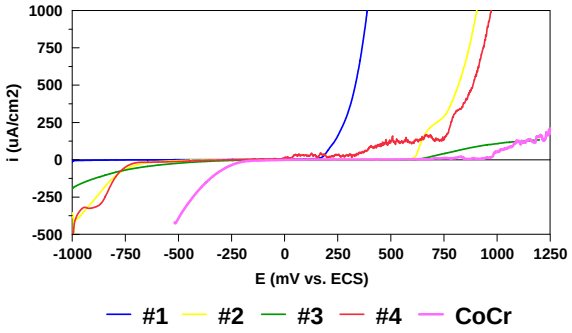


**Fig. 5** Potentiodynamic polarization curves in linear system of alloys #1 to # 4 in comparison with a conventional Co-Cr alloy.

The potentiodynamic curves displayed in Fig. 5 reveal important differences in the behaviour of the studied alloys (#1 - #4) as compared to the conventional Co-Cr alloy. The worst behaviour was given by the alloys containing only gold (#1 and #4), confirming the results of Kappert and Schuster[3]. Au is not miscible to Co and Cr.

## CONCLUSIONS

Alloys #1 and #4 showed a very complexe microstructure compared to the other studied alloys. The round "inclusions" with a diameter up to 0.1 mm are in part non miscible phases with a very low corrosion resistance. From the point of view of corrosion behaviour, the classical Co-Cr alloy is the best material followed by the alloys #2 and #3 (addition of respectively 4 % and 25 % of precious metals). The worst alloys, were #1 and #4 (with only addition of 2 % of Au). Scientifically speaking Co-Cr dental alloys enriched with precious metals is a non-sense.

## Reference

1. L. Reclaru; J.-M. Meyer, Effects of fluorides on titanium and other dental alloys in dentistry; *Biomaterials* **19** (1998), 85-92.

2. G. Petzow; Metallographisches, keramographisches, plastographisches Aetzen; Editions Gebrüder Borntraeger, Berlin – Stuttgart, 1994, p. 92.

3. H.F. Kappert, M. Schuster; *Dental Labor* **43** (3) (2000), 352 – 354.

European Cells and Materials Vol. 7. Suppl. 2, 2004 (page 53) ISSN 1473-2262

# Seeding Strategies for 3D Silk Scaffolds Using Human Mesenchymal Stem Cells

HM. Ruedlinger, S. Hofmann, A. Koch, C. Carugo, HP. Merkle, L. Meinel

*Galenische Pharmazie, ETH Zürich, Winterthurerstrasse 190, CH-8057 Zurich, meinel@mit.edu*

**INTRODUCTION:** Initial steps of the cultivation of engineered tissues in bioreactors involve cell seeding of three-dimensional scaffolds. These procedures usually require a high yield, to maximize the utilization of donor cells, a minimal time in suspension for anchorage-dependent and shear-sensitive cells, and spatially uniform distribution of attached cells, for rapid and uniform tissue regeneration. Our hypothesis was that dynamic seeding strategies are superior to static seeding in terms of total cell number, cell viability, attachment to the scaffold, and homogenous distribution of cells as compared to static seeding.

**METHODS:** Highly porous silk-fibroin scaffolds (8 mm in diameter and 2 mm thick) with pore diameters of 112 µm, 400 µm, and scaffolds with 112 µm at one end and 400 µm at the other, were (i) seeded with human mesenchymal stem cells (MSC) in well-mixed spinner flasks (dynamic seeding) or (ii) MSC were first suspended in a gel –gel is liquid below 20°C - and this cell-liquid suspension was applied to scaffolds and directly transferred to 37°C (static seeding).

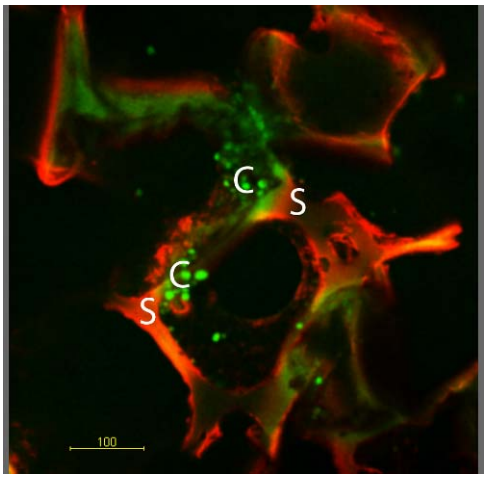


*Fig. 1: Dynamic seeding results in direct attachment of cells (C) to the silk lattice (S).*

**RESULTS:** Substantially more cells were deposited on the scaffolds – as determined by total DNA content - using static seeding regimens, and the number of living cells – as determined by MTT transformation – and the ratio of viable to total MSC was the same for both seeding protocols. Pore size did not have significant impact on MSC number or viability. MSC attached to the scaffold lattice when seeded dynamically (**Figure 1**) whereas statically seeded cells were found in the scaffold's void spaces and entrapped in the gel (**Figure 2**). As determined by live-dead staining and confocal microscopy, all MSCs were alive when seeded dynamically, whereas dead cells – although few in number - were randomly observed and entrapped within the gel matrix between the scaffold rods (**Figure 2**).

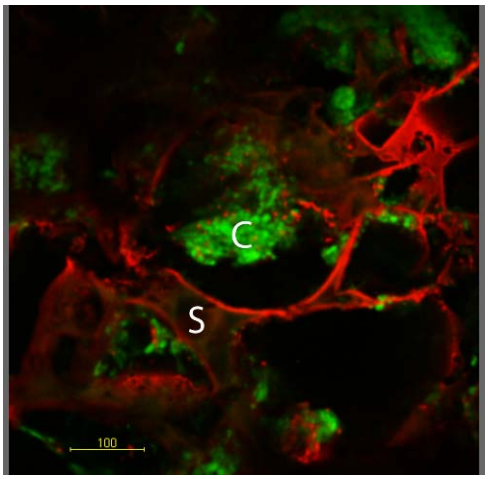


*Fig. 2: Statically seeded cells (C) reside in void areas within the silk network (S).*

**DISCUSSION & CONCLUSIONS:** Our hypothesis as mentioned above was not fully confirmed as the same levels of living cells were found using either seeding protocol. However, dynamically seeded cells distributed homogenously over the scaffold area and cells were attached to the scaffold, whereas static regimens resulted in clusters of cells entrapped in the gel matrix after 2 days.
The proximity of the cells to the scaffold lattice and the proportion of living cells suggests dynamic approaches superior to static seeding for three-dimensional silk scaffolds.

European Cells and Materials Vol. 7. Suppl. 2, 2004 (page 54) ISSN 1473-2262

# Enhanced bone regeneration by a biodegradable bioactive PLGA membrane

B. San Miguel[1,2,3], F.E. Weber[1,3]

[1] *Institute for Oral Biology, Section Bioengineering, University of Zurich, Switzerland.*
[2] *Laboratory for surface Science and Technology, Dept. of Materials, ETH-Zürich, Switzerland.*
[3] *Dept. Of Cranio-Maxillofacial Surgery, University Hospital Zürich, Switzerland.*

**INTRODUCTION**: Guided bone regeneration is a procedure where a membrane is used to create a compartment that can easily be occupied by bone. In order to avoid a second surgery, normally required for the removal of the membrane, a biodegradable guided bone regeneration membrane made out of L-lactide, D,L-lactide, polyglycolide and trimethylene carbonate was developed. To overcome the intrinsic rigidity of the PLGA material, a plasticizer (NMP) was used; this substance has recently been shown to be bioactive, as it enhances bone maturation in vitro as well as bone regeneration in vivo [1].

**METHODS:** *Alkaline phosphatase activity (ALP)*, an early osteoblast marker method, is based on the hydrolysis of *p*-nitrophenolphosphate into *p*-nitrophenol under alkaline conditions. *Alizarin Red mineralization* assay relies on the chelation of the dye "Alizarin red S" with a calcium molecule. *Histomorphometry analysis*: a 6 mm in diameter defect is drilled into the rabbit calvaria followed by membrane implantation. After 4 weeks, the correspondent tissue blocks are removed, embedded in methyl-methacrylate, cut, polished, and surface stained with Goldner Trichrome. All experiments were carried out in triplicate for statistical analysis.

**RESULTS:** The effect of NMP and its combination with human recombinant BMP-2 (rhBMP-2) was tested on a pre-osteoblastic cell line (MC3T3-E1) *in vitro,* both by Alkaline phosphatase activity (early osteoblastic marker) and Alizarin red mineralization assays. *In vivo*, the polymeric NMP-loaded membranes were implanted together with similar membranes without NMP, and empty defects (controls).

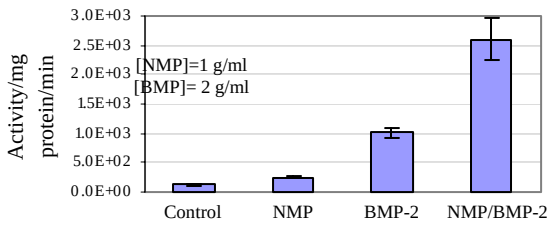


*Fig.1: Effect of NMP, rhBMP-2 and NMP/ rhBMP-2 on ALP activity of MC3T3-E1 cells cultured on TCPS in medium supplemented with ascorbic acid, after 2 weeks.*

*Fig.2: Effect of NMP on calcium phosphate deposition and mineralization by Alizarin Red staining after 4 weeks. Control without NMP (left) vs. sample containing 2.5 mM NMP (right).*

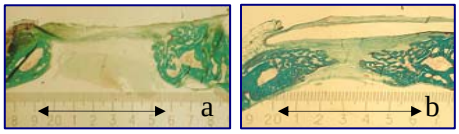


*Fig.3: Histological in vivo results from empty defect (a) Vs membrane loaded with NMP (b). In the control samples bone failed to bridge the defect after 4 weeks of implantation, while membrane-treated defects were almost bridged. Bone stains dark green whereas fibrous tissue light green. Arrow indicates initial 6mm width defect.*

**DISCUSSION & CONCLUSIONS**: The combination of rhBMP-2 and N-methyl-2-pyrrolidone (NMP) on MC3T3-E1 pre-osteoblastic cells seeded onto TCPS, promotes both their differentiation into mature osteoblasts (ALP activity) and the formation of mineral-like nodules (Alizarin red assay) in vitro.
Studies performed in vivo show that a guided bone regeneration membrane releasing NMP enhances bone formation. In this model the activation of autologous BMP by NMP was sufficient to enhance bone regeneration substantially.

**REFERENCES:** [1] F.E. Weber, H.G. Schmökel, E. Pirhonen (2003) *The first bioactive, degradable membrane for guided bone regeneration*, Abstractbook 1854, IADR, Gothenburg [2] C.H. Hammerle and R.E. Jung (2000) *Bone augmentation by means of barrier membranes* Periodontology **33**:36-53. [3] H.D. Zegzula, J.M. Wozney, J.O. Hollinger (1997) *Bone formation with use of rhBMP-2,* Journal of Bone and Joint Surgery. American Vol. **79**: 1778-90.

**FUNDING:** This study is supported by a grant from Inion OY, Tampere-Finland.

European Cells and Materials Vol. 7. Suppl. 2, 2004 (pages 55-56) ISSN 1473-2262

# Mechanical Properties of Fibre-Reinforced Dental Composites Subjected to Hydrothermal and Mechanical Ageing

A.Schütt[1], G. Bürki[2], P. Schwaller[2], J. Michler[2], M. Cattani-Lorente[1], P. Vallitu[3], S. Bouillaguet[1]

*[1] Dental Medicine, Geneva, Switzerland , [2] EMPA, Thun, Switzerland, [3]Turku University, Finland*

**INTRODUCTION:** Among the different materials used in dentistry, fiber-reinforced composite materials (FRC) are gaining popularity. Silanized glass-fibers are preferred by clinicians due to their mechanical properties, aesthetic qualities as well as their ability to chemically bond to dental composite resin materials. Interface properties are critical to the performance of fiber-reinforced composites because high masticatory forces are transfered across this interface.
Research findings have reported a degradation of the mechanical properties of fiber-reinforced polymers after water storage[1]. Other report has shown that mechanical fatigue, that occurs clinically, may also contribute to the reduction in mechanical properties of FRCs after ageing[2]. It is speculated that both the plasticization of the polymer matrix and the degradation of the fiber matrix-bond are implicated in this process. Therefore the objectives of this study were to compare the mechanical properties of two commercially available FRC systems after aqueous ageing and mechanical loading. Our first hypothesis was that the plasticization of the polymer matrix and the hydrolytic degradation of the fiber could be better demonstrated by measuring the changes in Young modulus of both components of FRCs using nanoindentation experiments. Our second hypothesis was that the degradation of interfacial adhesion between the fibers and the resin matrix could be assessed by using a micro push-out test.

**MATERIAL & METHODS:** Two commercially available FRC systems were tested: EverStick (StickTech) and Vectris Pontic (Ivoclar), consisting of longitudinal silanized glass fibers pre-impregnated with either a polymer-monomer gel, or photopolymerizing dimethacrylate resins.

For each material, eighteen specimens (2x2x25mm) were prepared using a stainless steel mould. The unpolymerized fiber reinforcements were cut into the length of 25 mm, placed into the mould, covered by polyethylene sheets and pressed between two glass plates. ES was light-cured for 40s on both sides and post-cured for 30 min (Liculite). VP specimens were light-cured 10 min under vacuum pressure (VS1) and post-cured for 10 min (Targis Power). The specimens were then polished using SiC paper (grit 800 -1200) and divided into three groups. The controls were stored at 37°C for 1 month in a dry environment. The second group was immersed in water and stored at 37°C for 1 month. The third group was submitted to a 300.000 cyclic stress at a frequency of 1Hz. A maximum cyclic force of 50 N was applied to the samples, which were simultaneously thermocycled in water at 5°C and 55°C during testing.

The flexural strength and the flexural elastic modulus were determined using a three-point bending test with an universal testing machine (Instron 1114) at a crosshead speed of 0.5 mm/min.

To measure the interfacial bonding strength and the Young's modulus of the matrix and fibers, the samples were embedded in a PMMA resin (Technovit 4071) and sectioned in the middle perpendicular to the long axis of the fibers with a diamond disc. The slices were then polished (SiC papers 1200-4000) down to 100μm and mounted on a grooved stub that were placed on the SEM stage (Zeiss DSM 962). A screw driven microindenter has been integrated with a scanning electron microscope (SEM) to perform fiber pushout tests on composites. The indenter is used to push fibers through thin sections while monitoring load and displacement. The displacement rate of the indenter was 0.31 μm/s and the maximum load of the instrument is 150 g (Touchstone Research Laboratory Ltd ). Ten fibers per specimen were tested.

A MTS nanoindenter XP with a Berkovich pyramid indenter was used to measure the Young's modulus of the fibers and the matrices. Ten indentations were made for each measurement with a 4 mN load. The Young's modulus was calculated using the algorithm of Oliver & Pharr [3].

The weight percentage of the fibers in the samples was estimated by calcination at 700°C for 3h.The data were compared with a two-way analysis of variance followed by a LSD multiple range test ($p<0.05$).

**RESULTS:** For each material, mean flexural strength and flexural elastic modulus values are given in Table 1. The Young modulus values for the fiber and the matrix and the interfacial adhesion are shown in Table 2.

Estimated mean fiber content by weight was 51±1% and 55±2% for ES and VP respectively.

*Table 1. Flexural strength (MPa) and flexural E modulus (GPa) of the two fiber-reinforced dental composites.*

| Material | Flx Strength | E |
|---|---|---|
| ES_control | 1164 (77) | 26.2 (1.9) |
| ES_water | 759 (69) | 25.5 (2.4) |
| ES_cycles | 847 (47) | 25.0 (3.4) |
| VP_control | 988 (105) | 32.7 (2.4) |
| VP_water | 746 (35) | 30.9 (0.8) |
| VP_cycles | 950 (64) | 34.7 (0.5) |

A two way analysis of variance showed no significant differences between the flexural strength of the two fiber reinforced composites ($p=0.2320$). However, there was a significant difference between the flexural strength of dry samples, samples immersed in water and fatigued samples ($p<0.0001$).

The elastic modulus of VP was significantly higher than the elastic modulus of ES ($p<0.0001$). Water storage and mechanical loading had no significant effect on the E modulus of both materials ($p=0.1447$)

*Table 2.Fiber and matrix Young modulus (GPa) and interfacial adhesion (Mpa) .*

| Material | $E_{fiber}$ | $E_{matrix}$ | Adhesion |
|---|---|---|---|
| ES_control | 76.8±3.6 | 4.9±0.2 | 103±9 |
| ES_water | 77.3±2.6 | 4.3±0.2 | 84±8 |
| ES_cycles | 73.9±5.4 | 5.8±2.1 | 87±11 |
| VP_control | 76.9±9.9 | 7.2±0.9 | 76±6 |
| VP_water | 69.3±5.9 | 5.2±0.2 | 62±9 |
| VP_cycles | 76.2±5.7 | 7.0±0.9 | 54±7 |

The results of the nanohardness test have shown that the Young elastic modulus of the glass fiber employed in both materials of are comparable ($p=0.5867$). Neither the storage conditions nor the mechanical fatigue significantly affected this property ($p=0.3615$). The Young's modulus of the ES matrix was significantly lower than the Young's modulus of VP ($p<0.0001$). The storage in water significantly decreased the matrix modulus, whereas the mechanical fatigue did not significantly affect this value.

ES showed a significantly higher interfacial adhesion than VP ($p<0.0001$). For ES and VP both water storage and cyclic fatigue resulted in a significant decrease of the adhesion ($p<0.0001$).

**DISCUSSION & CONCLUSIONS:** The two FRC materials tested showed similar flexural strength. VP was however stiffer than ES, probably because this material is based on a dimethacrylate matrix with a higher Young modulus than the polymeric matrix of ES. Moreover samples of VP showed a slightly higher fiber content than specimens of ES.

Occlusion forces that occur in the oral cavity have been simulated by submitting the samples to a bending cyclic fatigue test. With respect to the control group, the fatigued samples showed a decrease of the flexural strength. A more marked reduction was however observed when the specimens were just stored in water. Water storage also significantly decreased the matrix Young's modulus for both FRC materials. This result supports the concept of a plasticization of the resin matrix by water sorption. This effect was not observed on the matrix of the fatigued samples, as the interaction time between water and the specimens was shorter.

A decrease of the interfacial adhesion is another factor that can account for the reduction of the mechanical strength. Water storage and cyclic fatigue similarly reduced the adhesion between the fibers and the matrix for both materials, although probably by two different and independent mechanisms.

In conclusion, both water storage and mechanical ageing reduced the ultimate flexural strength of the two commercially available FRC tested. A decrease of the interfacial adhesion is one of the cause of the reduction of the mechanical properties, although the plasticization of the resin matrix cannot be ruled-out.

**REFERENCES:** [1] PK Vallittu (2000). *Int J Prosthodont* **13**:334-339 [2] JL Drummond, MS Bapna (2003). *Dent Mater* **19**:226-231 [3] WC Oliver, GA Pharr (1992) *J Mater Res* **7**:1564-1583

**ACKNOWLEDGEMENTS:** We gratefully acknowledge StickTech and Vivadent for kindly furnishing the materials used in this study.

# The influence of TGF-ß3 on bone regeneration in an ovine tibia defect - qualitative and quantitative histology -

S.Terhorst[1], U.Schlegel[1], T.Arvinte[2], M.Glatt[2], O.Maissen[1], BA.Rahn[1]

*[1] AO Research Institute, Davos, Switzerland. [2] Novartis Pharma, Basel, Switzerland.*

**INTRODUCTION:** The transplantation of autologous bone is often required for the treatment of large segmental bone defects. It can cause donor site morbidity and is of limited availability [1]. A possible approach is to design an artificial bone substitute, which ideally should stimulate cell differentiation, guide bone formation and provide cells which produce bone matrix [2]. The goal of this study was to investigate the osteoinductive potential of the Transforming Growth Factor-β3 (TGF-β3), which is known to regulate functions associated with bone formation [3].

**METHODS:** Cortical segmental defects of 18 mm length were created in ovine tibiae and treated with: (i): autologous cancellous bone, taken from the iliac crest, n=4; (ii): Poly (L/DL – Lactide) 80/20% sponges (PLA) [4] loaded with recombinant human TGF-β3 in a concentration of 50 µg/cm$^3$, n=4; (iii): PLA only, n=4; and (iv): 2 defects were left empty. For stabilization of the defects with full load bearing external fixations were used. After 4 and 6 weeks calcein green and after 8 and 10 weeks xylenol orange were administered for *in vivo* labeling of bone formation. After 12 weeks undecalcified specimens were embedded in methyl methacrylate. 100 µm thick sections were examined with contact radiography and fluorescence microscopy to measure the activity and amount of mineralization with Zeiss KS 400.3 and image pro plus 3.0. In the operator based qualitative evaluation of Giemsa/Eosin stained sections with bright field light microscopy points of interest were specified on samples, representing bone regeneration, bony bridging, vessel formation, soft tissue in-growth and foreign body reactions. For statistical analyses the Kruskal Wallis test and the Wilcoxon rank sum test were used ($p \leq 0.5$).

**RESULTS:** Contact radiographs showed the most mineralized bone area in the defect after 12 weeks in the bone graft group (i). TGF-β3/PLA (ii) showed significantly more amount of calcium deposition over 12 weeks than PLA only (iii). Median values for the amount of mineralization after 12 weeks: (i) 45.1 %, (ii) 24.2 %, (iii) 5.18 %, (iv) 7.17 %.

Fluorescence microscopy showed at 4 and 6 weeks significantly more activity of mineralization in the bone graft group (i) compared to TGF-β3/PLA (ii) and PLA only (iii). The deposition of xylenol orange showed no significant differences between the groups at 8 and 10 weeks.

The qualitative analyses of the Giemsa/Eosin stained sections showed after 12 weeks the highest activity of bone formation in the bone graft group (i), where many round osteoblasts surrounded by wide ostoid seams were seen. Many osteoclasts and eroded surfaces as signs of resorption were mainly seen in the TGF-β3/PLA group (ii). A bony bridging, crossing the defect was shown in 3 of 4 specimens of the bone graft group (i). Most vessels were seen in the TGF-β3/PLA group (ii). Transverse connective tissue structures occluding the proximal and distal medullar cavities as signs of highest soft tissue in-growth were seen in the empty defects (iv). Most foreign body giant cells were found in the PLA only group (iii).

**DISCUSSION & CONCLUSIONS:** The study showed that TGF-β3 enhanced bone formation, but the stimulation did not reach the potential of bone graft. Possible reasons could be an inaccurate dose or suboptimal release characteristics of TGF-β3. Furthermore PLA did not show a sufficient potential for bone regeneration enhancement. Optimization in material type and structure of the carrier as well as in the release kinetics of the Growth Factor may provide improved results.

TGF-β3 showed an osteoinductive potential. However effects of TGF-β3 loaded on PLA were inferior to an autologous cancellous bone graft in an ovine segmental tibia defect after 12 weeks.

**REFERENCES:** [1]B.N. Summers and S.M. Eisenstein (1989) *J Bone Joint Surg. Br.* **71(4)**:677-80. [2]P. Hardouin, K. Anselme, B. Flautre, et al (2000) *Joint Bone Spine* **67(5)**:419-24. [3]P. ten Dijke, K.K. Iwata, C. Goddard, et al (1990) *Mol. Cell Biol.* **10(9)**:4473-79. [4]Z. Gugala and S. Gogolewski (1998) *24th Annual Meeting of the Society for Biomaterials, San Diego, California, U.S.A.*:417.

**ACKNOWLEDGEMENTS:** Polymeric Implants: Sylwester Gogolewski; Statistics: Dominik Pfluger; Microscopy: Christoph Sprecher; Histology: Nora Goudsouzian.

European Cells and Materials Vol. 7. Suppl. 2, 2004 (pages 58-59) ISSN 1473-2262

# Mineralization of Hydroxyapatite over Collagen Type I

G.Verde-Carvallo, A.Guarino, G.González*

*Instituto Venezolano de Investigaciones Científicas (IVIC), Caracas, Venezuela.*

**INTRODUCTION:** Bone is a specialized form of connective tissue, that similar to others connective tissues, consists of cells and extracellular matrix. The difference between bone and others tissues, is the mineralization of the matrix, which provide the bone hardness for support and protection. The composition of the mineral matrix in cortical bone is ~70% of Hydroxyapatite and ~30% organic (largely collagen). In order to develop bone substitutes, Hydroxyapatite (HAp) has been intensively studied from de viewpoints of biocompatibility, bioactivity and osteoconductivity similar to bone, and collagen has also been studied for the osteoinductive properties and bioresorbability [1]. To achieve properties that are similar to the properties of bone, it is necessary to mimic not only the composition of the natural bone but also its structure, where HAp nanocrystals align their c-axes along collagen fibers. In the present investigation HAp-collagen composites have been made by two different methods of synthesis. The orientations of the structures have been observed by electron diffraction patterns.

**METHODS:** Two different methods were used to produce the Hap/collagen composite. The starting materials used for the first reaction (method a) were $(NH_4)_2HPO_4$ and $Ca(OH)_2$ , with a ratio Ca/P 1,67. A $Ca(OH)_2$ aqueous suspension and a solution $(NH_4)_2HPO_4$ with collagen type I were gradually added into a reaction vessel with a pH ~10,5. The weight ratio of HAp/collagen was fixed at 80/20. Then, the precipitate was aged at 40ºC for 24 h, the pH was gradually lowered to 8 by centrifugation at 10000 rpm. Finally the solid collected was dried at 60ºC under vacuum. The second reaction (method b) was made with $H_3PO_4$ aqueous solution in presence of collagen type I and $Ca(OH)_2$ suspension with a final pH 8,5 following the same procedure described above[2].

Characterization of HAp/collagen was made by X-ray diffraction (XRD) analyses. In preparing samples for transmission electron microscopy (TEM) observation, the dried powder was re-suspended in distilled water; a drop of the suspension was placed on a collodion-coated and carbon-reinforced copper electron microscope grid. After air drying, the sample was observed. The self-assembly phenomena of the HAp crystals that formed on the bio-organic templates were assessed using electron diffraction patterns.

**RESULTS:** Figure 1 shows the results of XRD measurements of both composites (a and b). The HAp peaks are broad, implying the nanocrystalline size of HAp. Figure 2 shows the TEM micrograph, where the mineral formed by the method *a* with $(NH_4)_2HPO_4$ have a crystal size of 10 nm width and 30 nm length and figure 3 shows the TEM micrographs of the synthesis by method *b* with $H_3PO_4$ and a crystal size of 10 width and 55 nm length.

*Fig.1:XRD for HAp synthesized with $(NH_4)_2HPO_4$ (method a) and with $H_3PO_4$ (method b).*

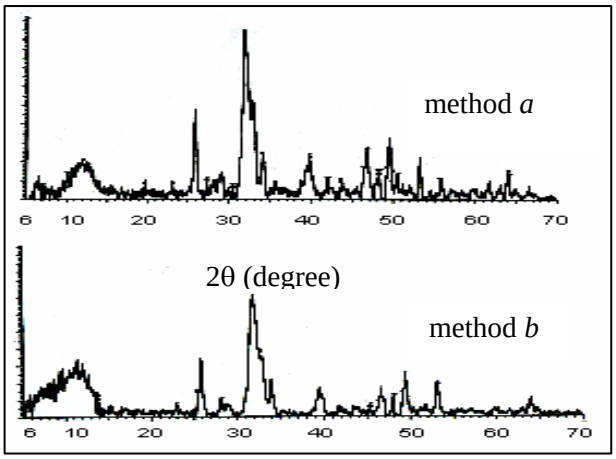


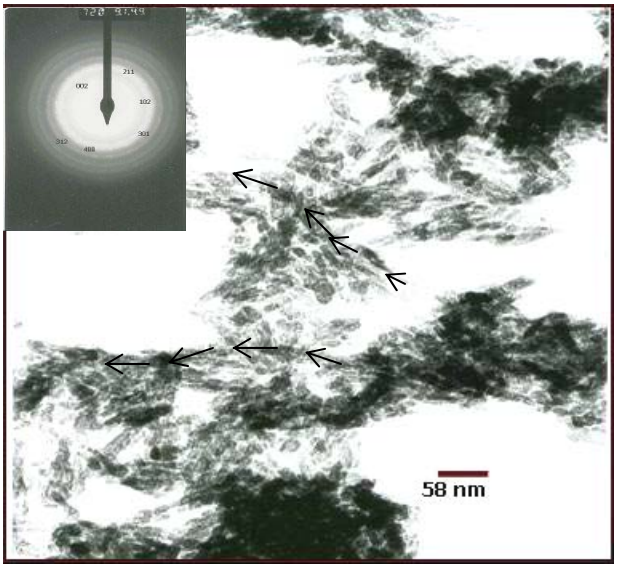


*Fig. 2: TEM micrograph and electron diffraction pattern of HAp/Coll by method a.*

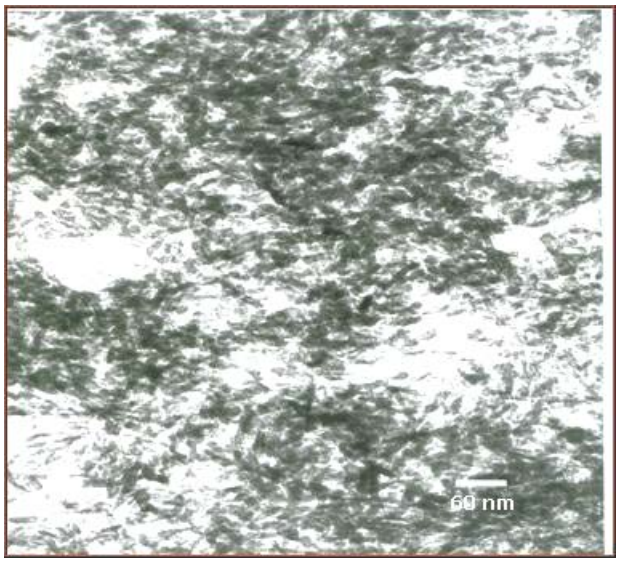


*Fig. 3: TEM micrograph of HAp/Coll by method b.*

**DISCUSSION & CONCLUSIONS:** The nucleation of Hydroxyapatite through the chemical interaction with collagen by two different methods of synthesis has been examined. The method *a* is not exactly a biomimetic synthesis, but the crystal size corresponds with that reported in literature for natural bone, the arrows show that crystals follows a oriented distribution over collagen fibrils, although diffraction pattern did not show any preferential orientation, perhaps it could not be clearly observed due to the large amount of HAP crystals present. Method *b* was made with an almost neutral pH, the crystals size is larger than the obtained with the first method although this size is still in good agreement with that of natural bone.

It has been under discussion for decades whether collagen acts as a promoter or inhibitor of the mineralization; however, recent studies point more in the direction that collagen has no effect on the mineralization[3]. In this work we could prove that an interaction exists between collagen and hydroxyapatite, and this was possible without the presence of noncollagenous proteins.

**REFERENCES:** [1] S-H. Rhee, J. Tanaka (1998) *J. Am.Ceram.Soc.*,81:3029-31, [2]S. Itoh, M. Kikuchi, et al (2002) *J Biomed. Mater. Res. (Appl. Biomater.)*,**63**:507-15. [3]A.L. Boskey (1996) *Connective Tissue Res.*,35:357.

**ACKNOWLEDGEMENTS:** we are grateful to Mirtha Romano for her technical support in TEM.